GEOPHY   IN   TE
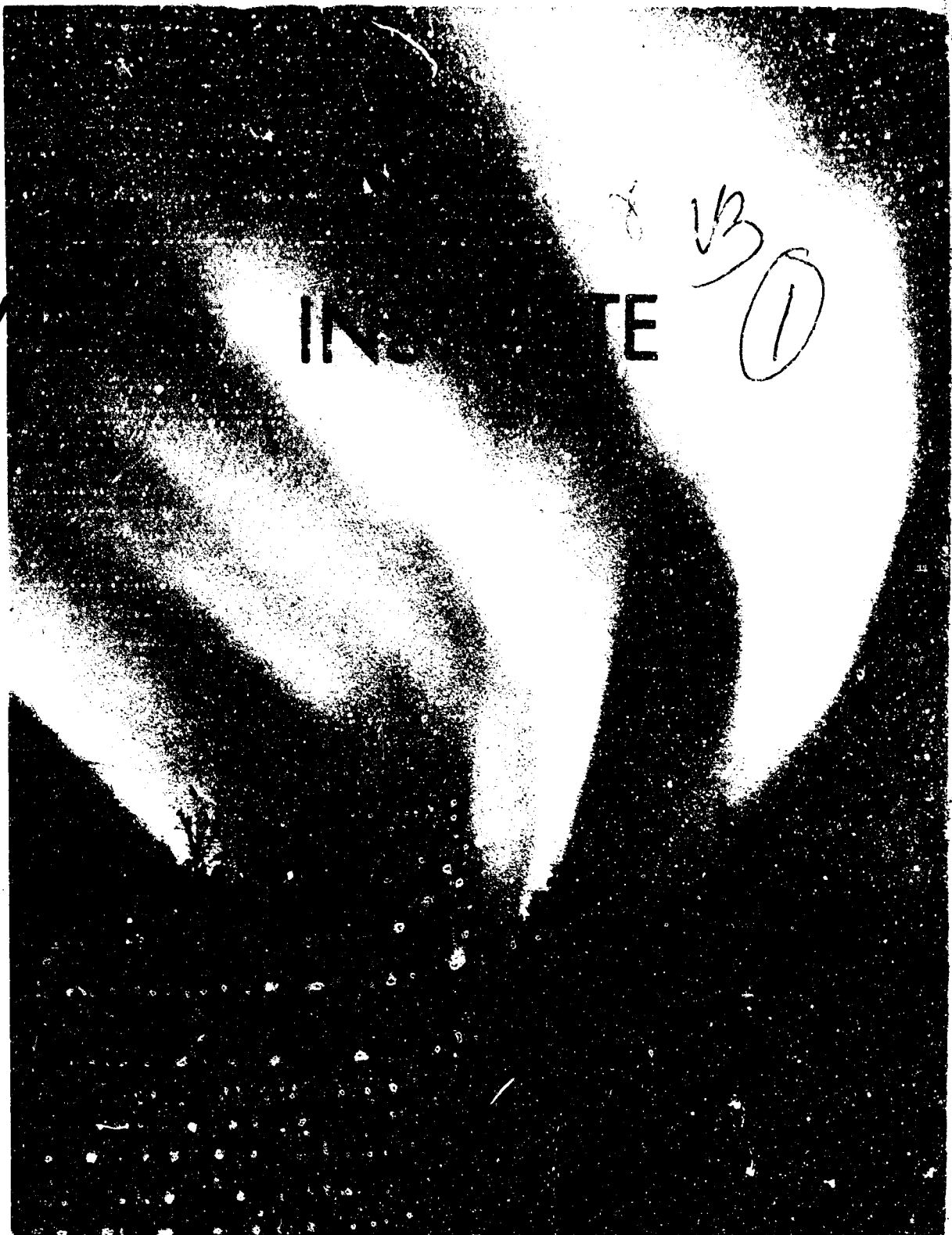
UNIVERSITY OF ALASKA

COLLEGE, ALASKA

UAG R-173

ICE FOG: LOW TEMPERATURE AIR POLLUTION

defined with Fairbanks, Alaska as type locality

by

Carl S. Benson
November, 1965

GEOPHYSICAL INSTITUTE

of the

UNIVERSITY OF ALASKA

ICE FOG: LOW TEMPERATURE AIR POLLUTION
Defined with Fairbanks, Alaska as type locality

by

Carl S. Benson

November 1965

Principal Investigator: Approved by:

                                                 K. B. Mather

Carl S. Benson   Keith B. Mather
                                                 Director

ABSTRACT

Stable pressure systems over interior Alaska sometimes produce prolonged, extreme (below -40°C) cold spells at the surface. The meteorological conditions responsible for two such cold spells are discussed in detail in Appendix A, where it is shown that the rate of radiative cooling of the air is enhanced by suspended ice crystals which are themselves a result of the initial cooling.

Radiation fogs formed during the onset of cold spells are generally of short duration because the air soon becomes desiccated. These fogs consist of supercooled water droplets until the air temperature goes below the "spontaneous freezing point" for water droplets (about -40°C); the fog then becomes an ice crystal fog, or simply "Ice Fog". During the cooling cycle water is gradually condensed out of the air until the droplets freeze. At this point there is a sharp, discontinuous decrease in the saturation vapor pressure of the air because it must be reckoned over ice rather than over water. The polluted air over Fairbanks allows droplets to begin freezing at the relatively high temperature of -35°C. Between -35 and -40°C the amount of water vapor condensed by freezing of supercooled water droplets is 3 to 5 times greater than the amount condensed by 1°C of cooling at these temperatures. This results in rapid and widespread formation of ice fog (Appendix B) which persists in the Fairbanks area as long as the cold spell lasts. The persistence of Fairbanks ice fog depends on a continual source of moisture (4.1×10^6 Kg H_2O per day) from human activities within the fog.

Ice fog crystals are an order of magnitude smaller than diamond dust, or cirrus cloud crystals, which in turn are an order of magnitude smaller than common snow crystals (0.01, 0.1 and 1 to 5 mm respectively). The differences in size are shown to result from differences in cooling rates over 5 orders of magnitude. Most of the ice fog crystals have settling rates which are slower than the upward velocity of air over the city center. The upward air movement is caused by convection cells driven by the 6°C "heat island" over Fairbanks. This causes a reduced precipitation rate which permits the density of ice fog in the city center to be three times greater than that in the outlying areas.

The inversions which occur during cold spells over Fairbanks begin at ground level and are among the strongest and most persistent in the world. They are three times stronger than those in the inversion layer over Los Angeles. Thus, the low-lying air over Fairbanks stagnates and becomes effectively decoupled from the atmosphere above, permitting high concentrations of all pollutants. The combustion of fuel oil, gasoline, and coal provides daily inputs of: 4.1×10^6 kg CO_2; 8.6×10^3 kg SO_2; and 60, 46 and 20 kg of Pb, Br and Cl respectively, into a lens-like layer of air resting on the surface with a total volume less than 3×10^9 m^3. The air pollution over Fairbanks during cold spells couldn't be worse, because the mechanisms for cleaning the air are virtually eliminated while all activities which pollute the air are increased.

TABLE OF CONTENTS

APPENDICES

APPENDIX A

    The Effect of Suspended Ice Crystals on Radiative Cooling.

APPENDIX B

    Nucleation and Freezing of Supercooled Water Droplets.

LIST OF FIGURES

INTRODUCTION

Problems involved with the formation of ice crystals in the atmosphere are covered voluminously in the literature of cloud physics. Ice fog is a special case for two reasons: (1) it is man-made, and (2) it forms as a result of injecting water vapor at temperatures generally exceeding $100^{\circ}C$ into a pre-cook l ($-35^{\circ}C$ or below) water-saturated air mass. The injected water vapor cools at rates 5 to 6 orders of magnitude greater than the most rapid cooling rates observed in the free atmosphere; this results in small crystals which fall very slowly. The abundant nuclei also resulting from combustion processes insure that the supercooled droplets freeze at temperatures above the spontaneous freezing point for small droplets, ie, $-40 \pm 1.5^{\circ}C$. Ice fog is a form of air pollution which appears at temperatures below $-35^{\circ}C$ in populated regions where topography, combined with strong inversions, causes air to stagnate.

The Stanford Research Institute carried on a study of ice fog at Eielson Air Force Base between 1951 and 1955. Their report (Robinson et al, 1955) is the most comprehensive available on the subject, yet several areas of research still need attention.

In 1961 the Geophysical Institute began studying ice fog in the greater Fairbanks area. Financial support has been provided by grants, DA-ENG-11-190-61-G3 and DA-ENG-27-021-62-G5, from the U.S. Army Cold Regions Research and Engineering Laboratory (CRREL), Hanover, N.H., and from the Geophysical Institute and the Physics Department of the University of Alaska. A preliminary account of this work was presented at the 15th Alaskan Science Conference in Fairbanks (Benson, Gotaas, Francis and Murcray, 1964).

Equipment was provided on loan from CRREL, the U.S. Air Force Arctic Aeromedical Laboratory, the Department of Atmospheric Sciences of the University of Washington, the Geophysical Institute of the University of Alaska, and the Signal Corps Meteorological team at Fort Wainwright.

1

Persons active on the project in addition to the principal investigator[*] may be separated into four groups:

1. Geophysical Institute staff supported by funds from the CRREL grants: Karl E. Francis;[**] Rudolph Domke, Electronics Technician; Carol Echols, Senior Research Assistant; Emil Peel, Senior Research Assistant; George Ryon, Technician; and Donald Williams, Field Assistant.

2. Geophysical Institute staff funded by the Geophysical Institute and Physics Department of the University of Alaska: Michael Almasi, Associate Electronics Engineer; Yngvar Gotaas, Meteorologist and Assistant Professor of Geophysics; and Wallace Murcray, Associate Professor of Geophysics.

3. Graduate students John P. Clark and Gary L. Richardson conducted studies on man-made water vapor sources which contributed to the research program and constituted partial fulfillment of their requirements for the masters degree in Engineering Management.

4. Army personnel from CRREL and Signal Corps included: Dr. Motoi Kumai (CRREL) who participated in the field work during both field seasons and made electron microscope studies on crystal nuclei at the University of Chicago. Mr. Stanley Bolsenga (CRREL) assisted in setting up meteorological instruments during the 1961-62 field season. Mr. H. O'Brien (CRREL) assisted Dr. Kumai during the 1962-63 field season. Mr. Sam Scott (CRREL) assisted in setting up instrumentation during the 1962-63 field season. Lt. Col. Ellis Pickett, commander of Ft. Wainwright Signal Corps Met. team, assisted in both field seasons by providing

---

[*]Due to prior commitments with National Science Foundation, Ohio State University, and the University of Wisconsin, Carl Benson was in Antarctica during the entire month of December 1961 and for the first 20 days of January 1962.

[**]Karl Francis originally intended to use this program as an M.S. thesis in Geophysics, but changed his field of interest and took an M.S. in Geography at Oregon State University. He worked as a technician on the project to assist with instrumentation in fall of 1963. During the 1961-62 field season he worked on field sampling techniques, including photomicrography in the field, and laid a good base for collecting and filing photos and formvar replicas of crystals.

2

storage space, equipment, and part-time helpers. Major E. Hoppe and Major W. Johnson USAF have contributed information and assistance on the ice fog problems at Eielson AFB.

The study underway at the Geophysical Institute began with three general objectives:

1. Genesis and morphology of ice crystal forms in ice fogs

2. Vertical distribution of temperature and crystal forms in ice fogs

3. Meso-micro-meteorological conditions associated with ice fog development and dissipation.

Observations were made during the winters of 1961-62 and 1962-63. The 1961-62 winter was unusually cold with six ice fog periods, the longest of which was 16 days (15-30 December 1961), a total of 40 days with ice fog were observed, and on 28 and 29 Dec. 1961, an all-time low of -52°C (-62°F) for the month of December was recorded in Fairbanks. The average temperature for the month of December 1961 was -31.1°C (-23.9°F), this is 8.2°C (14.8°F) below normal; December 1964 averaged -32.5°C (-26.5°F), or 10.4°C (18.8°F) below normal. The 1962-63 winter was unusually warm with five ice fog events of short duration which totaled 25 days. The temperature records for these two winters are shown in Figure 1; the range of average max-min values is indicated by the cross hatch pattern.

In pursuance of objective 1, techniques were worked out during the 1961-62 field season for obtaining formvar replicas of crystals and for use of a microscope with camera to photograph both the crystals themselves and the replicas. Among other things, this involved construction of a heated jacket for the microscope camera. Formvar replicas and direct photography collections were made simultaneously to provide a basis for evaluating the formvar technique in these studies. The replication technique was modified slightly from that described by Schaefer (1941).
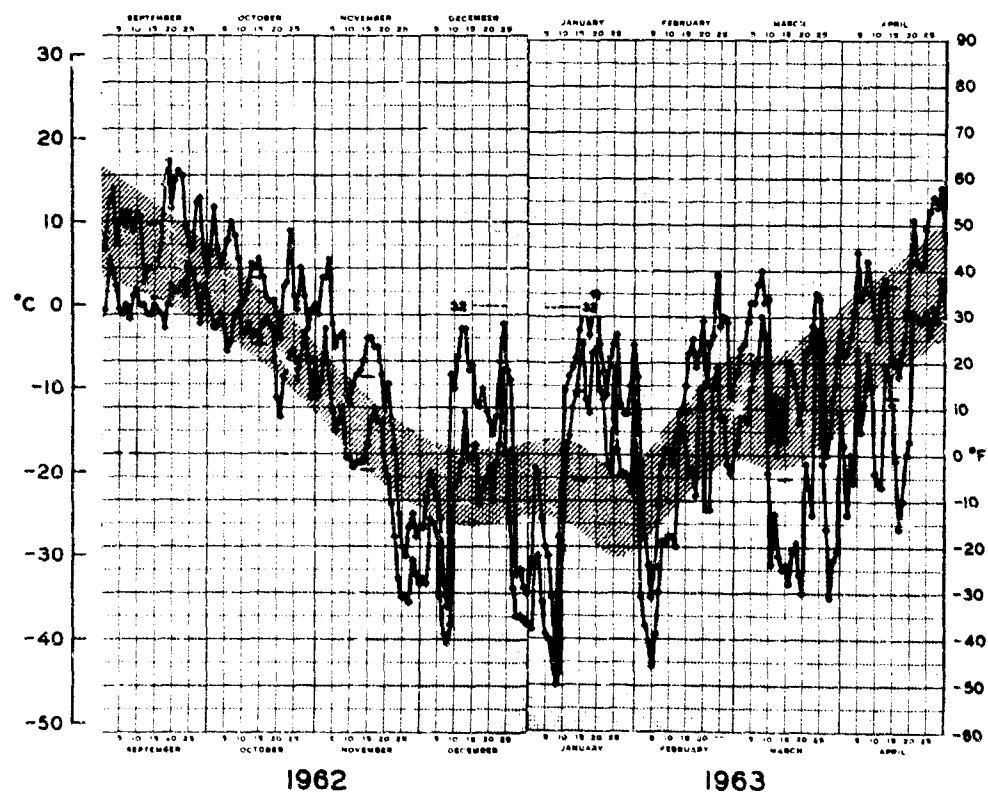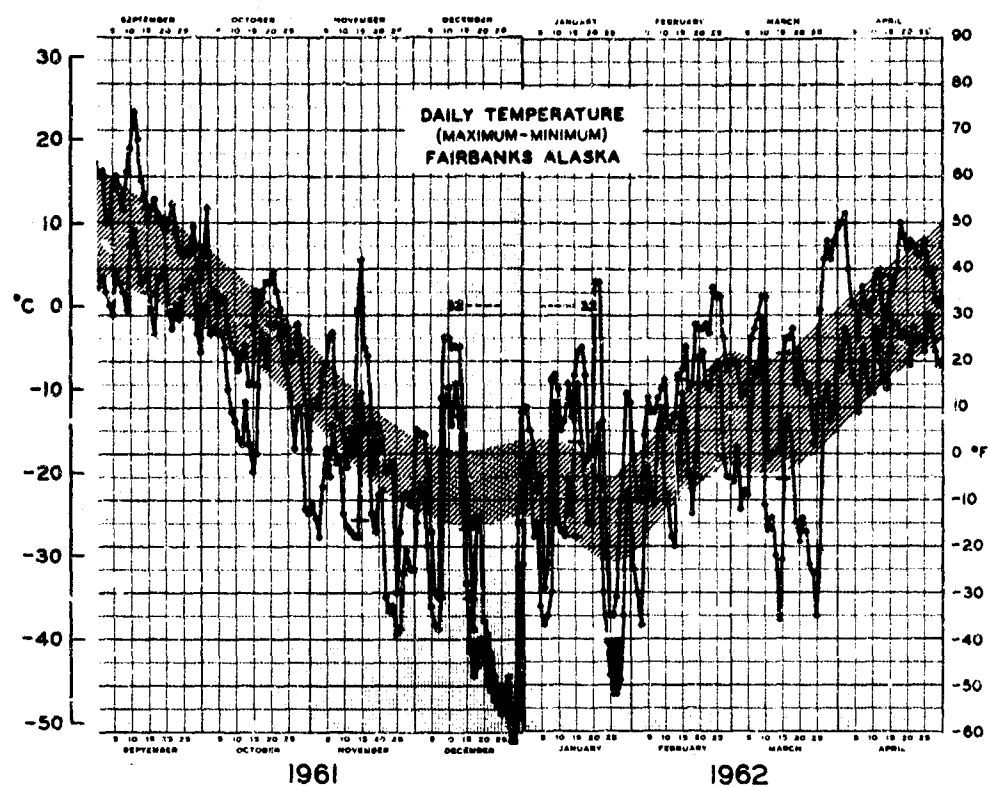
Fig. 1. Daily maximum and minimum temperatures for the winters 1961-62 and 1962-63. The range of average maximum and minimum values is shown by the cross-hatched pattern; the blackened pattern represents temperatures below -40°C.

Crystals were also collected on collodion-coated electron microscope grids. After the crystals or droplets were photographed and allowed to evaporate, their residues were examined for crystal nuclei under an electron microscope by Dr. Motoi Kumai of CRREL. Some results of this work were presented by Kumai (1964). A total of 364 direct photomicrographs were made of 295 Argonne electron microscope grid collections which include snow crystals as well as a wide size spectrum of ice fog crystals. The combination of morphological studies and electron microscopy is intended to cover the widest possible temperature ranges. During the 1962-63 field season foruvar replicas were made periodically at stations in the mesometeorological network described below.

Objectives 2 and 3 listed above will be discussed together. During the 1961-62 field season a small micrometeorological program was attempted When equipment originally expected from the Signal Corps could not be provided, a mid-winter attempt was made to install equipment flown to Alaska by CRREL in December 1961. However, the primary product of this effort was experience because of the combination of extreme cold (for six consecutive days the maximum air temperature remained below -45°C (-50°F), together with activities associated with the crystal sampling program.

Nuclei counts were made with a small particle detector during the winter of 1961-62 with the counter at ambient air temperature. The action of the counter depends on maintaining a moist blotter inside the instrument. Thus, readings should be expected to vary according to whether the air temperature is above or below 0°C. Even though it is recognized that there may be significant seasonal variations in nuclei, measurements were repeated during May of 1962 in the same region to provide counts at temperatures above 0°C.

A meso-micrometeorology network consisting of four 15 m towers and 8 thermographs was set up and maintained during the 1962-63 field season. The

4

towers had thermocouples at 1, 2, 4, 8, and 15 m above ground, as well as at the ground-snow interface. The thermographs were placed in shelters mounted 2 m above the ground. Locations of towers and thermographs are shown in Figure 2. The stations located along the slope of Birch Hill were intended to provide a record of air temperature 2 m above ground throughout this nearly 200 m variation in altitude. Maintenance of this instrumental network was time-consuming, and power failures plus erratic or non-function of various components, resulted in some broken records throughout the season. The data have been reduced and selected time intervals of: (1) cooling periods, (2) low temperature periods, and (3) warming periods, have been extracted for detailed presentation in this report. All data are on file in useful form and, in addition to providing valuable spatial information on ice fog, they suggest new approaches to the overall problem.

Several experimental devices were designed and used to provide information on horizontal and vertical variation of significant variables. During the 1962-63 field season FAA clearance was obtained, as well as approval from the Army Aviation group, to fly a 34 m^3 (1200 ft^3) Seyfang balloon. The balloon was provided on loan by CRREL and berthed at Fort Wainwright in Hanger 1. Experience was gained in operating the balloon and a sampling apparatus was designed for use with it. This apparatus permitted collection of formvar replicas of crystals at selected altitudes with simultaneous measurement of wind and air temperature. The wind measurements were made with a Beckman & Whitley K114 portable anemometer and counter system provided by the University of Washington. A trailer was outfitted to provide heated working space for use with the blimp and for microscopic examination of crystals.

A wiresonde unit was developed and mounted on pack boards. The unit can be easily transported by two men and permits temperature and wind profiles to be made at any desired point. Wiresonde wind measurements were calibrated by

Fig. 2. Map of Fairbanks and vicinity with test stations and principal roads indicated. The symbols are:

⊕ Micrometeorological towers with thermocouples at 1,2,4,8 and 15 m above ground during 1962-63 winter.

△ Triangulation control points where observations and photographs have been made of ice fog and other atmospheric phenomena over the Fairbanks area.

0 Thermographs located 2 m above ground during 1962-63 winter. Thermographs were also run at points ⊕ 1, ⊕ 2, △ 5, and △ 18.

Records from points 10, 11, 15 and 29 were not complete througout the 1962-63 season. Daily maximum and minimum values are available from the U.S.C. and G.S. station at point 17.

The U.S. Weather Bureau Station is at point 21.

● Power plants:
    Point 23, Ft. Wainwright North Power Plant
        24, Ft. Wainwright South Power Plant
        25, Golden Valley Electric Association Power Plant
        26, Municipal Utilities System of Fairbanks, Power Plant
        27, University of Alaska Heating Plant,

The Fairbanks Sewage Treatment Plant is at point 31.

X Limited observation points, used as base of temperature traverses (especially point 22, Van Horn Road and Cushman intersection) and for snow studies (points 28 and 29).

The altitudes of key points are:	Meters	Feet
1. Birch Hill Middle	300	986
2. Ski Lodge	140	458
3. Aeromedical Lab. River Site	137	449
4. Aeromedical Laboratory	140	458
5. Birch-Hill West (B.M.)	333	1096
6. Ski Slope Top	310	1018
7. Ski Slope Middle	240	787
8. Ski Slope Bottom	176	576
9. Peger Road Site	130	425
10. Phillips Field	132	433
15. Goldstream	180	590
18. Ester Dome	720	2364
19. VABM (Ditch)	270	885
20. Top of Chena Ridge	457	1500
21. U.S. Weather Bureau, Fairbanks Airport (B.M.)	132	433
Hanger #1 Runway (B.M.)	137	448
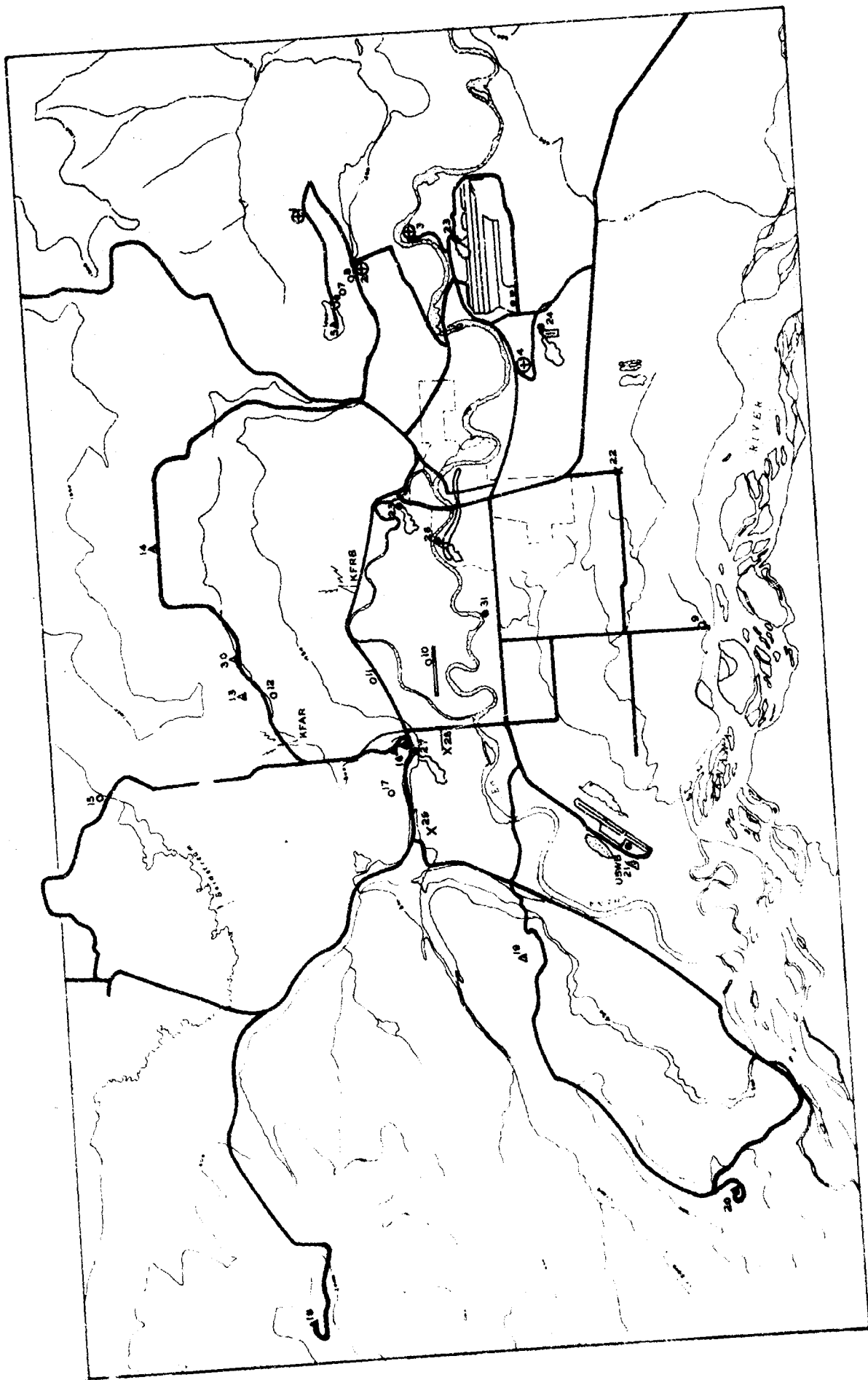
Figure 2

flying the wiresonde balloon alongside the blimp-supported anemometer mentioned above. Smoke bombs were used in conjunction with the wiresonde to measure low-level wind velocities.

A resistance thermometer mounted 2 m above the ground in front of an automobile proved effective in measuring the "heat island" produced by the city of Fairbanks.

In connection with crystal growth, the most difficult (yet one of the most important) parameters to measure is humidity. A frost point apparatus was designed and preliminary experiments indicate it to be a promising approach to the problem. Plans are underway to make comparative field tests of it, alongside of several other methods.

The original scope of the problem was broadened to include an analysis of meteorological conditions which produce prolonged cold spells. The two extreme periods of the 1961-1962 winter (15-29 December and 23-29 January) were analyzed using surface and upper air data from the U.S. Weather Bureau at Fairbanks, together with data from the meso-micrometeorological program. Data from the latter source were used to study the structure of the lowest air layers when strong inversions prevailed during the 1962-1963 winter, with special emphasis on the cold spell of 5-10 Jan 1963. In general, the cooling rates observed at the onset of cold spells, from the surface up to 3000 m are too large to be satisfactorily explained by advection and/or by radiative heat losses from the snow surface. This problem is discussed in Appendix A with the conclusion that radiative heat loss from suspended ice crystals is an important factor in rapid cooling; this process also influences humidity measurements made in air containing ice crystals.

Temperature variations which showed up on the instrument records prompted the use of vehicle-mounted thermometers, to examine variations caused by heat

sources and sinks in the area. Local temperature differences produce circulation of air within the ice fog. This effect first showed up on thermograph and thermocouple records from along the slope of Birch Hill; it is associated with wave motion of the lower air layers.

Ice crystals which form and grow as the free atmosphere cools are larger and have better developed crystal faces than do ice fog crystals. These variations in crystal size and shape result from variations in the conditions of formation and growth. The rate of crystallization is, of course, a very important growth parameter and it varies over a range of 5 to 6 orders of magnitude when one compares atmospheric cooling rates with those of exhaust gases. In particular, a marked difference in size and perfection of form is observed between ice fog crystals formed from automobile exhaust gases which cool 10 to $100^{\circ}C$ per sec, and "diamond dust" crystals formed in the first km above the surface in air cooling 3 to $4^{\circ}C$ per 12 hours.

Crystal twinning also depends on environmental conditions during growth. According to Vance (1961) primary twinning is favored by euhedral growth and rapid crystallization. Collections of ice fog crystals always contain many twinned crystals, whereas twins are not prevalent in diamond dust or snow crystals. Both ice fog and diamond dust crystals have good opportunity for euhedral growth so cooling rate is probably the most important factor in producing the morphological differences. The cooling rates are such that if primary twinning is involved, the observations in ice crystals agree with Vance's feldspar observations. However, most twins in ice fog crystals are probably secondary twins formed by crystals colliding and then orienting while in contact so that they twin on the 0001 plane. The 0001 plane is almost invariably the twinning plane. This essentially leads to synneusis twinning, and ice fog offers an excellent opportunity to study the mechanism of synneusis twinning in

7

a stress-free environment as compared with cases in magmas where stresses cannot be eliminated (Ross, 1957; Vance, 1961).

Calculations of the total output of water vapor from Eielson Air Force Base and from the Fairbanks - Ft. Wainwright area have been made and compared with the amount of water the air can hold at saturation at various temperatures. The over-saturation in some areas causes the air pollution problem represented by ice fog to be very acute. The water contained in the ice crystals and super-cooled droplets may, in itself, cause physiological problems. However, there is much besides water in the ice fog. Some of the other components of air pollution such as the amounts of carbon dioxide, sulfur, and lead (from gasoline) can be calculated along with the calculation of water vapor produced by combustion processes.

In addition to these calculations the air pollution in the greater Fairbanks area may be measured by using the winter snow pack as a collection device. The winter snow cover was sampled from top to bottom in the spring of 1963, '64 and '65 at selected locations. The melt water derived from the snow was subjected to measurements of specific electrical conductance in our laboratory; isotopic ratios have been measured on the same samples by Dr. Iving Friedmann, U.S.G.S., Denver, Colorado. The electrical conductance of water from Fairbanks area snow is an order of magnitude greater than in the outlying areas with fairly well defined boundaries. Similarly the conductance of water derived solely from material precipitated out of ice fog is an order of magnitude greater than that of the city snow pack.

A measure of the overall dirtiness of the polluted snow has been undertaken by measuring the total particulate material in the snow cover. This study supplements the measurements of electrical conductance which depends only on the ions present, and was done in cooperation with Dr. H. Bader and Mr. W. Hamilton of the University of Miami, Coral Gables, Florida.

Direct measurements of air pollution were made during the 1964-1965 winter in conjunction with Drs. J. W. Winchester and R. Duce of the Massachusetts Institute of Technology. These studies are initially concentrating on Lead and the Halogens. Although this research goes beyond the original scope of the ice fog study it is mentioned here because it has grown directly out of the original study, and will certainly continue.

The plan of this paper is first to discuss some essential aspects of air pollution in general. Then the Fairbanks problem will be presented with a discussion of sources of pollution. A general development of an ice fog event will then be described, followed by a detailed treatment of the factors which produce two such events. Finally, the air structure in and around the city will be discussed in terms of its important effect on the ice fog-air pollution situation.

Acknowledgements:

9

One generally thinks of Alaska as a big place with few people and clean air. Generally this is correct. However, parts of Alaska's thin population live in crowded, but isolated, communities, some of which are like small bubbles of urban United States. Unfortunately, in some instances this analogy is complete enough to include the most extreme cases of water and air pollution. These notes are concerned with a type of low temperature air pollution which is well known by the name "ice fog".

Ice fog is primarily a man-made air pollution problem which becomes a nuisance whenever temperatures go below $-35^{\circ}C$ in the Fairbanks - Ft. Wainwright area of interior Alaska. It is produced by water vapor output from automobile exhaust, power plant stacks, household chimneys and other sources associated with urban environments. Aside from local sources of water vapor, such as hot springs and caribou herds, ice fog is restricted to populated areas. Its thickness is generally about 10 m, and rarely exceeds 30 m; however, both its vertical thickness, and its density, increase as temperature decreases, especially below $-40^{\circ}C$ when street-level visibility in Fairbanks is reduced to less than 30 m.[*] The reduction of visibility by ice fog, although serious in itself, is only one of the more obvious manifestations. The air structure over Fairbanks during cold spells, even when temperatures are not low enough to produce ice fog, is very stable and produces concentrations of atmospheric pollutants which are as bad as any on earth.

Before discussing ice fog itself, several general aspects of air pollution will be considered and "low temperature air pollution" will be introduced here as a fourth "type" of air pollution with Fairbanks, Alaska as the type locality.

---

[*]Prolonged cold spells such as the one of 19-30 December 1961 (240 consecutive hours below $-40^{\circ}C$, including six consecutive days below $-45^{\circ}C$ with a minimum of $-52^{\circ}C$ ($-62^{\circ}F$)) cause cold-weather failure of mechanical parts in vehicles etc., as well as acute visibility problems for pedestrians, automobiles and aircraft. During this cold spell photos from hill tops indicate that the ice fog built up to an extreme thickness of almost 50 m in downtown Fairbanks on 29 December 1961.

To define pure, unpolluted air, or conversely, to define air pollution is not a simple task. It may depend on the point of view of the investigator or on the details of a specific problem. A chemist, physicist, biologist, surgeon, or city planner could each write his own definition of air pollution; but basically, it is a disease of civilization, which unfortunately is destined to increase concurrently with our exponential increase in population. The complexity of the problem, including a useful definition, is well stated by Haagen-Smit (1959, p. 1).

> "This control ...(of air pollution)... is beset with many
> difficulties, not all of an engineering nature. Since air
> pollution has been defined as 'the presence of unwanted
> material in the air' its very concept is highly subjective.
> The cure for this community disease reaches into the domains
> of the legal, as well as the medical professions. Its
> emotional nature is well illustrated by the controversy
> between smokers and non-smokers regarding the cleanliness
> of the air."

Air pollution, ie, "the presence of unwanted material in the air", varies in specific details from one locality to the next. The total quantity of pollutants put into the air is, of course, important but may be offset by combinations of topographic and meteorologic parameters. Thus, serious air pollution problems in Los Angeles have been widely recognized for over 20 years. On the other hand, aside from grumps about coal dust, the air pollution problems of Chicago have attracted relatively minor attention. These are good examples because each city is associated with slogans which relate to the purity of their air.

Chicago earns its nickname "The windy city". The often times bone-chilling wind from Lake Michigan does an effective job of diluting pollutants generated by the massive industrial complex and concentrated urban area from Gary, Indiana to Evanston, Illinois.

The cliche "Sunny California", especially in the Los Angeles basin where winds are generally calm, has attracted many people. The industry, and

11

especially the automobiles, which accompany these people discharge exhaust
products into the air which undergo complex photochemical reactions when acted
on by sunlight. Ironically, this sunshine encouraged the localized population
explosion in the first place. These photochemical reactions produce the "Los
Angeles type" of air pollution (Haagen-Smit, 1952). As pointed out by Chambers
(1962, p. 9) this is "referred to as smog in deference to local usage, although
it is actually not identical to the smoke fog of Great Britain from which the
term is derived." Indeed, "smog" is a poor term for this type of air pollution
because it has retarded popular appreciation that the problem involves complex
photochemical processes in the atmosphere.

Types of Air Pollution

It was mentioned above that "Ice Fog: Low-Temperature Air Pollution" would
be introduced as a fourth "type" of air pollution. Briefly, the "types" are:

(1) Coal Smoke and Gases --

> "... have been the chief atmospheric pollutants in all parts of
> the industrial world for more than 400 years. In spite of
> the recent rapid shift to petroleum and natural gas, coal
> smoke still is a major contributor to poor air quality in
> all but a few metropolitan areas" (Chambers, 1962, p. 7).

(2) Specific Toxicants -- fortunately, the damages which can be clearly
related to specific toxicants are infrequent and generally well isolated.

> "Perhaps the most publicized recent example of serious air
> pollution by an identified toxicant was the episode at Posa
> Rica, near Mexico City, in which numbers of people were
> affected and a few died from exposure to hydrogen sulfide.
> Metallic fumes and acid mists from metallurgical processing
> have occasionally rendered downwind regions wholly uninhabit-
> able for plants as well as men. Fluorides escaping from
> aluminum processing and other industrial sources have
> been the cause of losses to cattle farmers. Malodorous
> pollutants from a wide variety of source types have produced
> responses ranging from public irritation to overt and
> wholesale illness" (Chambers, 1962, p. 8).

(3) Los Angeles type Smog -- is by no means restricted to Los Angeles; it appears in any modern city whose economy is geared to the use of petroleum fuels. As stated by Chambers (1962, p. 9) it "has become the infamous prototype of similar developments appearing with increasing frequency in metropolitan areas of the United States and in some other countries". Observations on smog in South American, European and U.S. cities are described by Went (1955).

(4) Ice Fog -- or Fairbanks type, Low Temperature Air Pollution -- occurs in concentrated centers of population where extremely strong inversions are able to form in quiet air by outgoing radition from snow surfaces. These inversions have high positive temperature gradients, $\frac{dT}{dz}$, and they begin at ground level. Low temperature refers to values below $-35^{\circ}C$. Some aspects of this type of air pollution form the substance of these notes.

In summary; the two requirements for air pollution are: (1) the availability of pollutants, and (2) a restriction in the volume of air which can dissolve these pollutants. Conditions controlling the latter requirement vary widely from place to place because they depend on meteorologic and topographic factors. The most stable atmospheric conditions occur under and within, inversion layers. The situation is well summarized by Went (1955, p. 65). "The height of the inversion layer and the horizontal air movement over a city determine the volume of air in which the emitted air pollutants are contained, and consequently determine their ultimate concentration."

Temperature Inversions

Air temperature usually decreases with increasing altitude, when it increases with altitude a "temperature inversion" exists. Although the term "temperature inversion" is widely used by the general public, it is poorly understood, sometimes even by people writing about air pollution.[*] For the present

[*]Donald Carr, a research chemist and author of a book dealing with air pollution (The Breath of Life Pub. by W. W. Norton 1965), in a recent article on Air Pollution (Saturday Review 27 Feb.1965) stated "Nobody knows what causes inversions!

13

purpose, we will briefly consider the two main causes of inversions which are easily illustrated by well-known examples.

(1) A temperature inversion forms in the boundary layer between two air masses when a warmer one flows over a cooler one. An excellent example occurs in the Los Angeles area where cool air from the Pacific Ocean is overridden by warmer air from the Mojave Desert. In this example the air temperature is relatively constant from ground level up to 400-500 m through the oceanic air, and then increases sharply as the desert air is encountered.

(2) Temperature inversions form at ground level when there is a net loss of heat from the earth's surface by outgoing longwave radiation. The radiative balance between the surface and the air aloft causes this cooling to proceed upward in the air as described in detail by Wexler (1936). These inversions become especially well developed at night over snow surfaces and are common both day and night in parts of the Arctic and Antarctic. Unfortunately, they are also common in Fairbanks. The important difference between these inversions, and those which form at the boundary between two air masses, is that the lower boundaries of radiation inversions are directly in contact with the ground. Thus there is no "height of the inversion layer", and the minimum possible volume of air is available to dissolve air pollutants if they are present.

The rate of change of temperature within the inversion layer, ie, the "steepness, or strength, of the inversion", is also important because the stability of the air increases with it. The steepness of radiation inversions increases as topographic features restrict low level air motion. Thus, the strongest inversion measured at the South Pole was $9.65^{o}C/100$ m on 21 April

14

2315 GMT 1958 (Dalrymple, 1964); this is a strong inversion, but the inversions measured during cold spells at Fairbanks, Alaska are among the steepest in the world with values of 10 to 30°C/100 m, common in the first 50 to 100 m (Fig. 3). These different ranges of values can be attributed to topography. The south pole area is essentially a flat plateau; Fairbanks is surrounded by hills on three sides which permits stagnant air to form at low levels similar to the situation in the Los Angeles Basin. However, the stability of the air over Fairbanks is far greater than that over Los Angeles for two reasons: (1) Since the inversion over Fairbanks begins at ground level there is no air available to mix with, dissolve, and carry away pollutants beneath the inversion layer as compared to the 400-500 m thickness available over Los Angeles, and (2) Fairbanks inversions are roughly three times steeper than those in the Los Angeles inversion layer. (Gradients in the Los Angeles inversion layer rarely exceed the extreme value cited above for the South Pole Station.) Figure 3 shows soundings from the South Pole, Fairbanks, and Los Angeles.

Low Temperature Air Pollution

In Fairbanks, the air pollution situation during winter cold spells couldn't be worse. Exceptionally strong inversions are almost always present when surface air temperatures go below -30°C; their strength increases as the temperature continues to drop into the -40 and -50°C range. Since these inversions form by radiative cooling from the surface they restrict turbulence in the lowest levels, beginning at the ground surface itself. This is far worse than the infamous Los Angeles case where the air below the inversion layer is 400 to 500 m thick.

The extreme nature of the Fairbanks case may also be appreciated when we realize that most other cities evolve enough heat to prevent slight inversions from forming. Indeed, "over cities it is rare to find inversions in the lowest

15

Fig. 3. Comparison of inversions over the South Pole, Fairbanks and
        Los Angeles.

The altitudes at these stations are:

South Pole	2792 m	above sea level
Fairbanks	135 m	" " "
Los Angeles (Santa Monica)	38 m	" " "

In this figure the stations are plotted at a common altitude to
allow direct comparison of their air temperature profiles above
the snow or ground surface.

Data are from radiosonde records. Lines A and B represent high
and low average positions of Los Angeles inversions (Johnson, 1953).

Curve	Location	Time and Date
1	South Pole	23:15 GMT 21 Apr 1958
2	Fairbanks, Alaska	12:00 GMT 26 Jan 1962
3	" "	00:00 GMT 22 Dec 1961
4	" "	12:00 GMT 26 Dec 1961
5	Los Angeles (Santa Monica)	12:00 GMT 13 Aug 1963
6	"	00:00 GMT 23 Sept 1963
7	"	00:00 GMT 25 Sept 1963
8	"	00:00 GMT 26 Sept 1963
9	"	12:00 GMT 26 Sept 1963
10	"	00:00 GMT 27 Sept 1963
A	Los Angeles	Average 13:00 120 WMT Jun 1949
B	"	" 19:00 " " Aug "

The inversion in the first 50 m over Fairbanks (curve 2) is three
times steeper than the strongest inversion observed at the South
Pole (curve 1, Dalrymple, 1964).

City heat sources combined with solar radiation tend to destroy
inversions over most cities. The sequence of curves 6, 7, 8, 9
and 10 shows the development and destruction of a "smog hosting"
inversion over Los Angeles.

The cooling over Fairbanks, represented by curves 3 and 4 was
accompanied by dense ice fog and development of a normal lapse
rate within the ice fog layer. The normal lapse rate results
from radiative heat exchange within the ice fog itself and from
city heat sources. However, the inversion itself is still due
to net outgoing radiation and remains steep even though its base
moves to the top of the ice fog layer. The consequences of heat
sources within the fog and below a strong inversion are discussed
in Chapter VII especially pp. 53-55.
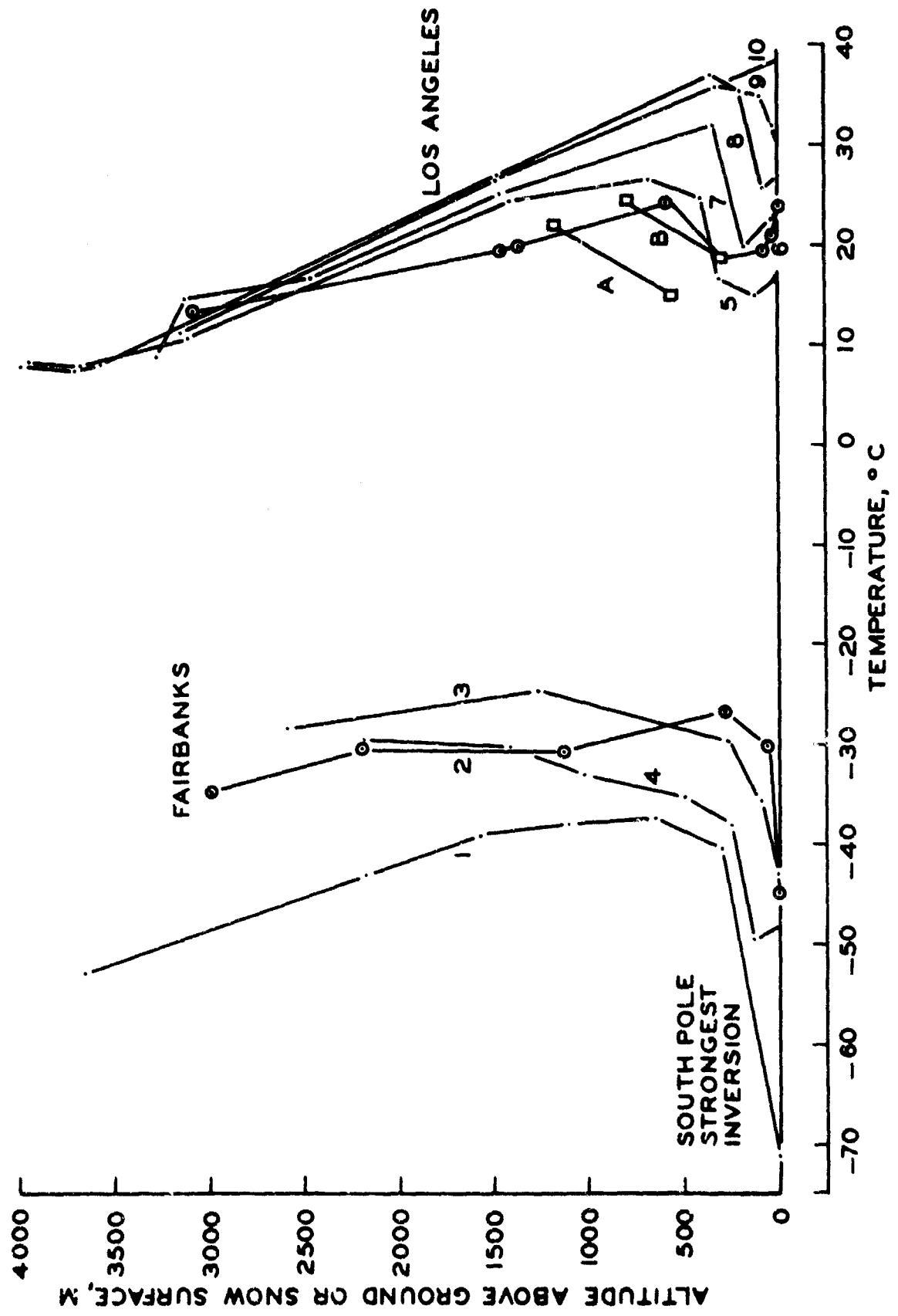
Figure 3

100 meters, and the city influence is still evident 200 to 300 meters above the surface" (Pack, 1964, p. 1121). The city influence of Fairbanks warms the air in the city so that it is about 6°C warmer than the surrounding areas, but this does not destroy the strong inversions which involve temperature increases of 10 to 15°C in the lowest 50 m. Unfortunately, the Fairbanks inversions are not only among the steepest in the world but they sometimes last for weeks at a time. This is a "semi-permanent nocturnal condition", to use Ball's (1960, p.9) descriptive terminology pertaining to Greenland and Antarctic conditions.

During cold spells the lower air levels have very low winds, almost always less than 2 m sec^{-1}; this is especially true for the first 500 m which is nearly contained by the hills around Fairbanks. The existing flow consists of katabatic (gravity drainage) winds which move down the Tanana valley. This has led to a widespread misconception that the katabatic flow drains cold air from the hills onto the flats, and especially into the lowest pockets. This would be a happy circumstance, if it occurred, because such drainage would tend to flush the air pollutants out of the city. However, the air in the flats is so much colder, and therefore denser, than that moving down from the hills, that the latter cannot penetrate, and moves across the cold low-lying pool of air as if it were a lake. Thus, the only flushing mechanism for Fairbanks air during cold spells is "turned off", and the dense surface layers are effectively decoupled from the air above. Unfortunately, it is precisely during these cold spells, when the air is most able to stagnate that the rate of polluting the atmosphere increases because of increased demands for heat and power. Indeed, in Fairbanks, the air pollution during winter cold spells couldn't be worse, because natural and man-made factors reinforce one another in ways which invariably lead to intensification, never mitigation, of the air pollution.

16

In most instances of air pollution, the sources of pollution are more obvious than are the meteorological condition responsible for their concentration. However, in Fairbanks, where the meteorological conditions described above are obviously capable of concentrating pollutants, the sources of pollution are not as obvious.

An important feature of ice fog is that water itself is a pollutant even in what would be considered negligibly small amounts at higher temperatures. While cold weather reduces the capability of the air to hold water in solution, it also causes an increase in the output of water from man-made sources, primarily from combustion processes. Let us again compare Los Angeles and Fairbanks. Obviously, Los Angeles has far more of any given type of combustion than Fairbanks, but air at $+ 20^{\circ}C$, in L.A., is capable of holding 255 times more water in solution than at $-45^{\circ}C$ in Fairbanks. The problem is, of course, intensified by the stronger inversions which rest on the surface in the Fairbanks area. Other man-made sources of water vapor in the Fairbanks-Ft. Wainwright area are: The cooling waters discharged from power plants, people and animals breathing, moisture leaks from houses and other buildings, steam lines, laundry plants, etc.

Combustion Products

Combustion of hydrocarbon fuels releases water and carbon dioxide to the air; the quantities involved for gasoline and fuel oil may be calculated by assuming complete combustion of the representative molecular species as follows:

	Molecular Weight of fuel	Molecular Weight Ratios	
		H_2O/Fuel	CO_2/Fuel

Gasoline

$C_8 H_{17} \xrightarrow[\text{excess } O_2]{\text{burned with}} 8\ CO_2 + 8.5\ H_2O$ 113   1.35   3.12

$C_8 H_{18} \xrightarrow[\text{excess } O_2]{\text{burned with}} 8\ CO_2 + 9\ H_2O$ 114   1.42   3.08   }(1)

Ave: 1.38   3.10

Fuel oil

$C_{16} H_{34} \xrightarrow[\text{excess } O_2]{\text{burned with}} 16\ CO_2 + 17\ H_2O$ 226   1.37   3.12

$C_{16} H_{32} \xrightarrow[\text{excess } O_2]{\text{burned with}} 16\ CO_2 + 16\ H_2O$ 224   1.29   3.12   }(2)

Ave: 1.33   3.13

Coal

The case for coal is slightly more complex because it contains water which is exhausted directly to the atmosphere as it is burned. The coal used in the Fairbanks-Ft. Wainwright area is from Healy, Alaska and it contains an average of 8% ash and 22% water according to tests run at the University of Alaska, (Hankinson, 1964). Thus 70% by weight is combustible material for which the benzene molecule, $C_6 H_6$, is representative.[*] To be conservative in estimating water sources for the atmosphere, we will assume that 20% of the coal, as received and burned in furnaces, is water; then, for the 70% combustible material we write:

	Molecular Weight of fuel	Molecular Weight Ratios	
		H_2O/Fuel	CO_2/Fuel

$C_6 H_6 \xrightarrow[\text{excess } O_2]{\text{burned with}} 16\ CO_2 + 16\ H_2O$ 78   0.69   3.38   (3)

The above equation, applicable to 70% of the mass burned, must be added to the 20% of the original mass which was H_2O.

---

[*]This is true for coals in general, see Van Krevelen (1961).

Thus, the net result is:

$$
\begin{array}{l}
0.10 \text{ Ash} \xrightarrow{\hspace{3cm}} \text{Negligible discharge to air} \\[4pt]
+\ 0.20\ H_2O \xrightarrow{\text{direct loss}} 0.20\ H_2O \\[4pt]
+\ 0.70\ C_6H_6 \xrightarrow[\text{excess } O_2]{\text{burned with}} 0.48\ H_2O\ +\ 2.36\ CO_2 \\[4pt]
1.00 \text{ Coal} \xrightarrow[\text{Combustion Products}]{\text{Direct loss} +} 0.68\ H_2O\ +\ 2.37\ CO_2
\end{array}
\quad\Bigg\}\quad (3a)
$$
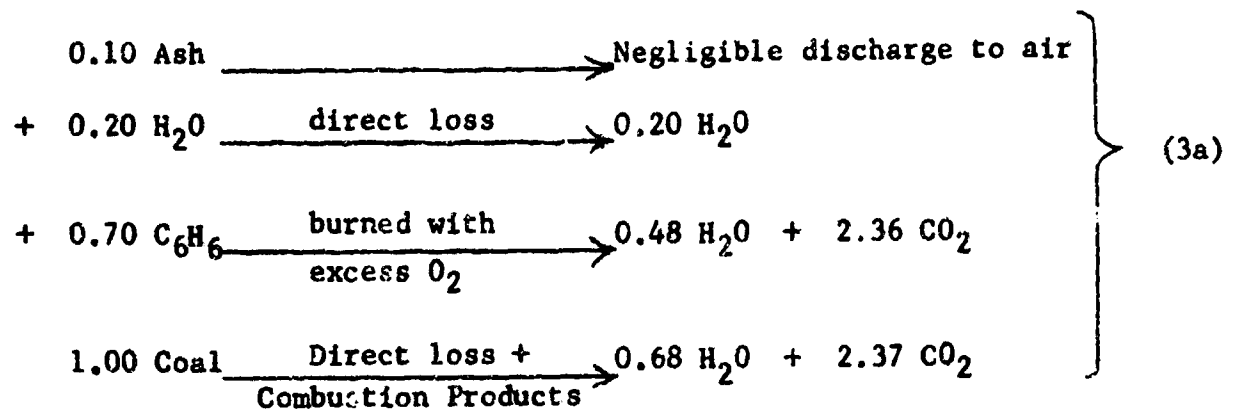
Totals

The amounts of gasoline, fuel oil and coal burned in the Fairbanks - Ft. Wainwright area are summarized in Figures 4, 5, 6, and 7. The quantities burned daily during cold spells are maximum values which can be estimated from the monthly values. The water and CO_2 produced are calculated from equations 1, 2, and 3a, with the following results:

Gasoline:		Gallons	Kg	Kg H_2O	Kg CO_2
	Monthly	900,000	2,700,000	3,720,000	8,400,000
	Daily	30,000	90,000	124,000	279,000

Fuel Oil:		Gallons	Kg	Kg H_2O	Kg CO_2
	Monthly	1,364,000	4,600,000	6,100,000	14,400,000
	Daily	45,000	152,000	202,000	475,000

Coal, Domestic:		lb	Kg	Kg H_2O	Kg CO_2
	Monthly	20,000,000	9,100,000	6,190,000	21,500,000
	Daily	670,000	305,000	207,000	720,000

Coal, Power Plants:		lb	Kg	Kg H_2O	Kg CO_2
	Monthly	74,000,000	33,600,000	23,850,000	79,400,000
	Daily	2,460,000	1,118,000	760,000	2,640,000

The total combustion products are:		Kg H_2O	Kg CO_2
	Monthly	39.9×10^6	123.7×10^6
	Daily	1.3×10^6	4.1×10^6

19
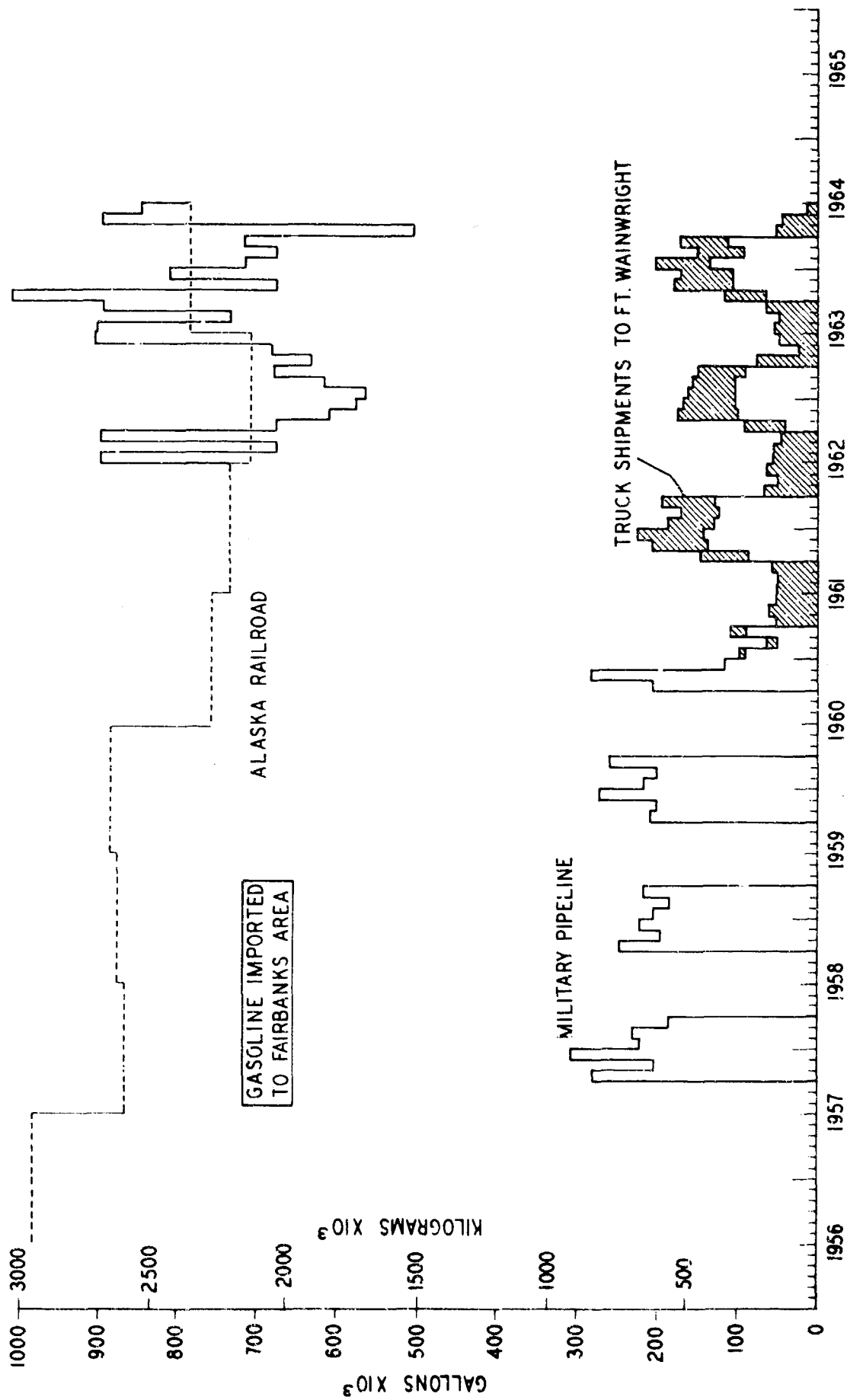
Fig. 4. Gasoline imported to Fairbanks and Ft. Wainwright. The three sources of gasoline in order of magnitudes are the Alaska Railroad, the military pipeline and truck shipments to the Ft. Wainwright Post Exchange Station. Pipeline data were obtained for the months Oct., Nov., Dec., Jan., Feb., and March. Railroad data are available as yearly averages except for the last two years when monthly quantities are available. When Ladd Air Force Base closed and became Ft. Wainwright in 1960, the amount of gasoline imported was reduced significantly as can easily be seen in this diagram.
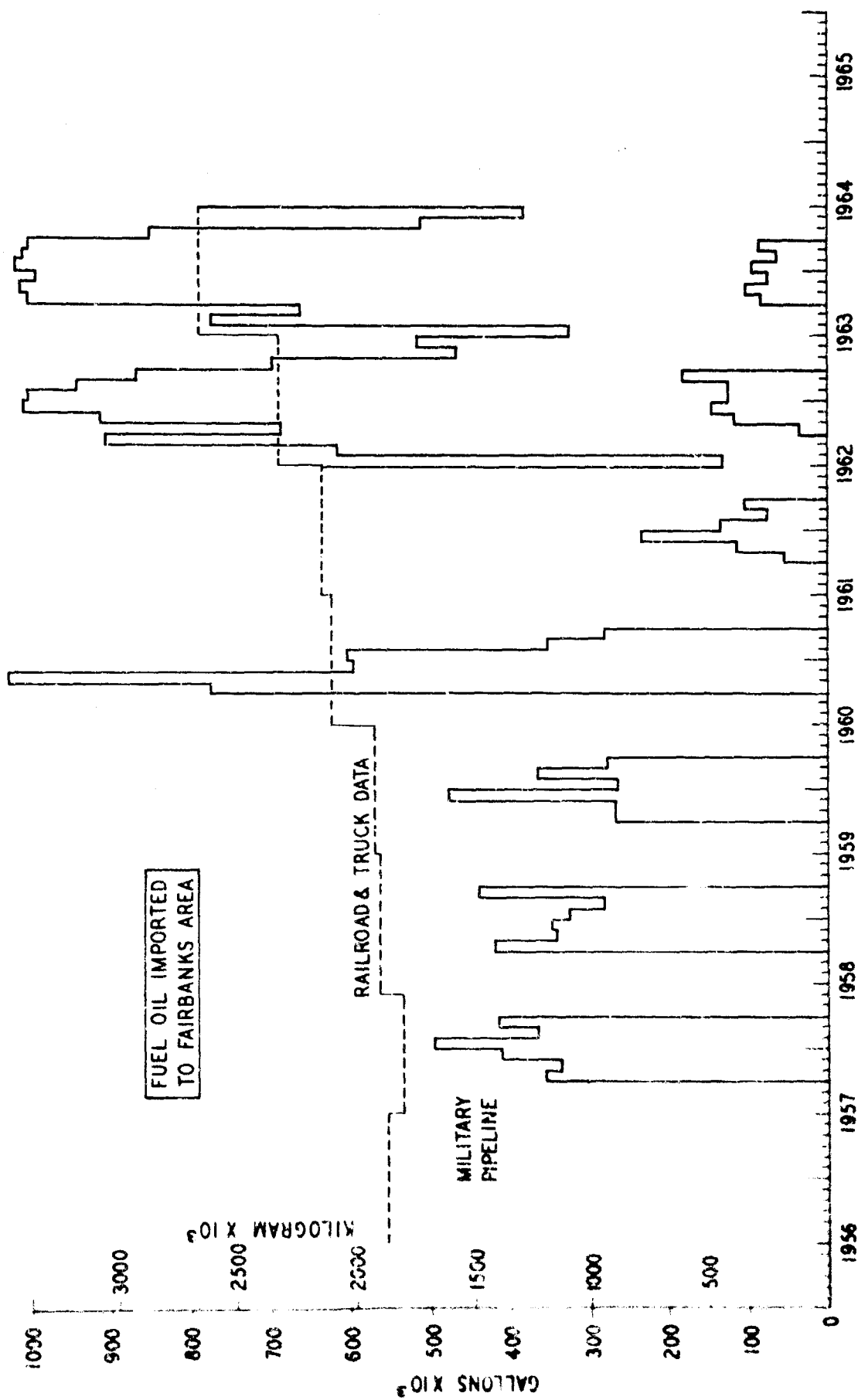
Fig. 5. Fuel oil imported to the Fairbanks area by railroad, truck and pipeline. As with the gasoline figures, annual railroad values are available except for the last two years when monthly averages were obtained. The transformation of Ladd AFB into Ft. Wainwright again shows up in the pipeline data. All fuel tanks were filled by the Air Force before the base was turned over to the Army; this resulted in the abnormally high monthly rates near the end of 1960.
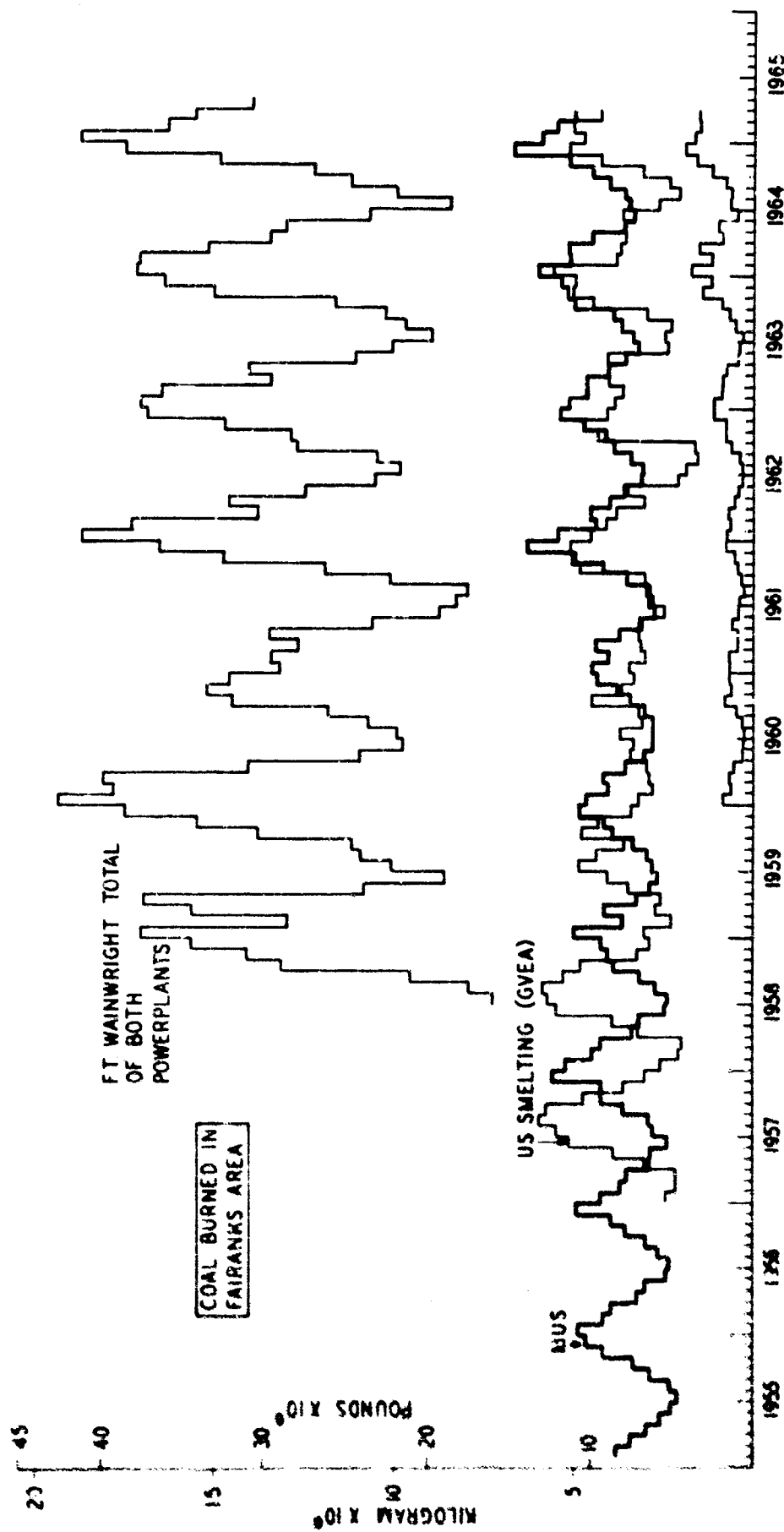
Fig. 6. Summary of coal burned in power plants at Ft. Wainwright and Fairbanks. The low fuel consumption in 1960 resulted from reduced use of buildings during the transfer of Ladd AFB to Ft. Wainwright. The Golden Valley Electric Association purchased the U.S. Smelting Refining and Mining Co. power plant in 1953. The gradual change from peak power production of this plant during summer mining operations, to peak production for winter power needs shows clearly from 1957 to the present. These data graphically portray the end of the gold mining era in Fairbanks. A steady increase in use of the University heating plant is also apparent. Unfortunately the increase since 1964 coincides with a 30 m (100 ft) lowering of the stack outlet.
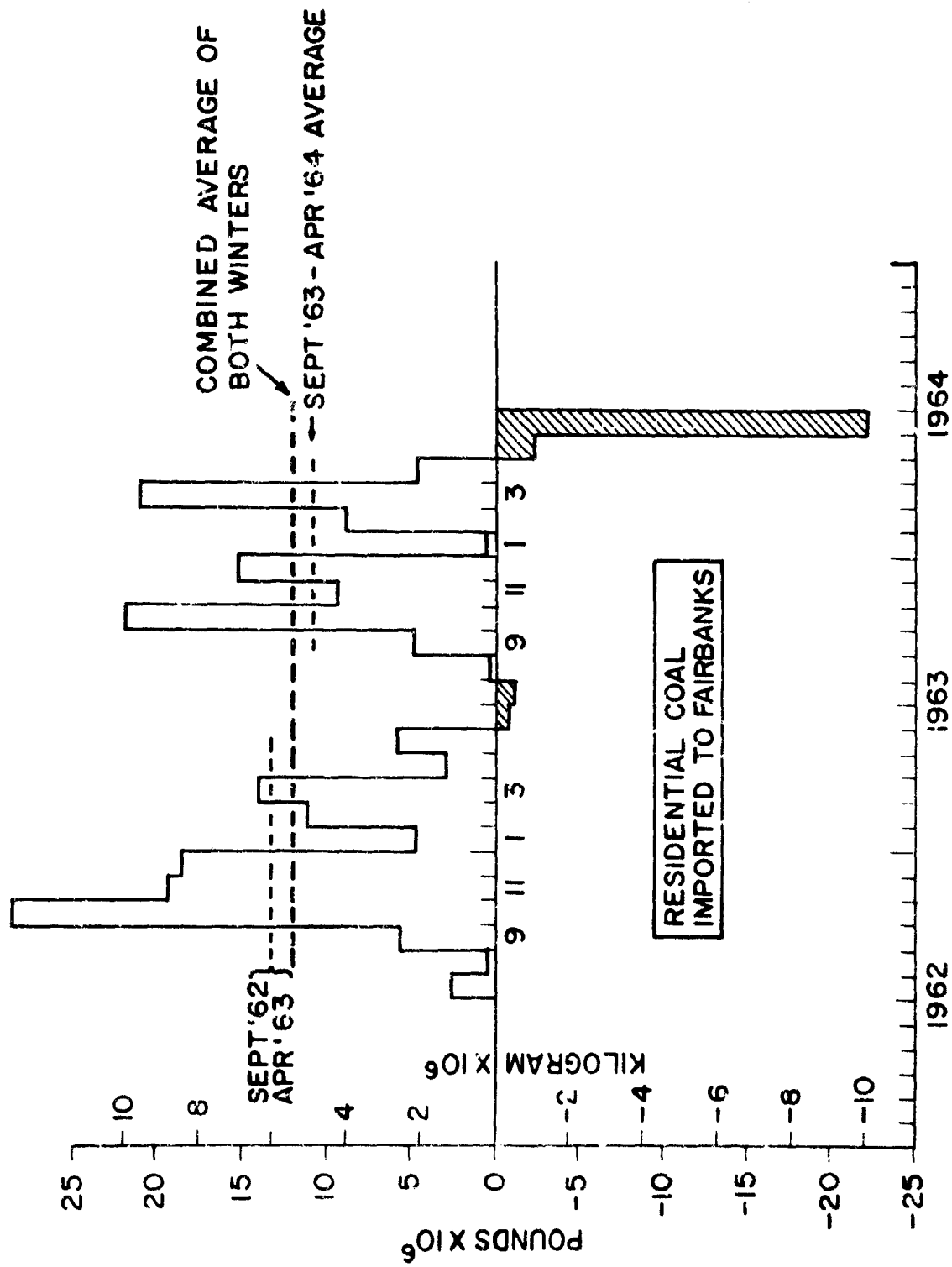
Fig. 7. Residential coal imports. This figure was prepared by subtracting power plant coal consumption from the coal imported by the Alaska Railroad. A stockpiling of coal is apparent in October and November of each year since the coal burned for domestic heating is certainly a maximum during December and January. The daily rate of consumption for cold spells during the two winters shown is estimated at 20 x 10⁶ lb (9 x 10⁶ kg).

Cooling Water from Power Plants

Power plants require a source of cool water to condense the steam produced in generating power. After this water absorbs heat from the steam lines it is discharged at a temperature of about 15°C, into direct contact with the bottom of the atmosphere. There are five power plants in the area; three of them obtain their cooling water from wells, whereas the other two use cooling ponds.

Power Plant	Point on Map	Abbreviations used in this paper	Source of Cooling Water
Ft. Wainwright, North	23	Ft. W.N.	Pond
Ft. Wainwright, South	24	Ft. W.S.	Pond
Golden Valley Electric Association, Inc.	25	G.V.E.A.	Wells
City of Fairbanks, Municipal Utilities System	26	M.U.S.	Wells
University of Alaska	27	U. of A.	Wells

The cooling ponds are essentially man-made lakes in contact with the ground water table. The large one used by the south power plant at Ft. Wainwright is the trapezoidally-shaped lake with an island in it, which lies about 1 km south of the west end of the runway (see the U.S.G.S. Fairbanks C-2 quadrangle, 1:63,360). The open-water area of the lake in winter, is about $1.3 \times 10^4 m^2$, or approximately half of the summer area. The cooling pond at Ft. Wainwright's north power plant is small ($242 m^2$); but it makes up for this by spraying the warm water through 32 nozzles located 2m above the open-water surface. When the air temperature is -45°C, the vapor pressure of this spray of water droplets at 15°C is about 200 times greater than the equilibrium vapor pressure of the ambient air. It would be hard to imagine a more efficient way of introducing water into a super-saturated air mass.

The power plants without cooling ponds pump water from wells, heat it, and discharge it into the Chena River, Noyes Slough and Deadman Slough. This hot water, which was originally out of contact with the atmosphere, now

maintains open-water surfaces through the winter for distances of about 2 km on the Chena River downstream from the M.U.S. power plant, and 4-5 km on Noyes Slough, downstream from the G.V.E.A. power plant. The greater length of open water from the G.V.E.A. plant is the result of two factors:

(a) The hot water discharge is the only source of water for Noyes Slough in the winter--in the MUS-Chena River situation the hot cooling water is mixed with the cold river water.

(b) The rate of discharging hot water from the G.V.E.A. plant is approximately twice that from the M.U.S. plant.

The U. of A. power plant maintains a small amount of open water surface near Deadman Slough. The University plant is primarily a heating plant with the campus heating system as its condenser; therefore its need for cooling water is relatively small. Similarly the M.U.S. plant produces heat for the city which serves, in part, as its condenser. The G.V.E.A. plant concentrates on producing electric power and uses a maximum amount of cooling water all of which is ejected into Noyes Slough.

To estimate the amount of water put into the atmosphere from power plant cooling waters it is necessary to analyze each case separately. A detailed analysis is given for the largest plant with results from the others summarized more briefly, and all of them tabulated on page 26.

South power plant, Ft. Wainwright

This is the largest power plant in the area (see comparative coal consumptions, Fig. 6). Its cooling pond is partly frozen in winter so that the en water surface of summertime, 2.6×10^4 m^2 is reduced to about 1.3×10^4 m^2 in winter. Water from the power plant is discharged into the pond at 15°C. It circulates through the cooling pond around the center island and is taken back into the plant at 5°C. It is a steady-state system, with flow to and

from the pond equal to 600 liters per second, or 51.8 x 10^9 cm^3 per day, and a net change of temperature equal to 10°C. This requires a heat loss from the cooling pond of 518 x 10^9 calories per day. This heat is lost by three processes which, in order of importance are:

(1) evaporation to the atmosphere,

(2) radiation to the sky, and

(3) conduction through the bottom of the pond.

Convection in the water reduces the amount of heat lost by conduction downward and increases the evaporative heat loss. The same is true for air motion across the pond. Although winds are low, almost always less than 2 m sec^{-1} under ice fog conditions, they do exist and their effect is to increase evaporative heat loss.

To make a conservative estimate of the water put into the air by evaporation, the following discussion maximizes heat losses from conduction and radiation and ascribes the remainder to evaporative heat loss.

(1) Conduction

The South Powe Plant cooling pond is 2.5 m deep. The maximum temperature observed at the bottom during summer was + 5°C with a surface temperature of 26°C (Merryman, 1964). Thus the maximum summer gradient would be 0.085°C cm^{-1}. It is reasonable to assume that the temperature at the bottom of the pond is never far from the maximum-density value of + 4°C. During winter the maximum temperature at the top of the pond near the hot-water outlet is 15°C; therefore the maximum temperature gradient in winter is 0.044°C cm^{-1}. The conductivity of water near 0°C is 0.0013 cal cm^{-1} sec^{-1} °C^{-1}. The following conditions will give a value of heat transfer greater than the upper bound which can be expected by conduction in this situation; assume:

(1) The extreme winter gradient of 0.044°C cm^{-1} for the entire open half of the pond,

22

(2) no convection in the water, and

(3) all heat conducted downward can be conducted away through the soil

below--this is obviously an extreme assumption because the temperature

gradient in the soil is at least one order of magnitude less than

in the water.

Using these extreme assumptions we obtain a vertical heat flux of:

$$k \frac{dT}{dz} = (0.0013)(0.044) = 57.2 \times 10^{-6} \text{ cal cm}^{-2} \text{ sec}^{-1},$$
$$= 493 \times 10^{-2} \text{ cal cm}^{-2} \text{ day}^{-1},$$

during winter we use half of the pond area, i.e., 1.3×10^8 cm^2, and obtain a

conductive heat loss of 493×10^{-2} cal cm^{-2} day^{-1} x 1.3×10^8 cm^2 = 0.64×10^9

cal day^{-1}. But the total heat to be lost is 518×10^9 cal day^{-1}; thus, the

extreme upper limit which can be handled by conduction is less than 0.1% of

the total and can be neglected.

(2) Radiation

Net radiative cooling of the earth's surface has been estimated and

measured by several methods.[*] Reasonable agreement exists between them when

applied to the cooling pond which is treated as a black-body with no cloud

cover. In particular, Wexler (1941) gives two formulae for the net outgoing

radiation at Fairbanks during clear weather, including coudiness up to 2/10;

these are especially useful here because they are based specifically on data

obtained in Fairbanks during 1936-1938 as follows:

Number of observations		Temperature range (^{o}C)	Formula, units cf Q are ly min^{-1} T is temperature ^{o}C
(a)	358	-1 to -44	$Q = 0.087 + 0.0012\ T$
(b)	222	-20 to -40	$Q = 0.105 + 0.0018\ T$

Here, we maximize the outgoing radiation by using formula (b) for the temper-

ature range -20 to -40C. The total pond area is 2.6×10^8 cm^2, but during

[*]A good summary, including a treatment of net fluxes from cloud tops and bases
is given by Haltiner and Martin (1957, pp. 128-132).

winter half is open water, and half is frozen with a snow cover on the ice.

Assume temperature of $+ 2^{\circ}C$ as an average for the open water area and $-40^{\circ}C$ for the snow cover. Then for the open water half of the pond $(1.3 \times 10^8 \text{ cm}^2)$

$$Q = 0.105 + 0.0036 = 0.1086 \text{ cal cm}^{-2} \text{ min}^{-1}$$
$$= 20.3 \times 10^9 \text{ cal day}^{-1},$$

and for the snow covered half

$$Q = 0.105 - 0.062 = 0.043 \text{ cal cm}^{-2} \text{ min}^{-1}$$
$$= 8.05 \times 10^9 \text{ cal day}^{-1}$$

Thus, the total loss by radiative cooling for clear sky, including up to 2/10 cloud cover, is about 28.35×10^9 cal day^{-1}. This is a maximum value and can be expected to decrease sharply to a negligible amount when a cloud of ice fog forms over the pond. However, even this maximum amount is only slightly over 5% of the total and leaves 490×10^9 cal day^{-1} to be lost by evaporation. During ice fog conditions the evaporative heat loss approaches the maximum value of 518×10^9 cal day^{-1}.

North power plant, Ft. Wainwright

The rate of discharge, sprayed through nozzles, into the cooling pond is 236 liters of water per second, or 20.4×10^9 cm^3 day^{-1}, at $15^{\circ}C$. The same amount is taken into the plant at $5^{\circ}C$, so the net change in temperature is $10^{\circ}C$ and the heat loss is 204×10^9 cal day^{-1}. If we use Wexler's formula for net radiative heat loss as above we obtain $Q = 1.086$ cal cm^{-2} min^{-1}. The area of the pond is 2.42×10^6 cm^2, so the radiative heat loss is 3.78×10^9 cal day^{-1}, but this is only 1.8% of the total and will decrease as ice fog forms over the pond. Therefore the evaporative heat loss during ice fog conditions will approach the maximum value of 204×10^9 cal day^{-1}.

Golden Valley Electric Association Power Plant

This plant discharges 440 liters of water per second, or 38×10^9 cm^3 per day, at a temperature of 15°C into Noyes Slough. The water comes from wells and is not recycled, and it cools to 0°C and eventually freezes at a distance varying from 4 to 7 km downstream from the outlet (Fig. 8). Since the temperature change is 15°C, the net cooling in the slough is then 570×10^9 cal day^{-1}. Because of the large bottom area, let us assume the relative conductive loss to be twice that of the South Power Plant at Ft. Wainwright, i.e. 0.2% of the total or 1.1×10^9 cal day^{-1}. The open water area averages about 3×10^8 cm^2, so clear-weather radiative heat loss is about 47×10^9 cal day^{-1}. This is about 8.25% of the total, and, as before, it represents the clear-water radiative heat loss so it will decrease as ice fog forms.

Municipal Utilities Power Plant

The cooling water discharges into the Chena River at a rate of 284 liters sec^{-1}, or 24.5×10^9 cm^3 day^{-1} at 15°C. As in the case of the G.V.E.A. plant the water is not recycled; it cools to 0°C and freezes in the river. The total heat output is 368×10^9 cal day^{-1}. The open water area is about 1.5×10^8 cm^2 so the clear-weather radiative cooling rate is about 24×10^9 cal day^{-1} or about 6.5% of the total. This case is a bit more complex than the others because some heat is lost by turbulent mixing with the Chena River. The rate of heat discharged by cooling water is 65% of that from the G.V.E.A. plant, but the open water area maintained by it is 50%. This difference can be accounted for if 15% of the heat from M.U.S. cooling water is dissipated through mixing with cold water of the Chena River. There is no such mixing in the case of the G.V.E.A. Power Plant because during winter it constitutes the only source of water (aside from unmentionable raw sewage which is added downstream) for Noyes Slough. Thus, in summary, the amount of heat dissipated
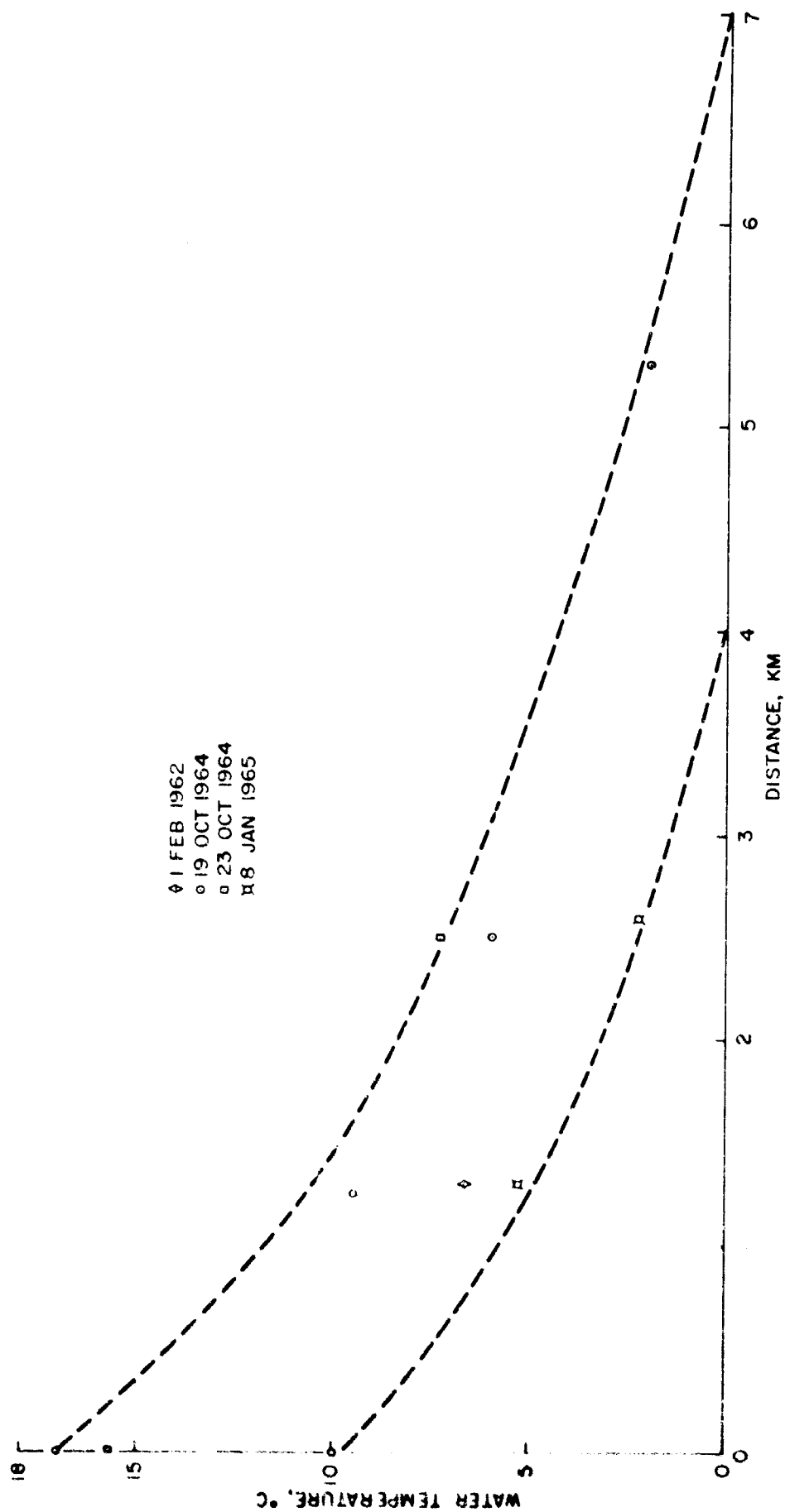
Fig. 8. Water temperature in Noyes Slough down-stream from GVEA power plant. Cooling water from the power plant is discharged into Noyes Slough at a rate of 440 liters per second at 15°C. The dashed curves are envelopes of maximum and minimum water temperatures in the slough based on the plotted data points. In particular, it is worth noting that the observation made on 1 Feb. 1962 followed the very cold weather shown in Fig. 1.

from cooling waters of the MUS plant is: 55×10^9 cal day^{-1} by mixing in the river, 313×10^9 cal day^{-1} by evaporation during ice fog conditions, and 289×10^9 cal day^{-1} by evaporation during clear-weather.

University Heating Plant

The cooling waters discharge at about 3.2 liter sec^{-1} or 0.3×10^9 cm^3 day^{-1}. The net cooling is 15°C so the heat loss is 4.5×10^9 cal day^{-1}. The majority of this heat is lost by evaporation and a conservative 5% deduction for other processes leaves the evaporative heat loss at 4.3×10^9 cal day^{-1}.

Summary

A	B	C	D	E	F	G	HI		JK	
							H	I	J	K
23	Ft.W.N.	236	15	5	10	204	200	204	333	340
24	Ft.W.S.	600	15	5	10	518	490	518	816	865
25	G.V.E.A.	440	15	0	15	570	522	569	870	949
26	M.U.S.	284	15	0	15	368	289	313	482	522
27	U. of A.	3.2	15	0	15	4.5	4.3	4.5	7.2	7.5
Totals		1563.2				1664.5	1505.3	1608.5	2508.2	2683.5

A   Point on Map
B   Power Plant
C   Discharge Rate of cooling water liters sec^{-1}
D   Initial Temperature of discharged cooling waters °C
E   Final temperature °C
F   Temperature difference ΔT°C
G   Heat loss cal day^{-1} x 10^9
HI   Evaporative heat loss cal day^{-1} x 10^9 during
   H   Clear weather
   I   Ice fog
JK Water released to the atmosphere by evaporation (g x 10^6 per day)
   J   Clear weather
   K   Ice fog

Miscellaneous Sources

There are many small leaks of moisture to the atmosphere in urban areas, these are difficult to evaluate. Examples are the moist air discharge from laundries, but air leaks from other buildings where the air is not considered moist must also be included. For example, air in a building with temperature of 25°C and 15% humidity contains 3.46 g H_2O per m^3. This corresponds to

saturated air at temperature of about -4 or -5°C (with respect to ice or water respectively); at -45°C this air would be 51 times oversaturated with respect to ice. When the door of such a building is opened during cold weather, there is a loss of warm air to the outside and the excess moisture contained in it must condense. Examples of miscellaneous sources will be followed by an estimate of the overall magnitude of this source.

The Fairbanks sewage treatment plant

This plant was put into operation in 1963. It discharges warm water (10°C) into the Chena River at a rate of 4.3×10^9 cm^3 day^{-1}. The water cools to 0°C in the river with a loss of 43×10^9 cal day^{-1}, which is sufficient to maintain an open water area of about 5×10^5 cm^2. If 20% of this heat is dissipated by mixing with the river water (as in the case of M.U.S. cooling water) together with radiation and conduction, we still have 34×10^9 cal day^{-1} to be lost by evaporation. This releases 56.6×10^6 g H_2O to the atmosphere daily.

In addition to this steady moisture input, the sewage treatment plant burns solids on Monday and Friday of each week. The furnace burns for 15 hours each time, using about 300 gallons (1000 Kg) of fuel oil. Water released from the fuel alone is 1330 Kg, and the amount of water originally in the solids, combined with that released from them during combustion is more than twice this amount; a conservative estimate would be 3×10^6 g H_2O. We may ignore the water put into the air from combustion of the oil itself since it is presumably included in the combustion analysis already made. In summary, during ice fog conditions the sewage treatment plant puts water into the air at a rate of 56.6×10^6 g H_2O per day, and twice each week this figure is increased, by the burning operation, to about 60×10^6 g H_2O per day.

University mine tunnel

The School of Mines at the University of Alaska has a mine under the campus. The entrance to this mine is under College Road at the east end of the new university heating plant. The mine tunnel is damp. To retard rotting of

the timbers, a fan was installed to blow warm, dry air from a utilidor near the old power plant into the mine tunnel. This air cools and absorbs moisture from the damp walls of the mine and is eventually exhausted to the outside air at the mine entrance. During cold weather this is a noticeable source of moisture as can be seen by the cloud formed, and by the following conservative estimate.

The area of the fan is about 0.2 m^2 and it moves air from the utilidor into the mine at a minimum speed of 10 m sec^{-1}, which results in a flow of $2 \text{ m}^3 \text{ sec}^{-1}$. The utilidor air has a temperature of $25^{\circ}C$ and 5% relative humidity. Thus it contains $1.5 \text{ g } H_2O \text{ m}^{-3}$, so the rate of moisture flow through the fan is $2.30 \text{ g } H_2O \text{ sec}^{-1}$, or $2 \times 10^5 \text{ g } H_2O$ per day. When the air leaves the mine tunnel its temperature is about $-10^{\circ}C$ and it is saturated, i.e., it contains $2.4 \text{ g } H_2O \text{ m}^{-3}$. This means that the water absorbed from the damp mine tunnel is about the same as the amount originally contained in the warm dry air which entered through the fan. And, the net discharge of water vapor from the mine tunnel is at least $4 \times 10^5 \text{ g } H_2O$ per day.

People and others that breathe

There are 30,000 people and about 2000 dogs in the Fairbanks-Ft. Wainwright area. The air that they exhale is saturated with water vapor at a temperature of $35^{\circ}C$. The dogs breathe at an average rate of 5.2 liters min^{-1} when they are resting (Altman and Dittmer, 1964, p. 220); this provides $7.5 \times 10^6 \text{ cm}^3$ of air per day which contains 39.63 g m^{-3} per dog, so the total moisture put into the air by 2000 Canis familiaris is at least $6 \times 10^5 \text{ g } H_2O$ per day. This is a conservative estimate because all of the dogs don't rest all of the time.

The people must be separated into two groups: 20,000 males and 10,000 females. At rest the tidal volumes are 750 cm^3 for males and 339 cm^3 for females but the rate of respirations is 11.7 per minute for both groups (Altman and Dittmer, 1964, p. 220). These rates increase with activity. For example,

28

in males the respiration and tidal volume are 17.1 per minute and 1673 cm^3 respectively for light work, and 2 per minute and 2030 cm^3 respectively for heavy work. As an overall average for an order of magnitude calculation, assume respiration rates of 15 per minute for both males and females and tidal volumes of 1500 cm^3 and 350 cm^3 respectively; this results in 28.8 x 10^6 g H_2O per day breathed into the air by Homo sapiens in the Fairbanks-Ft. Wainwright area.

Water is also put into the air by perspiration from the entire body surface. This continuous process is insensible except when the rate increases to the extent that it takes the liquid form of sweat. According to Best and Taylor (1952, p. 54) perspiration releases 70% as much moisture as is exhaled from the lungs. However, Kuno (1956, pp. 27-28) shows that the perspiration loss generally exceeds the loss by respiration and, in any event, it can always be taken as at least equal to it. Therefore, the moisture output from breathing by people can be safely doubled, to give a combined perspiration and respiration loss of about 58 x 10^6 g H_2O per day.

The fact that animals create their own clouds of ice fog has been long recognized and used to the advantage of hunters. Stefansson (1913, p. 235) describes an occasion when the temperature was..."considerably below -50°F"... during a hunt for caribou...

> "There was not a breath of air stirring...... There were
> only a few clearings in the woods, but whereever the animals
> were you could discover their presence by the clouds of
> steam that rose from them high above the tops of the
> trees.
>
> There are few things one sees in the North so nearly
> beyond belief as certain of the phenomena of intense
> cold as I saw and heard them that day. It turned out
> that the woods were full of caribou, and whereever a band
> was running you could not only see the steam rising from it
> and revealing its presence, even on the other side of a
> fairly high hill, but, more remarkable still, the air was
> so calm that where an animal ran past rapidly he left behind
> him a cloud of steam hovering over his trail and marking
> it out plainly for a mile behind him."

The following statement is from Carey (1964):

"January 1957 was a particularly cold winter, and I was trapping marten in the upper Kuskokwim, not far from the SW corner of McKinley Park. Several thousand caribou were wintering in the area in scattered small bands. On several occasions when I chanced upon these caribou along my trails. I observed that they were surrounded by a pall of ice fog, especially when the temperature was $-45^{\circ}C$ or lower. On one occasion I stood on a low ridge and noted a cloud of ice fog hanging in and over small spruce in a valley a mile or so distant. This was generated by a small band of caribou, perhaps 15, feeding there.

I have also noted moose in an aura of ice fog when the temperature is low.

On numerous occasions I have seen dog teams leave a trail of ice fog behind them on the trail. This is best observed when traveling directly away from the sun. When one turns and looks back directly into the low sunlight the trail will be hazy with ice fog."

Such observations clearly indicate the extreme stability of the lowest layers of air during cold weather, and how little moisture is required to make ice fog.

The many other miscellaneous sources of moisture will not be analyzed in detail, also all wood-burning fires are ignored. A minimum, but hopefully reasonable, estimation of all of these sources will be made by considering the university mine tunnel, the sewage treatment plant, and the total moisture loss from people by the processes discussed above.

Summary of Man-made Water Sources for the Fairbanks Atmosphere

I. Combustion Products	$\times 10^6$ g H_2O per day
(a) Gasoline	124
(b) Fuel oil	202
(c) Coal, domestic	207
	(Sub total = 533)
(d) Coal power plants	760
	(Sub total = 1293)
II. Cooling water from power plants	2600
III. Miscellaneous, (leaks from steam lines, houses, university mine shaft, sewage, people and animals breathing, etc.)	170
Total	4063 $\times 10^6$ g H_2O per day

For calculations in this paper the total input rate will be rounded off to 4100 $\times 10^6$ g H_2O per day.

SOURCES OF POLLUTION, II PRODUCTS OTHER THAN WATER

Electrical Conductance and Particulates

The small ice crystals which make up ice fog are often associated with impurities. This is especially true of those formed from combustion products. A very simple but effective way to investigate this is to use the snow cover as a collection filter. The snow cover forms before, and remains until after, the period of worst ice-fog air pollution conditions. At the end of March and in early April of 1963, 1964 and 1965, 68, 36, and 12 samples, respectively, were taken from the snow pack at selected points in and around Fairbanks. These were channel samples from top to bottom of the snow cover. Measurements of the specific electrical conductance were made on each melted snow sample, the values range from less than 10 μ mho in the outlying areas to greater than 100 μ mho in the city as summarized in Figures 9, 10, and 11.

Two samples were taken at each of the 36 sites in 1964; one set was sealed in specially prepared bottles and shipped to Mr. Wayne Hamilton of the University of Miami for analysis with equipment designed by himself and Dr. Henri Bader for analysis of particulate material in polar snow. All particles smaller than 10 μ diameter were counted and grouped into eleven class intervals. Material coarser than 10 μ is being treated separately, the results, including chemical analyses will be presented in a separate paper. The particulate content smaller than 10 μ diameter is expressed in terms of the volume of solid matter per unit volume of the melt water obtained from the sample. Figure 12 is a contour map showing total values and representative histograms of effective particle diameters are shown in Figures 13, 14, and 15.

Particulate counts from outlying areas, which are relatively unpolluted show peak frequencies in the smallest end of the size spectrum. Examples are samples 21 and 54 (Fig. 13). Sample 54 contains slightly over five times

APRIL 1963
SPECIFIC ELECTRICAL
CONDUCTANCE
μ mho cm^{-1}
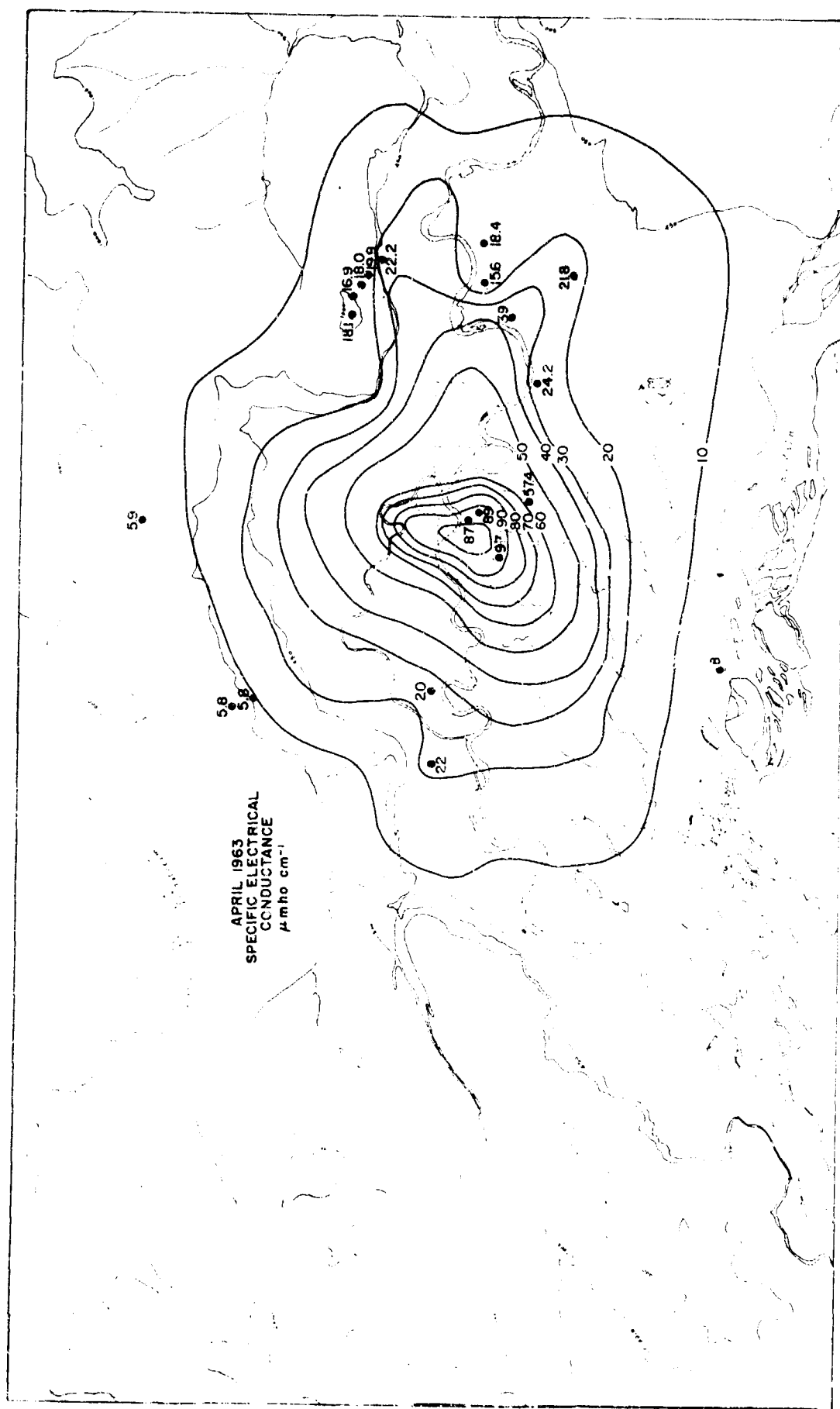
Fig. 9. Measurements of specific electrical conductance (μ mho cm^{-1}) were made on melt water derived from snow samples taken at selected points in and around Fairbanks. The snow pack was sampled from top to bottom at each point. No significant melting had occurred prior to sampling in April 1963.
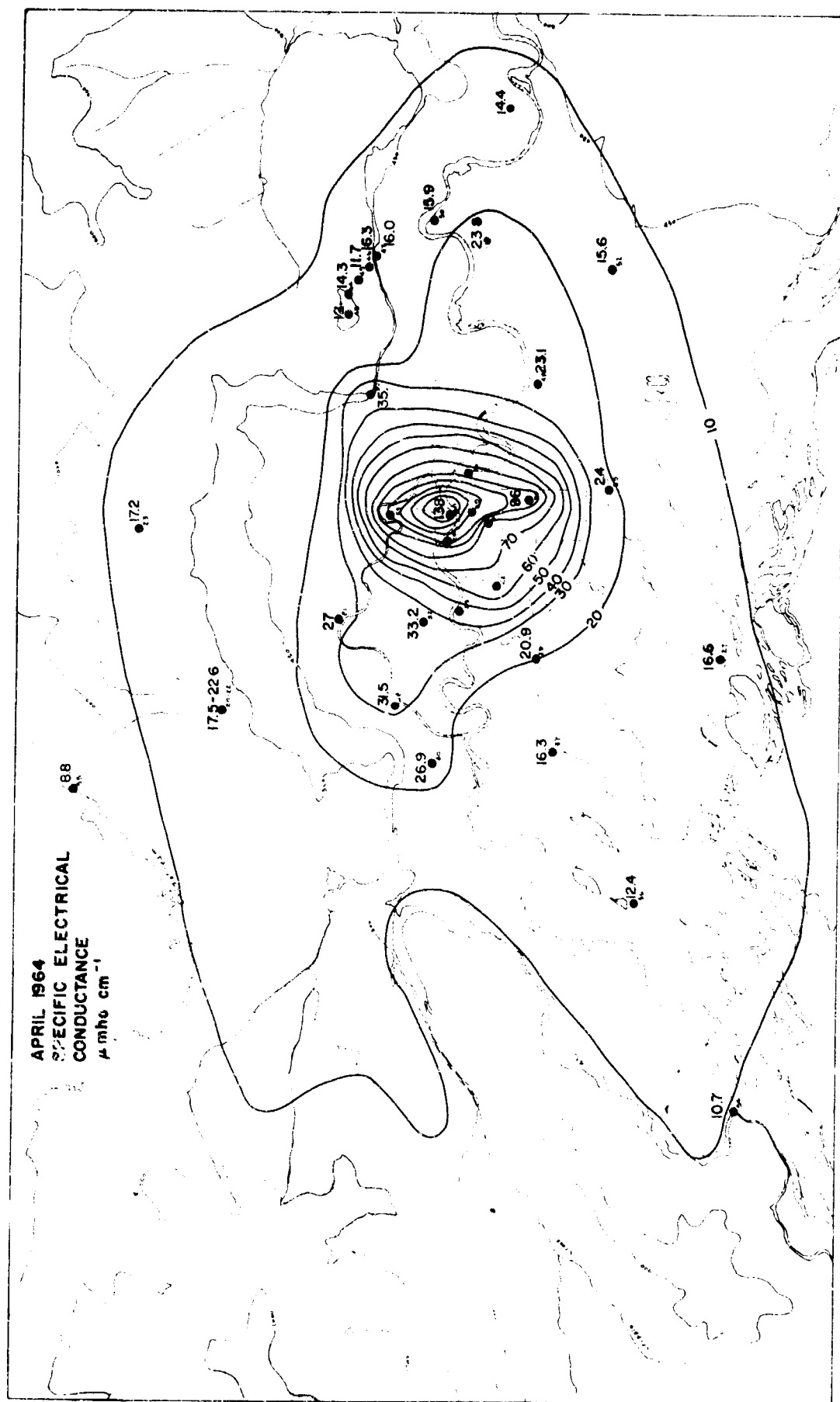
Fig. 10. Specific electrical conductance (μ mho cm^{-1}) measurements made in April 1964 in the same way as described in Fig. 9.
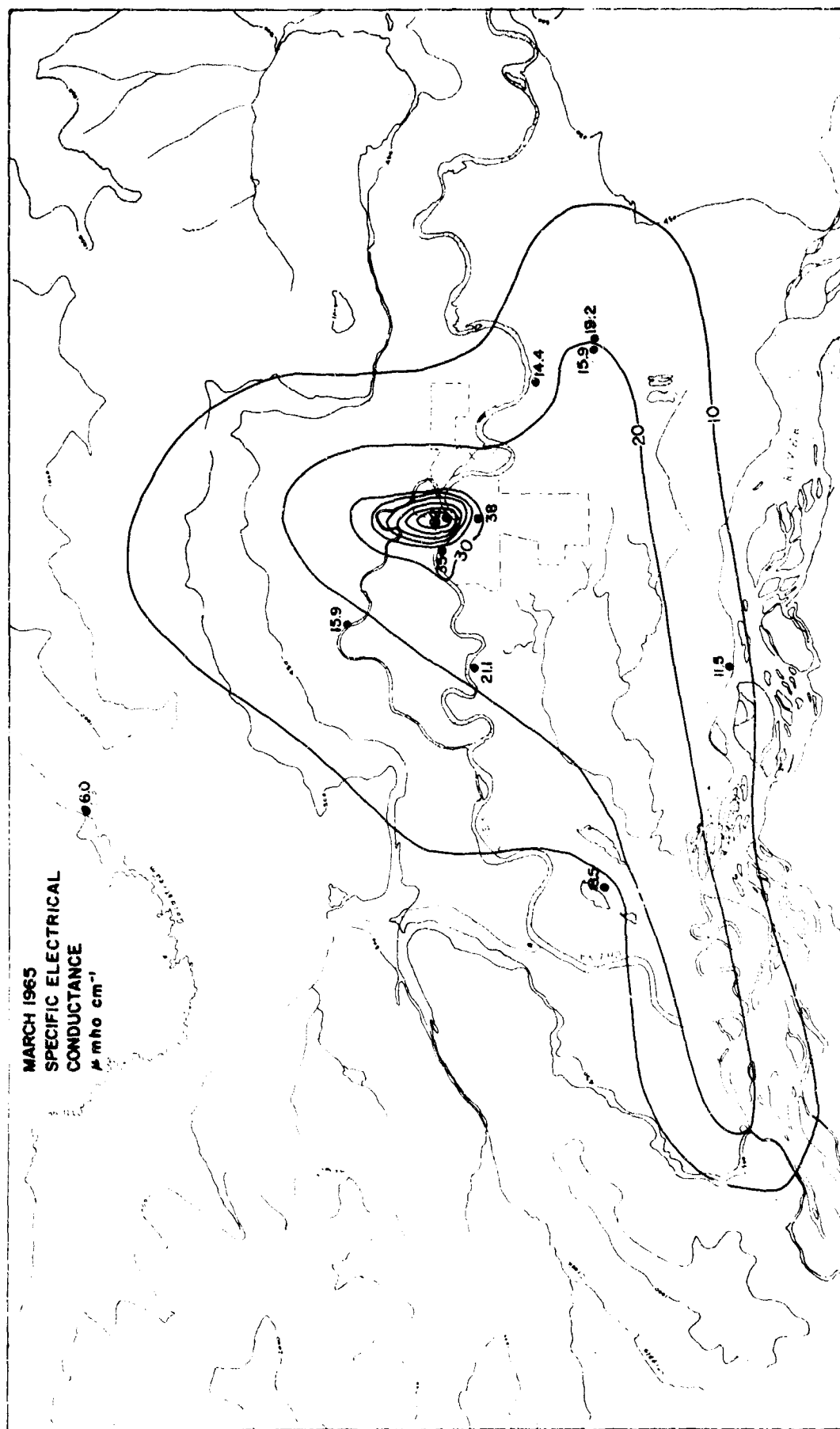
Fig. 11. Specific electrical conductance (μ mho cm^{-1}) measurements made in March 1965 in the same way as described in Fig. 9. An unusually early warm spell produced some melting prior to sampling in 1965. This is most likely the reason for the lower conductance values (see pp. 34-35).
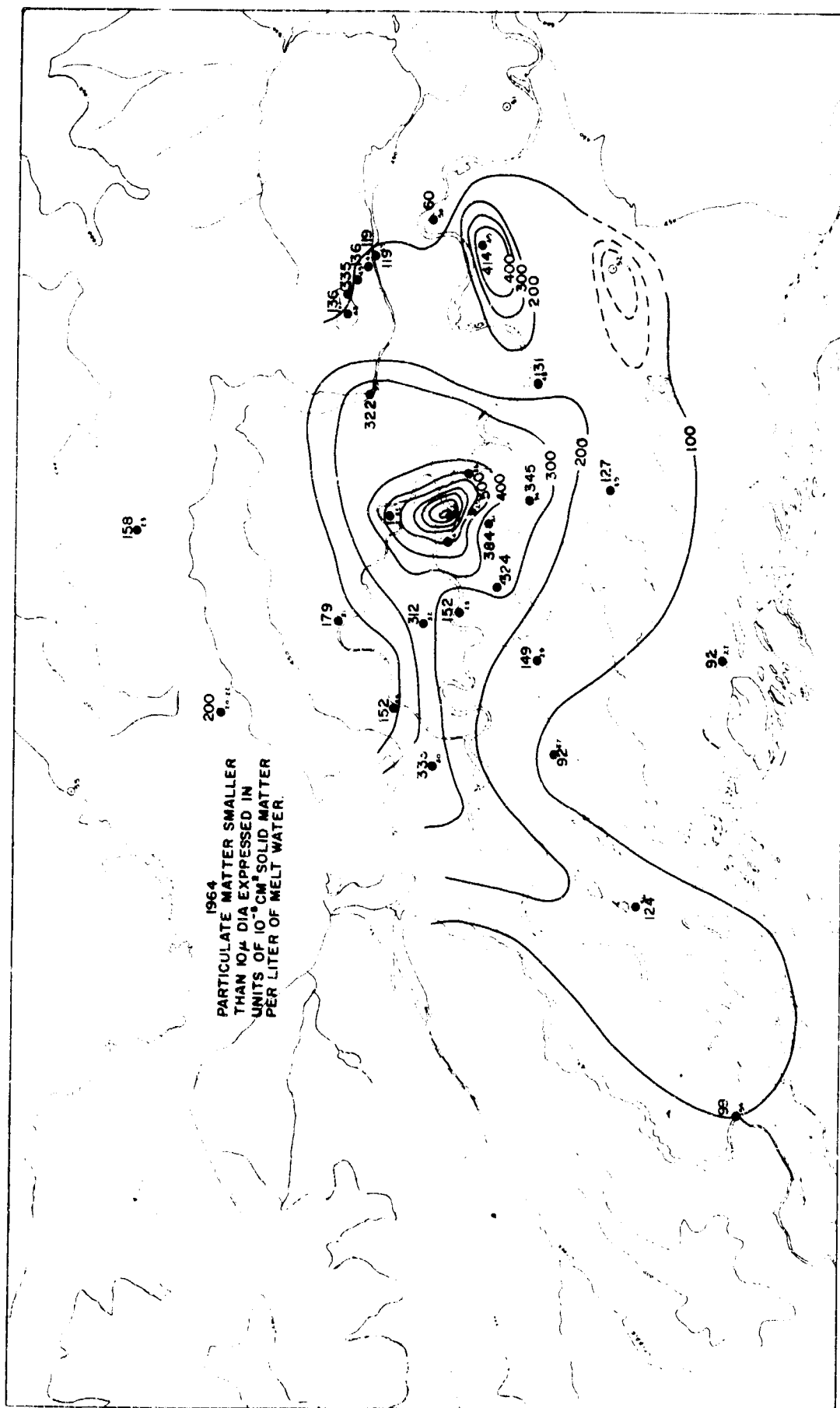
Fig. 12. Particulate matter obtained from snow samples taken concurrently and at the same places as the 1964 conductance samples. Only the fraction of particles smaller than 10 μ diameter are included in this analysis.
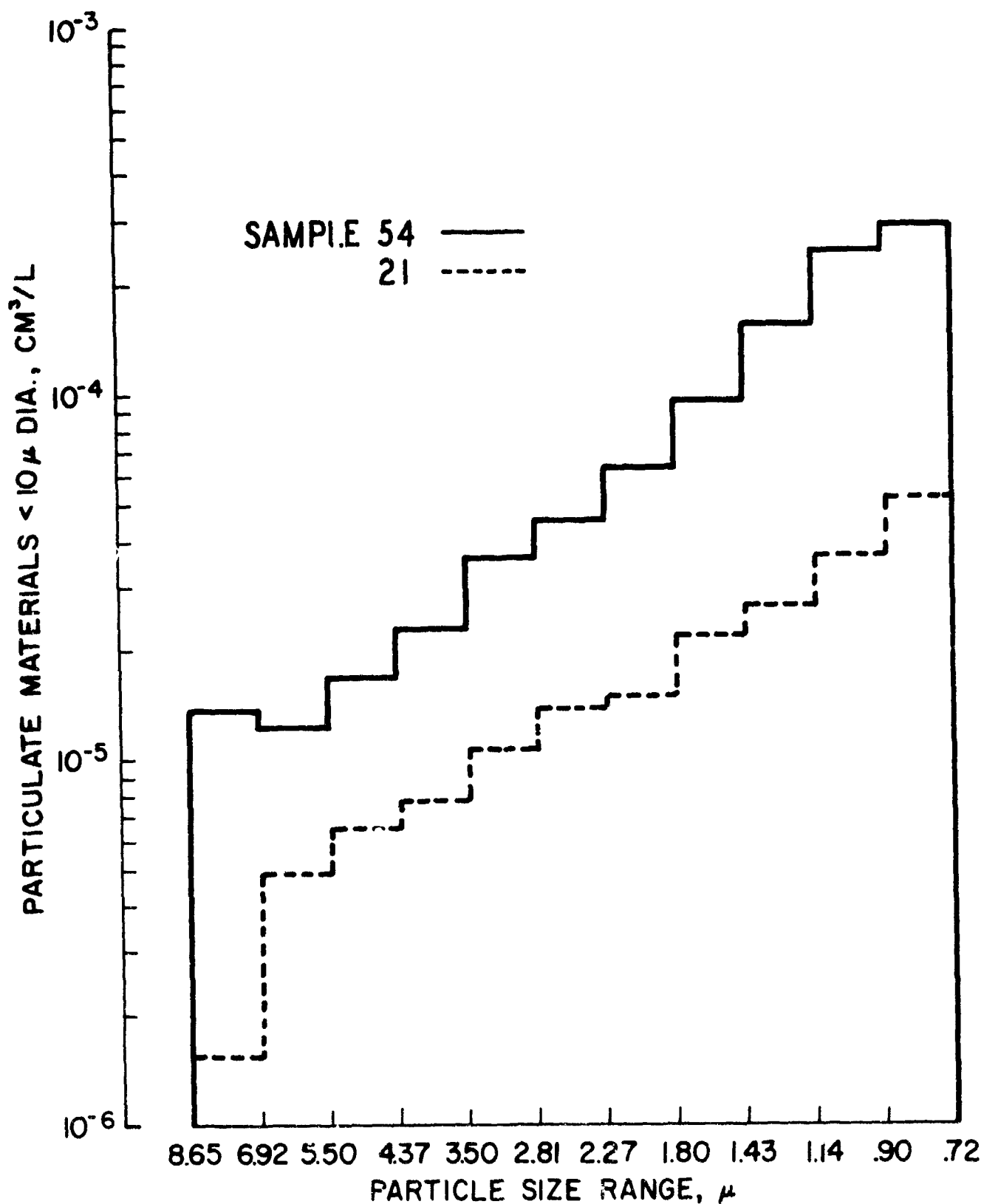
Fig. 13. Histograms of particles less than 10 μ diameter from samples 21 and 54. Sample 54 was taken downstream in the katabatic flow across the city. Sample 21 was obtained from a point unaffected by air drainage across Fairbanks and 75 m higher than sample 54. These samples are from fairly unpolluted areas and show only a single maximum which lies at the smallest end of the size spectrum.
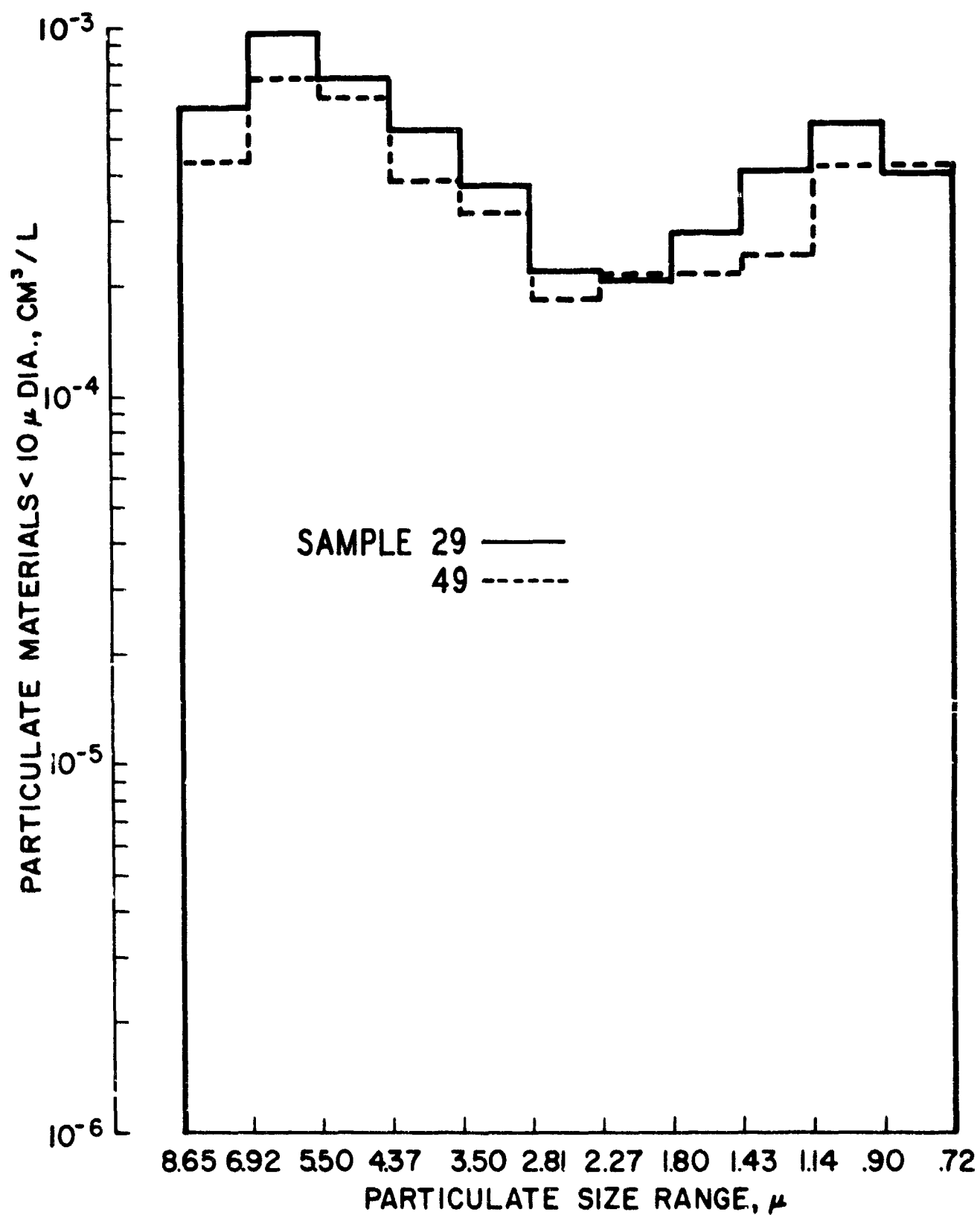
Fig. 14. Histograms of particles less than 10 μ diameter from samples 29 and 49. These are typical of samples from mildly polluted areas in that they show two maxima, one at the smallest end of the size spectrum and one in the 5 to 6 μ range.
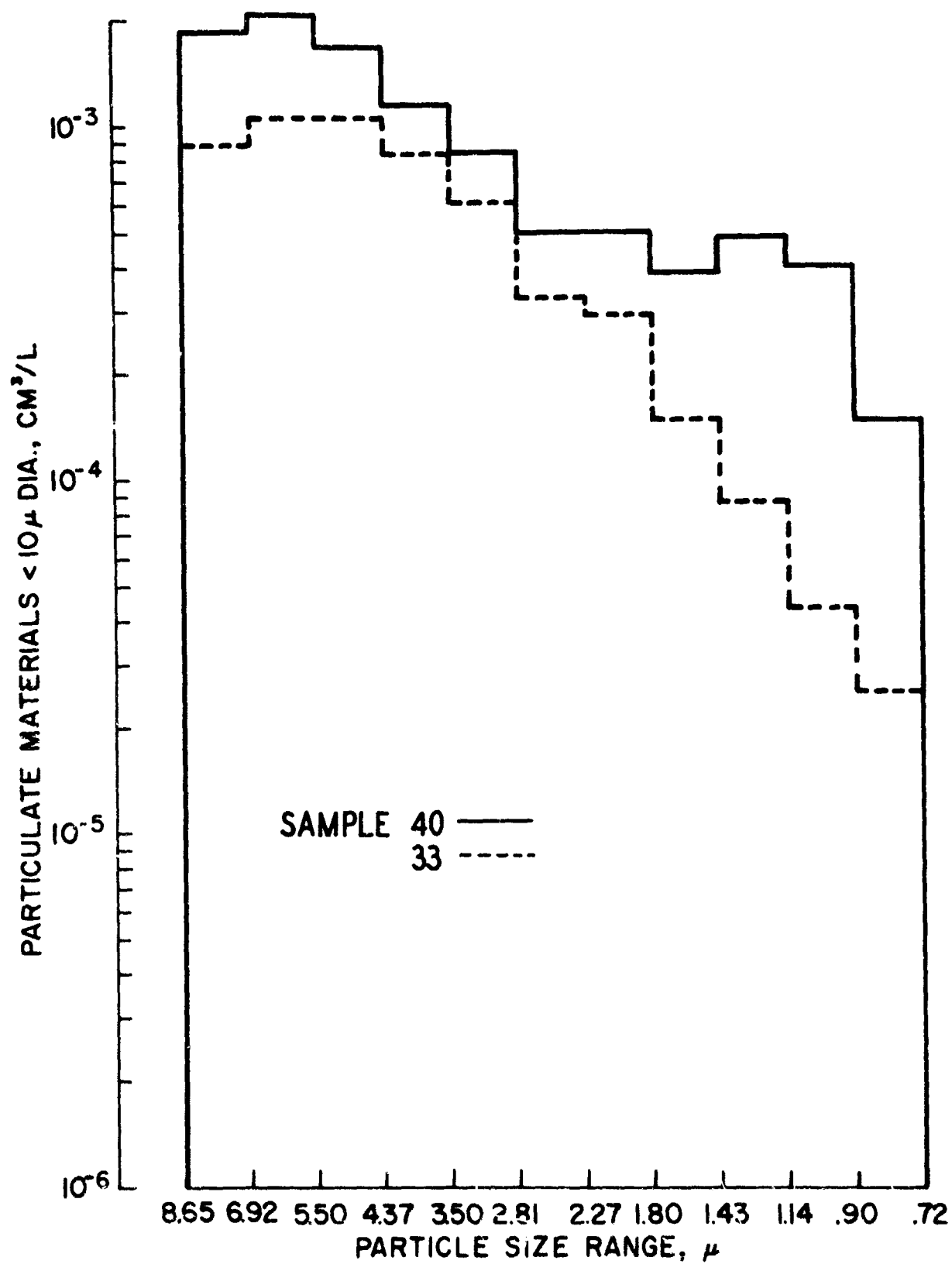
Fig. 15. Histograms of particles less than 10 μ diameter from samples
33 and 40 which are from extremely polluted areas and show a single
maximum in the coarsest size range (see p. 32 and Chapter VII).

more particulate matter than does sample 21, 98.8×10^{-3} cm^3 per liter and 19.4×10^{-3} cm^3 per liter respectively. Sample 54 was taken downstream of t! katabatic flow across the city. Sample 21 was obtained from a point 75 m higher in altitude than sample 54, and out of the region affected by drainage from Fairbanks.

Most samples in polluted areas show two maxima, one at the smallest end of the spectrum and one in the 5 to 6 μ range. Examples are samples 29 and 49 in Figure 14.

Some samples from extremely polluted areas, where dirt is easily visible in the snow and melt water derived from it, show only one maximum and it lies in the coarsest size range. Examples are samples 33 and 40 in Figure 15. The relative lack of particulates in the fine size range of sample 33 is partly due to some of the finer particles being lost while filtering out the particles greater than 10 μ diameter. It may also be partly due to upward air movement over heated parts of the city. This aspect of the problem will be treated in more detail in the section on air structure in the inversion layer.

The 1964 data on particulate matter less than 10 μ diameter and electrical conductance of the melt water are combined in Figure 16. The samples are separated into four groups:

Group	Particulate matter (<10 μ diam) $Q \times 10^{-3}$ cm^3 ℓ^{-1}	Specific electrical conductance, K μ mho cm^{-1}
I	$150 < Q < 1000$	$40 < K < 140$
II	$300 < Q < 425$	$10 < K < 40$
III	$100 < Q < 200$	$10 < K < 35$
IV	$15 < Q < 100$	$10 < K < 25$

The boundaries between groups are arbitrary. However, from Figure 16 we see that samples with specific conductance values greater than 40 μ mho cm^{-1} are, without exception, from the downtown area and include all of the dirtiest
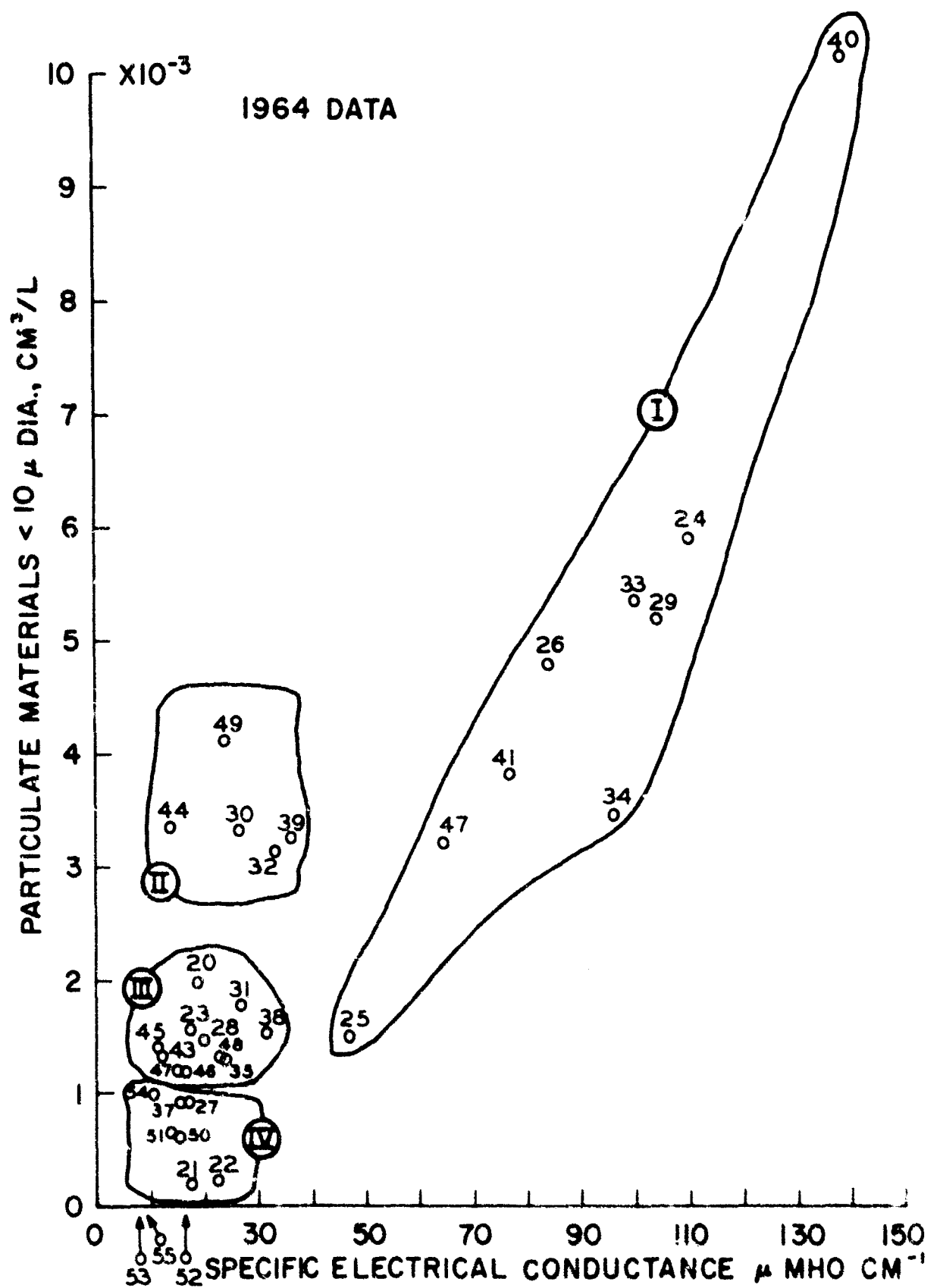
Fig. 16. Particulate material plotted against specific electrical conductance values for the 1964 data (see p. 32).

samples. At the other extreme, the cleanest samples in group IV are all well-removed from the city and have conductance values less than 25μ mho cm^{-1}.

The maximum values of electrical conductance are found in the downtown business district of Fairbanks. They decrease sharply to less than half of their maximum values within a 2 km radius of the corner of second and Cushman streets. This well-defined sharp decrease in values away from the center of town is not as apparent in the case of particulate material (Fig. 12).

The values of electrical conductance discussed so far pertain to melt water derived from the entire snow-pack. During the winter of 1964-1965, a collecting stand with 1 m^2 of clear plastic was placed near the corner of Fourth and Cushman streets in an undisturbed empty lot. The objective was to collect undiluted ice fog residue. Thus, periods of snowfall were eliminated and the sampler was set up only during ice fog events. Out of six attempts two were successful, one produced 80 and the other 98 g H_2O, with .38 g and .51 g solid material respectively, ie about 0.5% in each case. The ice fog deposit had a grey color due to carbonaceous material which proved difficult to wash from the plastic sheet. The specific electrical conductance for one sample was 730 to 770 μ mho cm^{-1} and 1600 to 1760 μ mho cm^{-1} for the other.* In summary, the electrical conductance of water derived from the complete undisturbed snow-pack in downtown Fairbanks is an order of magnitude greater than values obtained from the snow-pack of outlying areas surrounding Fairbanks. Similarly the undiluted material, precipitated solely from ice fog, has conductance values an order of magnitude greater than measured in the downtown snow-pack.

The electrical conductance is, of course, due to free ions in the melt water. But the source of these ions, and their location in, or on, the ice

*The latter sample had 5 small drops of yellow oil on the plastic sheet. The oil was separated from the residue before analysis. The origin of the oil drops is unknown, but they were excluded from the test sample and probably did not contribute much to the conductance.

crystals is not immediately clear. They could be associated with the crystal nuclei which are found in each crystal, or they could be concentrated on the crystal surfaces. The latter alternative seems most likely according to the following reasoning.

The ice crystals form by freezing of supercooled water droplets--or by freezing of a supercooled liquid layer on a foreign particle. In any case whether a droplet per se exists or whether it is a liquid surface on a solid object the phenomenon is the same, ie, nucleation and crystallization of supercooled water.[*] The nuclei remains imbedded in the crystal but as this crystal continues to grow impurities are excluded, as much as possible, and pushed toward the crystal boundaries. This tends to concentrate ions on crystal surfaces. The boundary region between ice crystals has an absorption coefficient for infrared radiation many times greater than that for the ice crystals away from the boundaries (Plyer 1924, 1926). This causes preferential melting to occur first at the grain boundaries, and gives rise to the commonly observed delineation of grain boundaries when ice begins to melt. Since this is the region where impurities are concentrated during crystallization, it is reasonable to expect that the very first melt water will remove a disproportionally large number of ions, and therefore have higher electrical conductance than subsequent melt water. The 1965 measurements are compatible with this explanation.

During 1965 the sampling program was nearly ruined by an unusually early heat wave in March[**] which produced some melting in the snow pack. This fact, together with the observation that the 1965 conductance values are only 40 to 50% of those measured during the two preceding years, suggests that the first melt water (which was too small in quantity to be determined by calculation of

[*]The problem of nucleation and freezing of supercooled water will be discussed in Appendix B on nucleation.

[**]The occurrence of this warm spell is the reason why only 12 samples were collected in 1965.

34

water content from depth-density measurements) removed up to 50% of the ions present in the total melt water derived from the snow pack. An investigation of the variation in conductance as snow melts is planned.

The particulate material, although concentrated in certain areas[*], is abundant throughout the entire Fairbanks - Ft. Wainwright area. The same is true of the small nuclei (less than 0.01 μ diam) as measured with the small particle detector, type CN, a modification of the Nolan Pollack counter; these nuclei counts are summarized by Kumai (1964). However, the ion concentration is more clearly defined and restricted to the downtown business district than is the overall particulate concentration.

Combustion Products

The combustion processes which were examined as sources of water vapor are also sources of other products.

Carbon dioxide

The calculation summarized on page 19 show the input rate of CO_2 to be 4.1×10^9 g per day.

Sulfur

The sulfur content of fuels varies widely.

> "Crude oil may contain small quantities of impurities,
> of which sulfur is the principal undesirable con-
> stituent. Sulfur in oil generally occurs as sulfides,
> mercaptans, polysulfides and thiophenes. A substantial
> portion of the domestic crude in the U.S. contains
> over 0.5% sulfur, and perhaps 10% of the crude contains
> about 2% sulfur..." (Elkin, H. F., 1962, p. 143).

U.S. Government specifications set the maximum allowable sulfur content for gasoline and fuel oil at 0.25%. Commercial sources in Fairbanks report gasoline sulfur contents varying from 0.05% to 0.13%. The average value used for calculations in the Los Angeles area by Magill and Benoliel (1952 p. 1349) was 0.13%. Since this is well below the amount contained in some fuel oils

---

[*]The largest particle sizes are associated with the burning of coal which causes obviously dirty snow in certain parts of Fairbanks.

and in military gasoline it will be used as an overall value to estimate the sulfur input from the gasoline and oil summary on page 19. The resulting figure is 3.15×10^5 g sulfur per day from combustion of gasoline and fuel oils.

The coal burned in the Fairbanks - Ft. Wainwright area comes from Healy, Alaska; according to Selvig and Ode (1957) its average sulfur content is 0.28%. Using the summary on page 19, we get input rates of 8.54×10^5 g sulfur per day from domestic sources and 31.3×10^5 g sulfur per day from power plants.

The total sulfur input to the atmosphere from combustion of coal, fuel oil and gasoline is 4.3×10^6 g per day. Since sulfur in the air is mainly present as SO_2, we may express the total output of sulfur oxide as 8.6×10^6 g per day.

Lead

Antiknock compounds are added to gasolines. Among the compounds used are:

1. Tetraethyl lead (TEL), $Pb(C_2H_5)_4$

2. Diphenyl-dimethyl lead, $Pb(C_6H_5)_2(CH_3)_2$

3. Diphenyl-diethyl lead, $Pb(C_6H_5)_2(C_2H_5)_2$

4. Dimethyl-diethyl lead, $Pb(CH_3)_2(C_2H_5)_2$

5. Methyl-triethyl lead, $PbCH_3(C_2H_5)_3$

6. Tetra-methyl lead, $Pb(CH_3)_4$

7. Iron carbonyl, $Fe(CO)_5$

8. Aniline, $C_6H_5NH_2$

Iron carbonyl has been used in Europe, but lead compounds are the cheapest, most effective, and most widely used. The extremely poisonous nature of tetraethyl lead is well known, and the care required in handling it has been emphasized for over 40 years (Midgley, 1925); however, all of the compounds listed are highly poisonous.

All lead compounds contain at least 3 halogen atoms for every lead atom. The halogens are added in an effort to prevent formation of lead oxide, which

is relatively non-volatile and causes trouble by fouling spark plugs etc.
Since tetrethyl lead (TEL) is the most commonly used additive a brief summary
of its properties is in order.

TEL consists of:

Compound	Per Cent of total	Formula Wt.	Weight contributed to solution
$Pb(C_2H_5)_4$	65%	323.45	210.00
$Br_2(C_2H_4)$	25%	187.88	46.90
$Cl_2(C_2H_4)$	10%	98.97	0.99
			267.89 Molecular wt. of solution

A simple calculation using the above data shows that the solution is 50% lead
by weight. The density of the TEL solution is 1.53 g cm^{-3}, so when the legal
limit of 3 m TEL is added per gallon we have 4.6 g per gallon; this results in
a net amount of 2.3 g Pb per gallon of gasoline. The amount of lead in gaso-
line used by the military may exceed this amount according to a Military
Specification dated 27 May 1963: MIL-G-3056B, Ammendment 2 in reference to
antiknock additives... "Metallic lead content not to exceed 3.17 g per gallon."
For purposes of computation we will assume a conservative 2 g Pb gal^{-1};
applying this to the summary for gasoline on page 19 we obtain a net input of
6×10^4 g Pb per day.

Halogens

From the above figures for TEL we see that 2 Br and 2 Cl atoms are
added for each Pb atom. The daily input of 290 moles of lead as calculated
above, demands 580 moles of Cl and Br, or 2.03×10^4 g Cl and 4.64×10^4 g Br
per day. The halogens do not always combine with lead as desired. Products
found in combustion chambers in addition to $PbBr_2$ and $PbCl_2$ include PbO,
$PbSO_4$, $PbO-PbBr_2$ and $PbO-PbSO_4$ (Obert,1950, p.290). Kumai (1964, p.25) shows

an electron microscope photo of PbO crystals in supercooled water droplets from automobile exhaust.

Summary

The daily input of pollutants other than water to Fairbanks-Ft. Wainwright atmosphere includes:

Compound	Daily input (Kg)
CO_2	4,100,000
SO_2	8,600
Pb	60
Br	46
Cl	20

The automobile combustion products listed above are probably the primary source of ions which contribute to the high electrical conductance values. Both the conductance values and the vehicle densities are greater in the downtown business district. Also, the potential for air pollution is aggravated during ice fog weather because many cars are left with engines idling for hours at a time in parking lots or at curbsides.

ECONOMIC GROWTH AND ICE FOG

So far we have discussed sources of pollution and estimated the quantities involved. No estimates of concentration of pollutants can be given without knowledge of (1) the volume of air which is available to hold these pollutants and (2) the rate of precipitation of the various pollutants. Before going into these aspects of the problem it is worthwhile to emphasize that the present rate of polluting the atmosphere in the Fairbanks area will increase. This is apparent from the steady increase in human activity which seems destined to continue.

The population growth is shown in Figure 17. The assessed valuations for real property in the city of Fairbanks are shown in Figure 17a. Inflation causes the curve to be steeper than if the dollar were stable, but even if one divides the 1964 valuation by three there is still an 8-fold increase in the 24 years between 1937 and 1964. Another growth index is the linear increase in number of telephone customers Figure 18, which still lags behind the demand for telephones. An especially important parameter is the number of vehicles registered in the Fairbanks area. Figure 19 shows that between 1948 and 1964 the number of vehicles registered in the Fairbanks area increased from 4000 to over 17,000. It is also important to note in this figure the decline in taxicabs from 174 to 48 during the same period. The latter observation indicates clearly that more private vehicles operate throughout the winter every year. This is partly the result of the headbolt heater, first marketed in 1948 and used in nearly all cars by 1950. Thus, the spread of ice fog has resulted from several interacting aspects of economic growth.

As the number of vehicles which operated through the winters increased, the Fairbanks traffic pattern spread. Minnie street was a dead end at Noyes Slough until 1953 when the Wendell Street bridge across the Chena River, and the Minnie street bridge across Noyes Slough were completed. This was followed by business establishments, and the area encompassed by ice fog rapidly increased to include all of the area from downtown Fairbanks to the north of Minnie Street.*

During at least the past five years, periods of low temperature have been associated with very thick ice fog in the downtown area (Fig. 36). The visibility is often less than 20 m at street level. This is in sharp contrast to the situation shown in Figure 20. This photo, taken in 1911 at -58°F (-50°C),** shows

ice fog from power plant and house chimneys but the street-level visibility is
*Thanks are due to Mr. Maury Smith, the Fairbanks "hometown reporter", for these historical comments. His home on Well St. was not encompassed by thick ice fog during the years 1939 to 1952, but since 1953 ice fog has been a nuisance.
**The temperature is verified by records from the University Experiment Station which show a high of -44°F (-42°C) and a low of -60°F (-51°C) for 24 Jan. 1911.
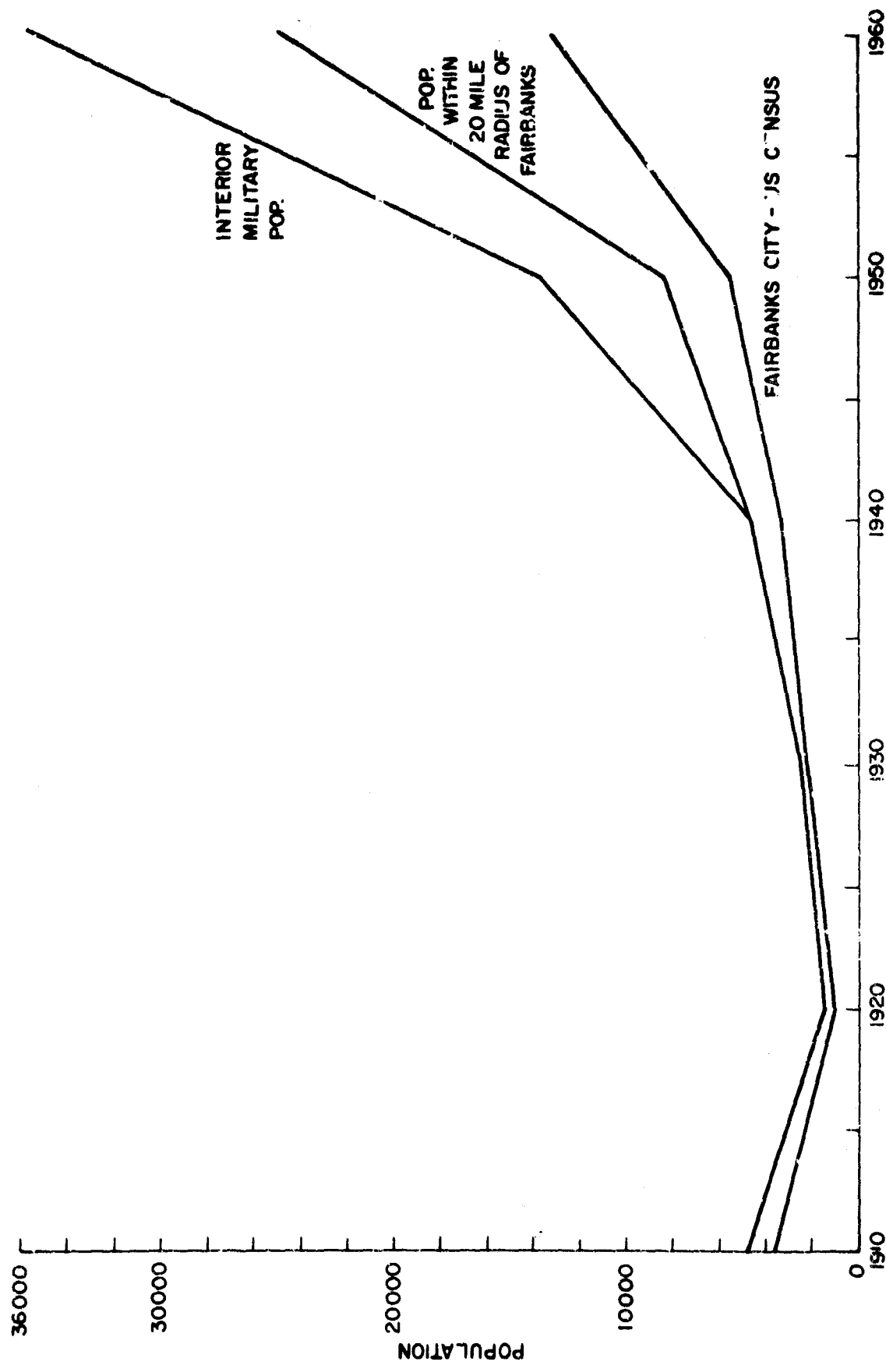
Fig. 17. Population of Fairbanks and vicinity, from U.S. Census records.
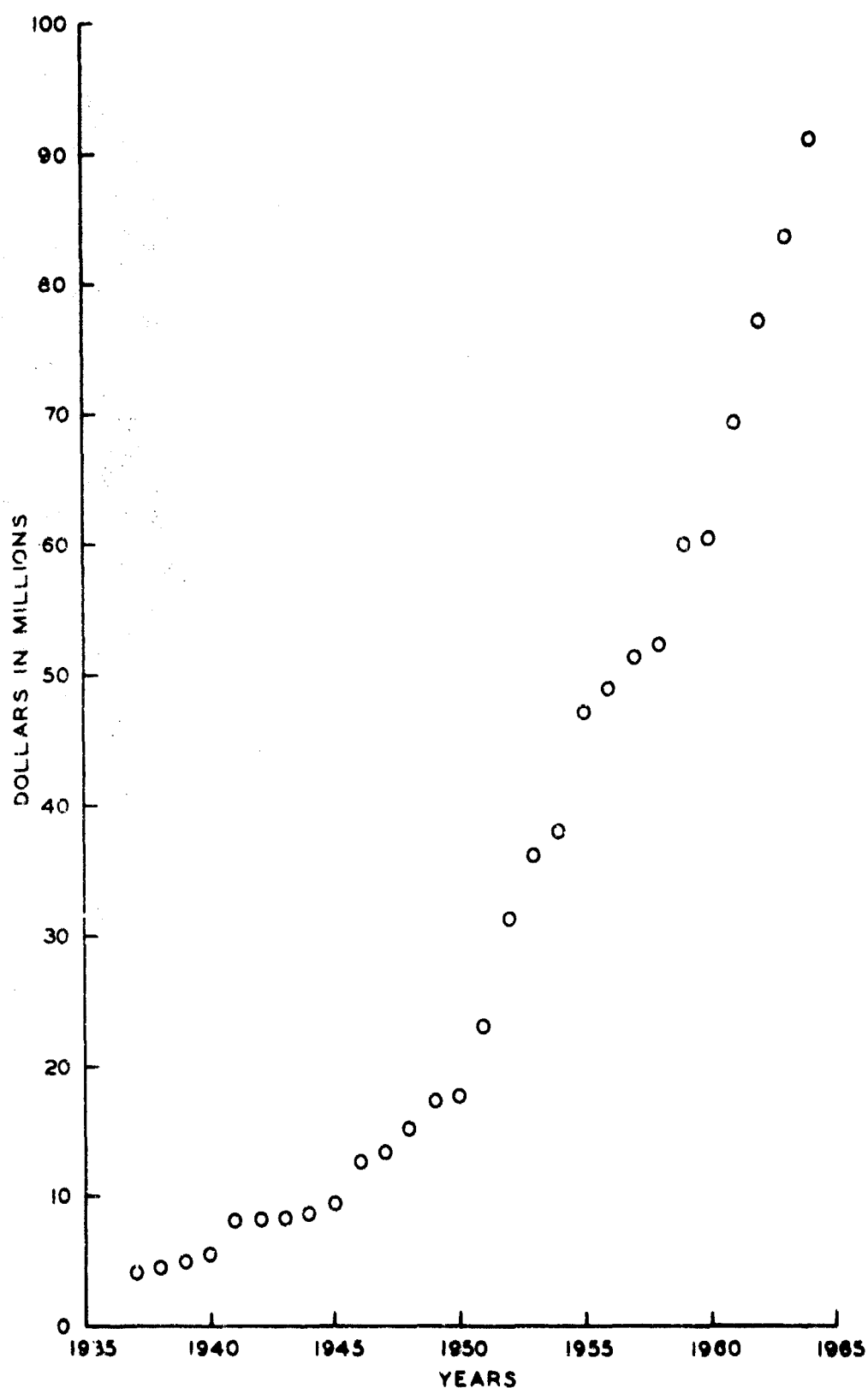
Fig. 17a. Assessed valuations (100% valuation) for real property in the city of Fairbanks. The information was compiled from Fairbanks city records by Mr. John Carlson, North Star Borough Tax Assessor.

THOUSANDS OF TELEPHONE CUSTOMERS AT
MUNICIPAL UTILITIES SYSTEM, FAIRBANKS ALASKA
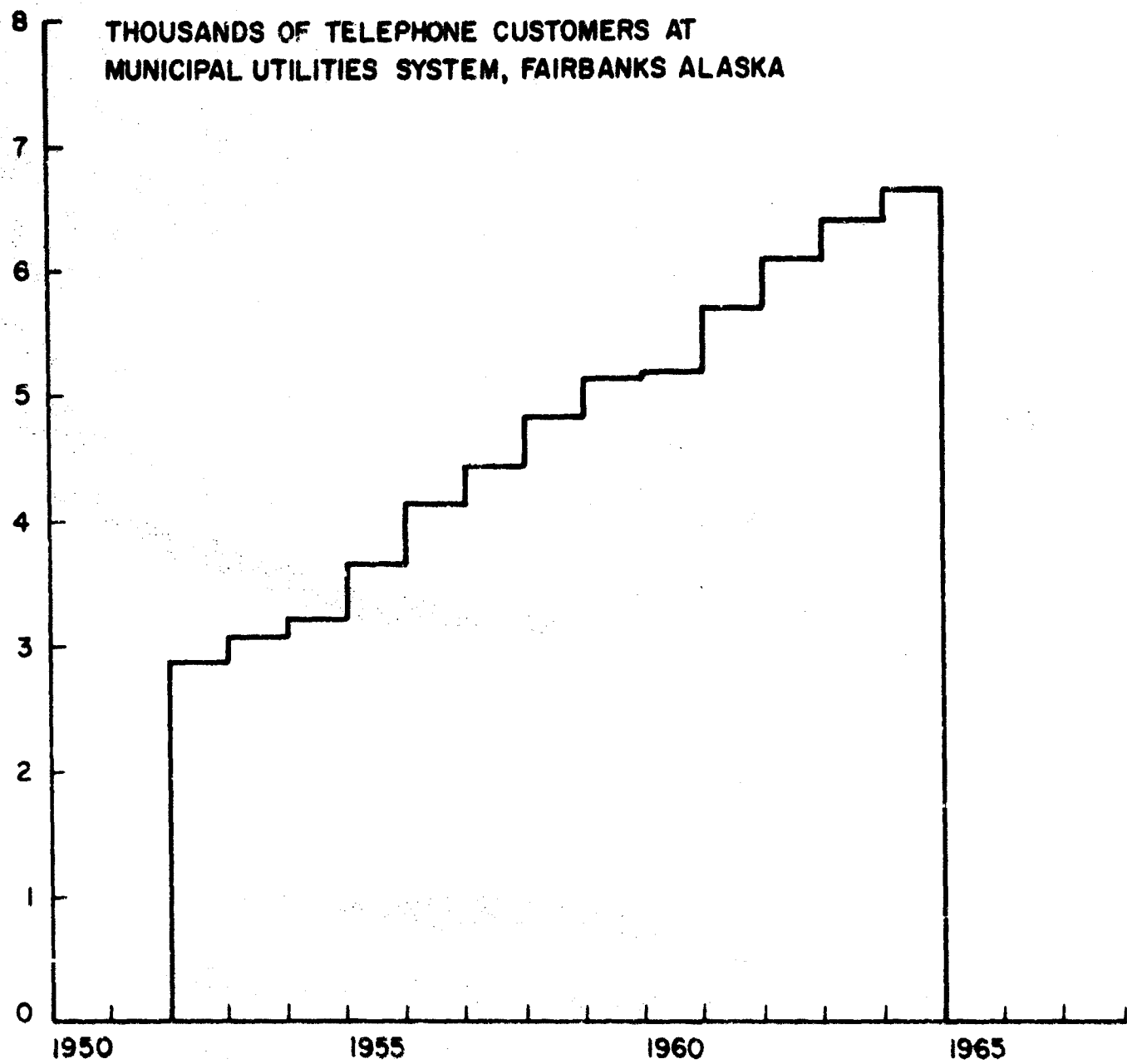
Fig. 18. Thousands of telephone customers at Municipal Utilities System
of Fairbanks, information provided by Mr. Harry Reimer of M.U.S.
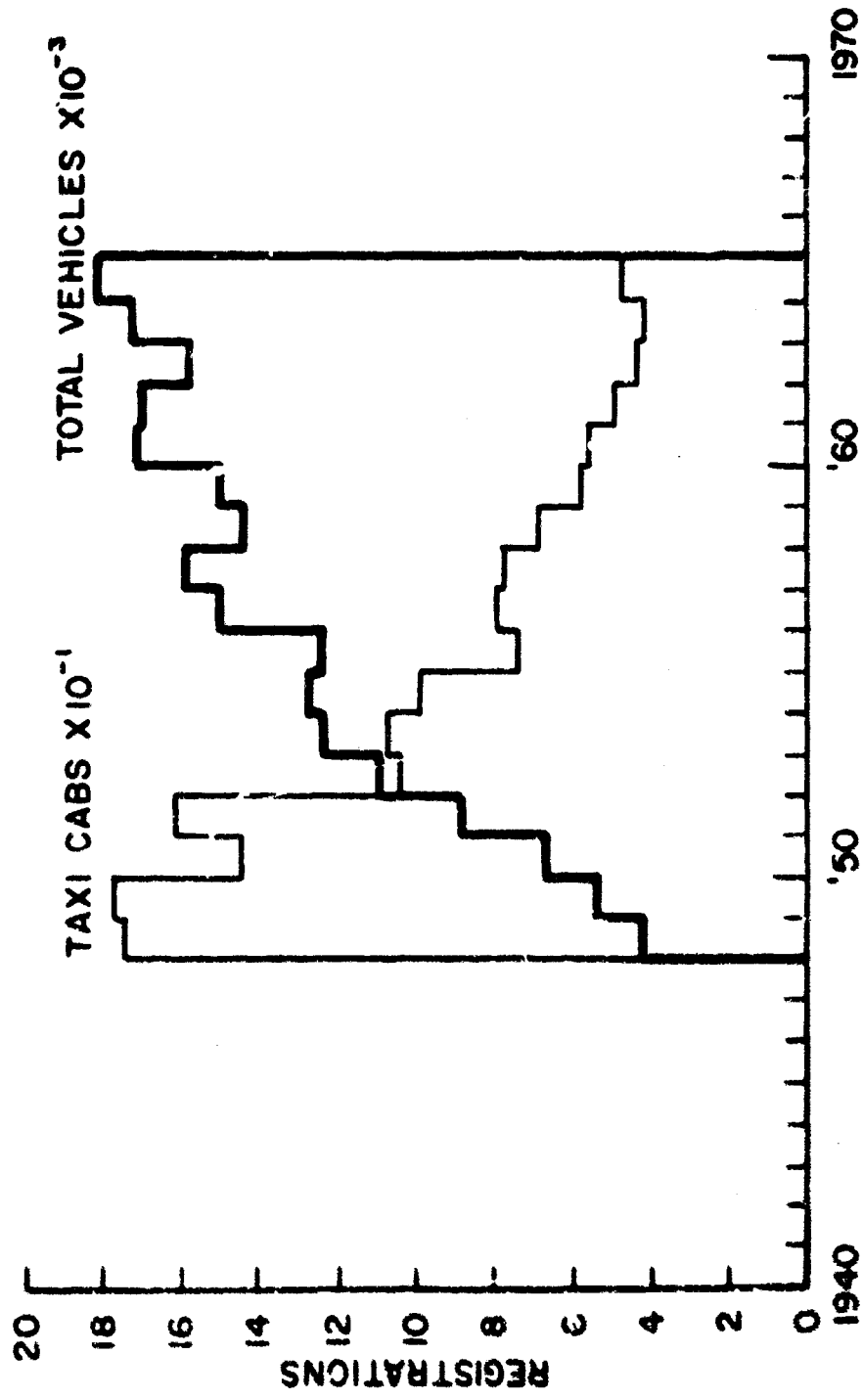
Fig. 19. Motor vehicles registered at the Fairbanks Office of the Department of Revenues Motor Vehicle Division, State of Alaska. The total number of vehicles increased from 4000 to over 17,000 while the number of taxi cabs in operation went from 174 to 48 in the same period of time; both statistics point toward a significant increase in the number of private vehicles in operation through the winter.

Fig. 20. -50°C (-58°F) 24 Jan. 1911, Fairbanks, Alaska.

Lithograph Reproduction by Commercial Printing Co., Fairbanks, Alaska

remarkably good. Dense ice fog would not permit a photo such as this be taken at temperatures lower than -35°C now. The only missing ingredients in the 1911 photo are 16,000 automobiles. If any vehicles were in Fairbanks during 1911, it is certainly not a bold assumption to claim that they were not operating on 24 January.

GENERAL PHYSICAL PROPERTIES OF ICE FOG

Optical Properties

The optical properties of ice fogs are different from those of other concentrations of ice crystals in the air such as cirrus clouds or "diamond dust" crystal displays. The latter consist of euhedral crystals generally larger than 30 μ diameter. They produce interesting halo phenomena as described on page 5 of Appendix A. At night the halo phenomena are mainly strong "vertical pillars" of light over automobile head lights, rotating beacon lights, etc. Halo phenomena are not present in ice fogs. Indeed, the optical effects of ice fog are similar to those of water droplet fogs, yet water droplets are not present in ice fogs as effectively demonstrated by Robinson, Thuman and Wiggins (1957 pp 97 98). Also, visibility is reduced by ice fogs to an incomparably greater degree than is the case for diamond dust crystal showers. These differences can be explained by considering the size and shape of the crystals involved.

The crystals present in ice fog range between 2 and 15 μ in diameter (Robinson, Thuman, and Wiggins, 1957; Kumai, 1964). Larger crystals - up to about 30 μ diameter - also occur, and in general they are more euhedral. Many of the small crystals lack definite crystal form to the extent that they have been referred to as "spherical" (Kumai, 1964). It also led to the definition of the term "droxtal" (Robinson, et al, 1955) unfortunately this term has carried the erroneous conception that ice fog crystals are not crystals. Once a supercooled droplet freezes, it becomes crystalline ice regardless of its shape, or

40

the presence or absence of crystal faces. No evidence of amorphous ice exists and the term "droxtal" is not used in this paper because of implications that have been associated with it. Indeed, although not essential to the proof of crystallinity, it may be noted that crystal faces are almost always identifiable on photomicrographs or when directly observing the crystals under a microscope.

The differences in size and shape of crystals between ice fog crystals and diamond dust or cirrus crystals are due to different rates of cooling and growth. In table 2, Appendix A we see that $4^{\circ}C$ per 12 hrs is a rapid cooling rate for the free atmosphere. Such cooling rates at low temperature cause water vapor to precipitate out of clear air in the form of well-developed crystals 30 to $100\,\mu$ in diameter, Figure 21. In this case, the atmosphere and the water vapor contained in it cool simultaneously and the crystals grow in a saturated air mass as long as cooling continues. The size and perfection of crystals increases with the original moisture content of the air and with the length of the cooling period, the limiting case is a snowstorm with large well-developed crystals (Fig. 22).

The above conditions are in sharp contrast to the situation prevailing when crystals form from cooling exhaust gases. These gases, originally at temperatures exceeding $100^{\circ}C$, cool more than $150^{\circ}C$ in less than 10 seconds when ejected into air of temperature $-35^{\circ}C$ or below. Their cooling rates are on the order of 10^6 greater than those in the free atmosphere. This rapid cooling condenses the water vapor into many small droplets which become supercooled, and at temperatures below -30 to $-35^{\circ}C$ they freeze. Crystal faces develop and twinning on the basal plane is common, (Fig. 23). But, in addition to the rapid cooling, this process differs from free atmosphere processes in that the crystals do not grow in a continuously saturated environment. Since the ability of these exhaust gases to hold moisture decreases by three orders of magnitude in several seconds, the crystals are almost immediately thrust into an atmosphere

41
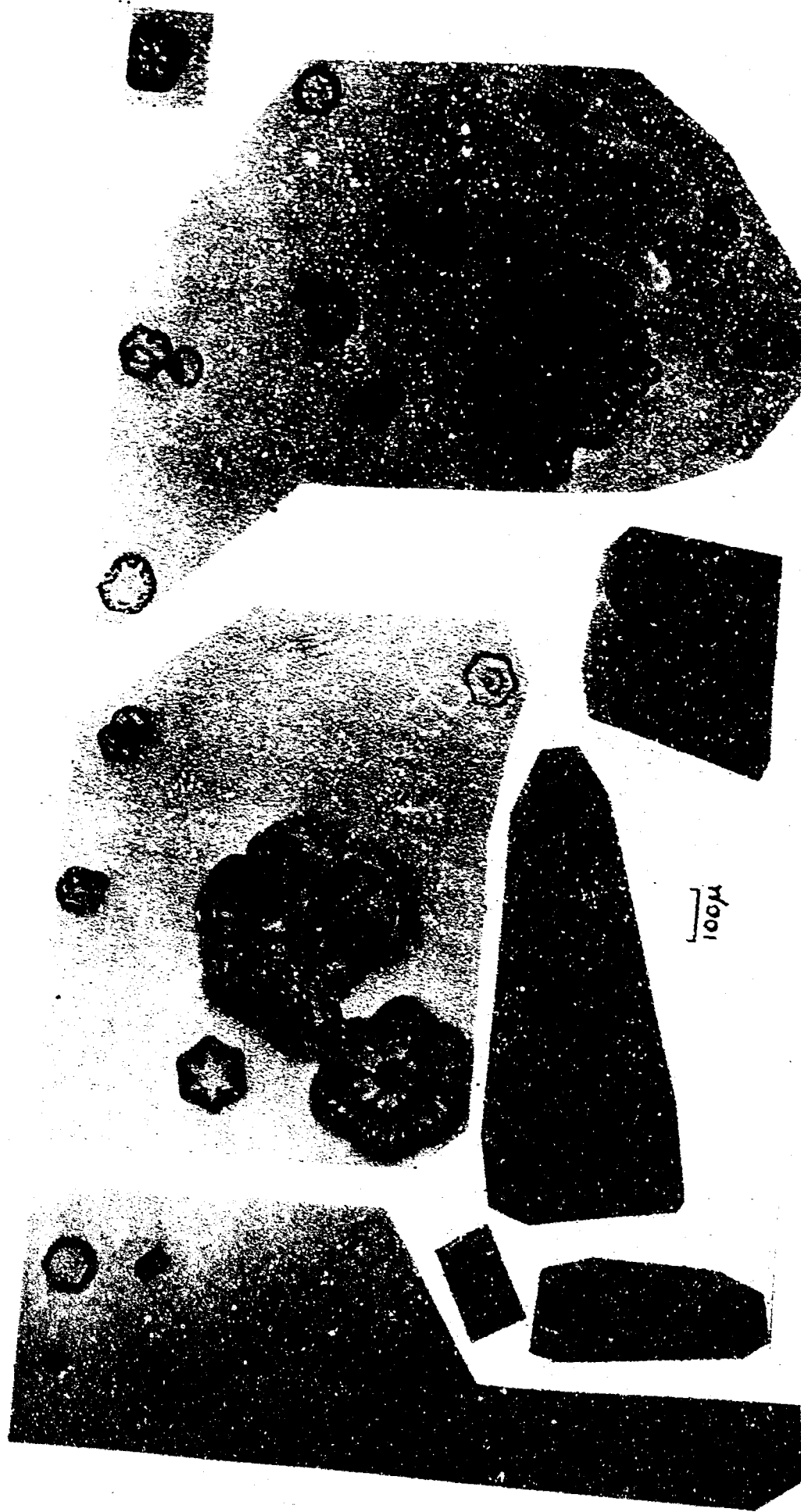
Fig. 21. Formvar replicas of diamond dust crystals about 0.1 mm diameter, which precipitated out of an otherwise clear sky during the morning of 8 Nov. 1961. (Photos by K. Francis).

100μ

Fig. 22. Small (1 mm) snow crystals from a light snowfall during afternoon of 8 Nov. 1961. Although these crystals are an order of magnitude larger than the diamond dust crystals which fell earlier in the day (Fig. 21) they are not large snow crystals; 5 mm is a common diameter for snow crystals. (Photos by K. Francis).

100μ
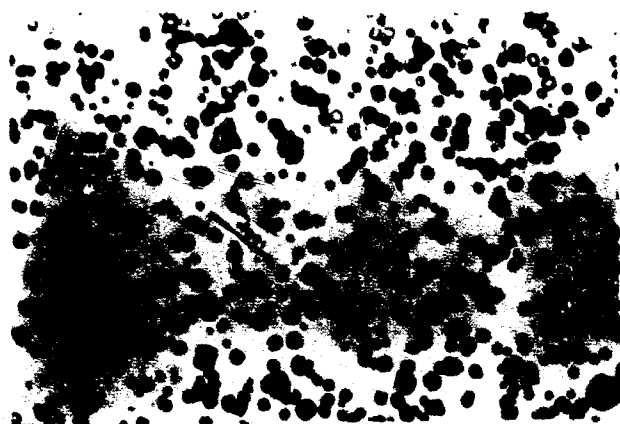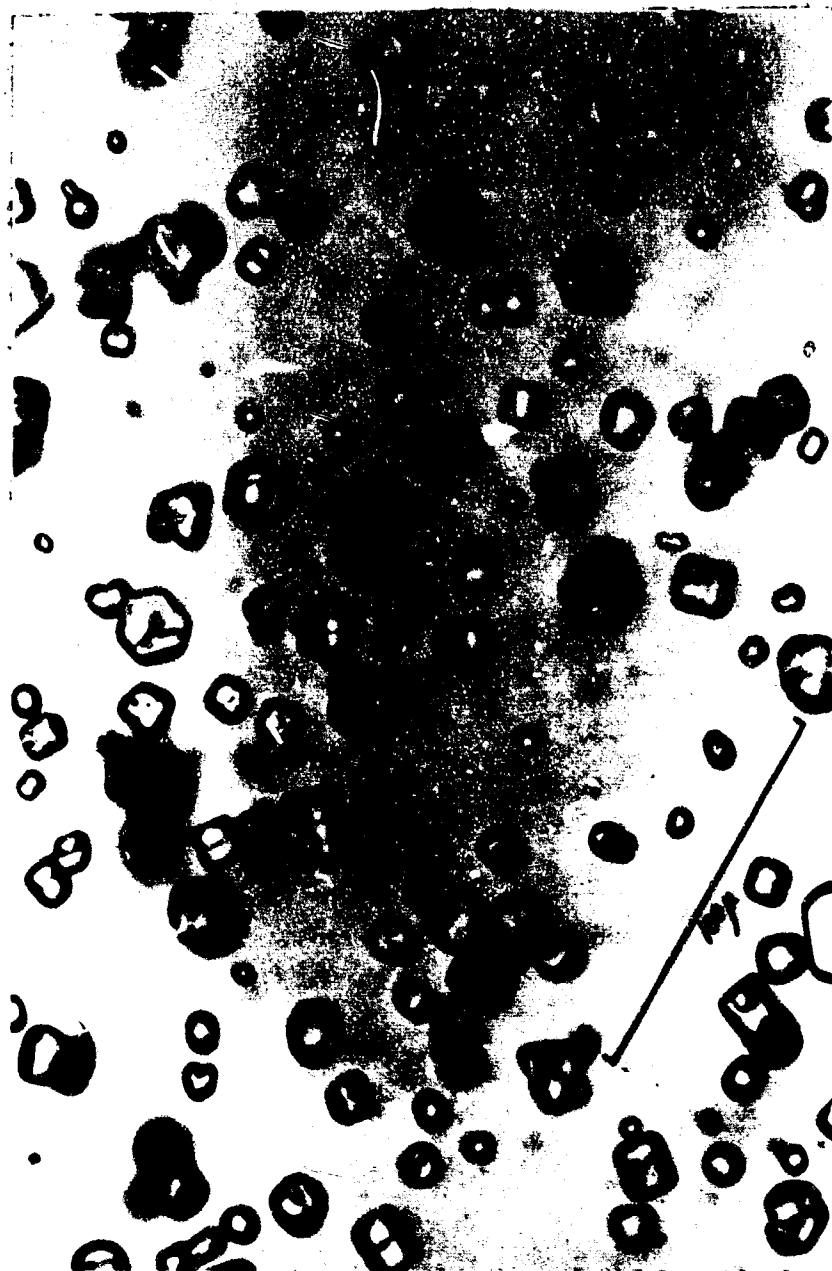
Fig. 23. Ice crystals collected from extremely dense ice fog, in a supermarket parking lot full of idling automobiles, in Fairbanks on 26 January 1962 at -39°C. The scale on the left is the same as in Figures 21 and 22; the scale on the right is a 5 fold enlargement. These crystals range downward in size from 25 μ, with an average in the 10 to 20 μ range. Many of the crystals shown are twinned on the 0001 plane. In general, ice fog, diamond dust, and snow crystals are of the order of 0.01, 0.1 and 1.0 mm respectively. (Photos by M. Kumai).

which, even though it may be saturated contains so little water vapor (0.2 g H_2O m^{-3} or less) that it permits extremely slow growth rates.

Consider the geometry of suspended ice crystals from the simplified point of view that crystals may be plates, i.e., flat segments of planes, at one extreme and needles, or segments of lines, at the other extreme. All gradations may exist between these extremes: the plates may thicken by growth parallel to the optic axis and the needles may become columns by growth normal to the optic axis. Between the extremes are equidimensional prisms with the sphere as a limiting case. Planar and needle-shaped crystals assume preferred orientations as they fall through the air. The pronounced halo phenomena observed when diamond dust crystals are in the air, are intensified by reflections from such orientated planar surfaces. The main reflection phenomena are vertical sun pillar and the horizontal parhelic circle, especially the two parhelia, or "sun dogs", which lie to the right and left of the sun along the parhelic circle. At night, vertical pillars formed by reflection from headlights are often very pronounced when plate-like "diamond dust" crystals are in the air, but are completely absent in ice fog. Ice fog crystals are so small and equidimensional that they fall with random orientation, much like water droplets. The lack of preferentially orientated reflecting surfaces and the density of particles in the air in water-droplet and ice fogs results in a lack of halo phenomena. During the onset of an ice fog event such as described in Appendix A one can observe the transition from diamond dust crystals to ice fog crystals and easily distinguish between them by the presence or absence of halo phenomena.

The pronounced reduction of visibility caused by ice fog as compared to crystal showers is explained by comparing crystal size, rather than shape. In general, smaller particles cause greater reduction to visibility than larger ones. Examples of this for droplets ranging from $5\,\mu$ to $200\,\mu$ in size, with corresponding visibilities ranging from 5 to over 500m (Went,1955, p. 67) may be applied to the comparison of ice fog and diamond dust crystals, where the order of

magnitude of diameters are 10 μ and 100 μ respectively (Figs. 21 and 23).
Diameters exceeding 1000 μ are observed in snow crystals (Fig. 22); however, one obviously cannot ignore other aspects of the problem which affect visibility such as the total rate of fall of material, after all the cliche' "blinding snow-storm" is not entirely restricted to fiction.

Cooling Rate of Exhaust Gases

The cooling of automobile exhaust gases was investigated at temperatures above and below freezing temperatures with results summarized in Figure 24. The thermistor probe was kept in mid stream of the exhaust plume and the speed of the gases varied from 20 m sec^{-1} near the outlet at fast idle to about 1 m sec^{-1} in the plume 1 to 2 m away from the outlet. With the engine idling steadily, a steady-state distribution of velocity may be assumed within the exhaust plume. The change of temperature with distance from the pipe outlet is proportional to the square of the difference between exhaust temperature and ambient air temperature:

$$\frac{dT}{dx} = -k (T - T_a)^2 \qquad (4)$$

where: T is temperature of the exhaust gas (C),

T_a is ambient air temperature,

and x is distance (cm) from the exhaust pipe outlet, measured in the center of the exhaust plume. k is a constant

The following data are typical:

Distance from Exhaust Pipe (cm)	Temperature °C
inside of pipe	100
20	31.5
30	19.5
40	9.0
40	4.0
100	-14.0
200	-25.0

Time, 21:40

Date, Mon 6 Jan 1964

Ambient air temperature = 28.7°C

43

$$\frac{dT}{dx} = -k(T - T_a)^2$$

	°C T_a	(ASSUM.) T_0	DATA PTS.	CURVE COMPUTED	$k(CM^{-1}°C^{-1}$
1)	~50	150	NONE	— · · — · · —	4.83×10^{-4}
2)	−28.7	296	O	——————	"
3)	−28.7	100	O	——————	"
4)	+24.4	89	□ SLOW IDLE	— · — · —	2.97×10^{-3}
5)	+24.4	160	△ FAST "	· · · · · · · ·	6.51×10^{-4}
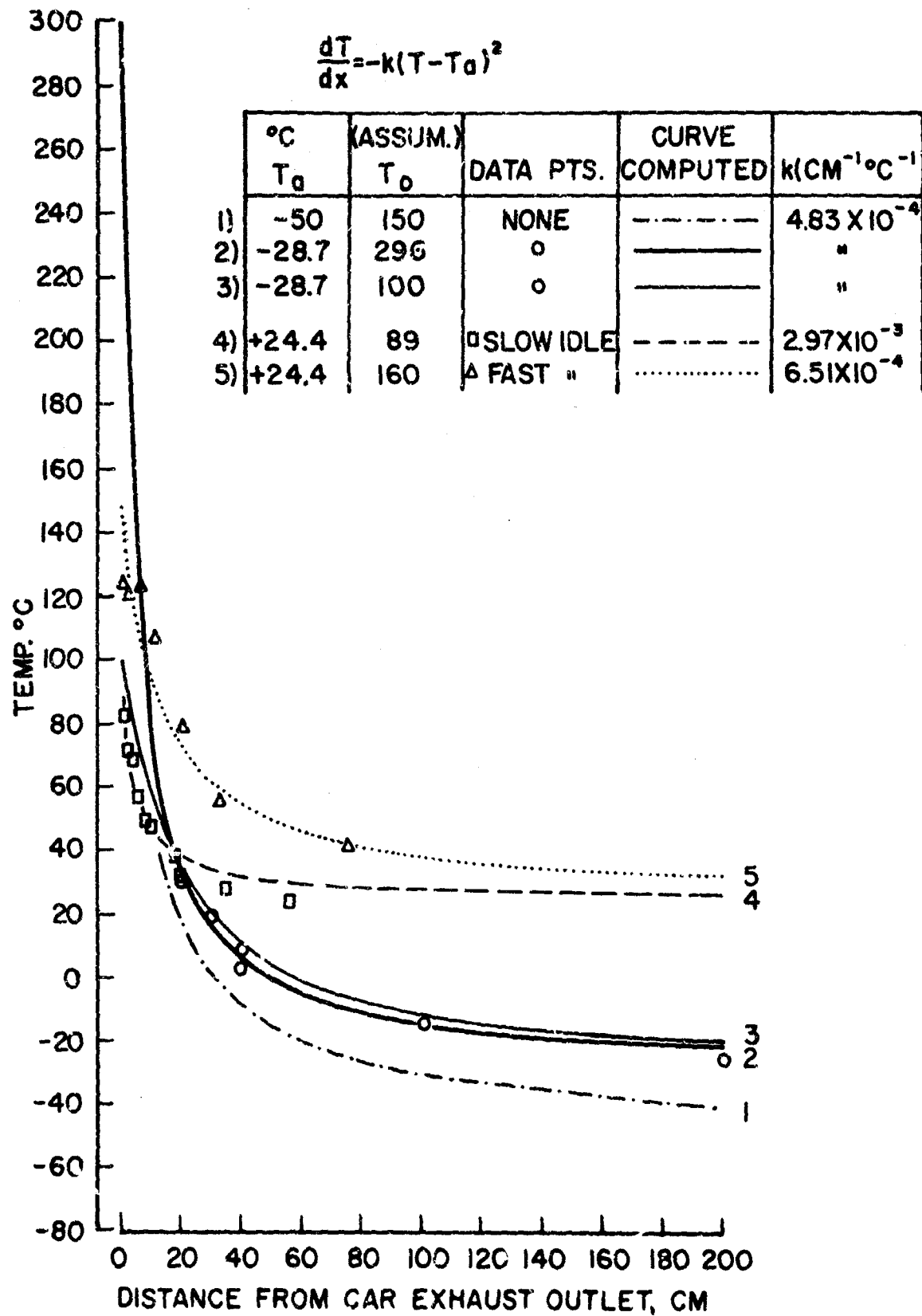
Fig. 24. Cooling rates of automobile exhaust gases. Temperatures were measured with a thermistor probe in the exhaust plume of an idling vehicle. The exhaust cooling rates for moving vehicles have not been mea̶   ̶ ̶ut should be more rapid.

If a very conservative average speed of 1 m sec^{-1} is assumed for the exhaust plume out to 200 cm in the above example we obtain cooling rates in excess of $\frac{60°C}{sec}$, or, 5×10^5 times greater than the rapid free-air cooling rate (see p.41). Using equation (4), a least squares fit to the above data give k = 4.83×10^{-4} cm^{-1} °C^{-1}, and place the exhaust pipe outlet temperature at 296°C; the data points and this curve are plotted in Figure 24. If we retain the value of k determined above and use 100°C as an extreme lower limit for the exhaust outlet temperature, the computed curve is only slightly altered and still affords a reasonable description of the exhaust cooling rate. The two warm-weather tests included in Figure 24, are also adequately described by equation (4).

Development of a Typical Ice Fog

From points 12, 13 and 30 (Fig. 2) the onset of an ice fog event has been repeatedly observed to have the following characteristics.

(1) A diffuse foggy layer consisting of well-formed crystals and ice fog crystals extends to an altitude of about 100 m above Fairbanks,

(2) The top of this cloud is ill-defined and has low density, an observer sees vertical "pillars of light" extending upward from lights at night. This phenomenon is especially noticeable over the rotating beacon lights on Birch Hill, because the pillars appear to flash on and off since they are only visible when the beacon points towards the observer. Also, automobile headlights may be detected at a distance by the vertical pillars above them as they move towards an observer.

(3) The above phenomena are observed throughout the rapid cooling phase at the start of a cold spell, but they are not observed in ice fog,

(4) At the end of the cooling phase, the air is dessicated to the extent that no more diamond dust crystals precipitate,

(5) The upper boundary of the fog becomes sharply defined and its altitude above the city is reduced to 10 or 20 m.

44

(6) When the air temperature goes below -35°C fog droplets begin to freeze. This increases the supersaturation of the air in a matter of hours to an extent that ice fog appears to form instantly (see Appendix B especially pp. 32-34).

(7) At this stage the water source from the free atmosphere is exhausted. Man-made water sources described earlier take over, and cause the ice fog layer to gradually thicken every day that the air temperature remains in the -40° to -50°C range (Fig. 27).

STRUCTURE OF THE POLLUTED AIR LAYER

Volume

The volumes occupied by ice fog at various stages of development have been estimated by combining measurements of areal extent and thickness. The estimates range from 1.0 to 265 x $10^7 m^3$. The basis of these estimates and some complexities involved in making them are outlined below.

Area

The areas covered by ice fog are summarized in Figure 26. These areal determinations were based on observations and photographs (Fig. 25) from the points designated by triangles on Figure 2. The inner area is covered by ice fog whenever ice fog is present. The area included in the dashed contour is affected when ice fog conditions last for several days. The outer solid-line contour includes the maximum ice fog cover during prolonged sieges. The areas measured by planimeter are: 61.6, 99.0 and 166 km^2 respectively.

Qualifications of the above figures are in order. The ice fog is not continuous, especially near the outer boundary. Patchy areas exist: (1) in the north east Approach Hill area at the east end of Ft. Wainwright (Fig. 25b), (2) near the university and (3) south and west of International Airport. The sizes of these patchy areas are approximately 10, 16, and 17 km^2, respectively. Generally an observer on Birch Hill (point 5) can see the Tanana River south and east of Fairbanks during ice fog periods. However, during December 1964 ice fog was observed to extend south of the Tanana River west of the junction

45

Fig. 25. Panoramic photos of ice fog from top of Birch Hill, (point 5, Fig. 2).

a. The thickest, most widespread ice fog observed so far, (29 Dec. 1961), it covered all buildings in downtown Fairbanks (see Figs. 1 and 27).

b. The patchy area at the east end of Ft. Wainwright on 27 Jan. 1962.

c. Wave forms on the top of the ice fog layer, on 14 Dec. 1964, (p. 52).
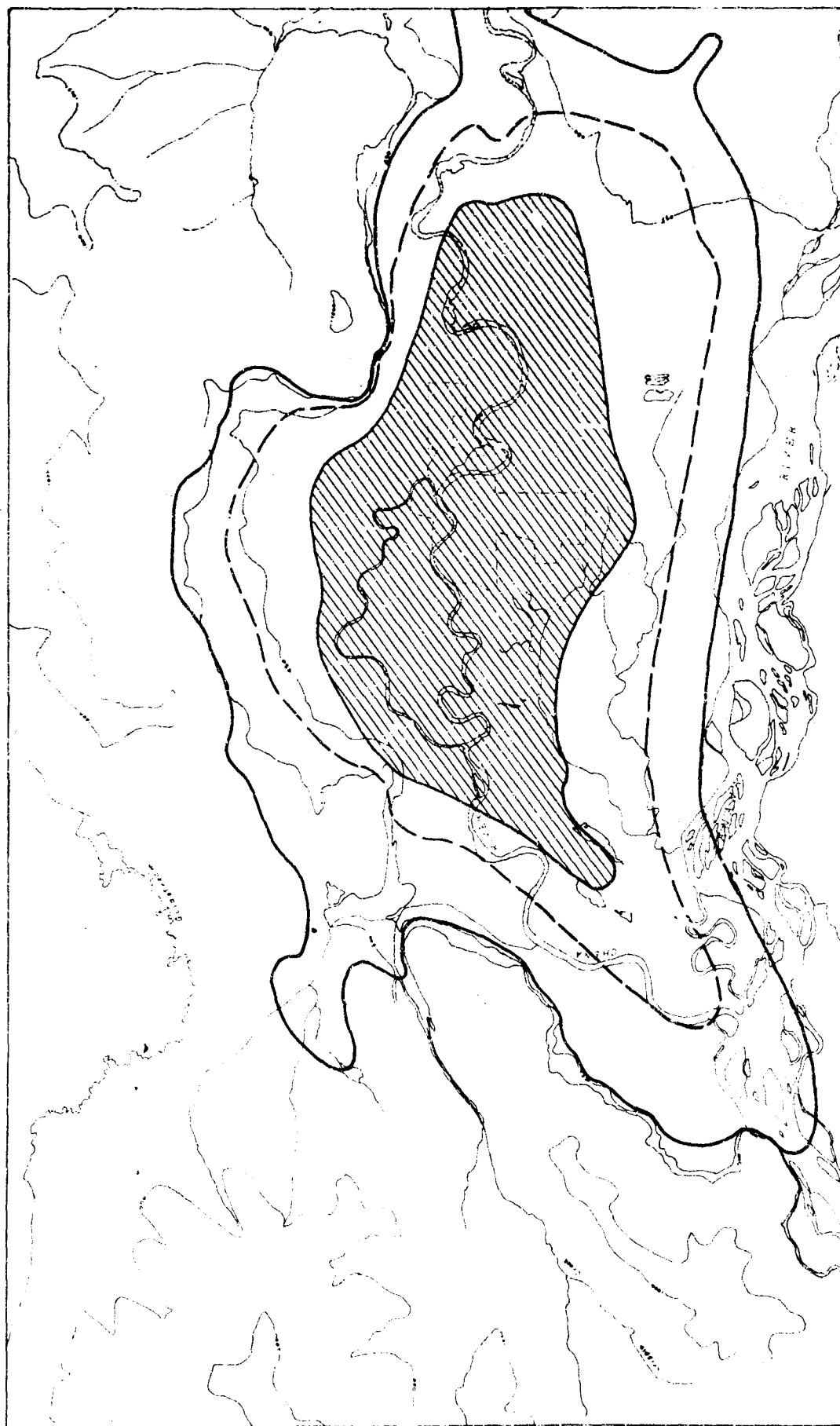
Fig. 26. Areal extent of ice fog. The cross hatched area is covered whenever ice fog is present. The area within the dashed line is covered after several days of ice fog, and the outer solid line includes the most extensive ice fogs. Recent observations from points 19 and 20 indicate that the southwestern border extends farther south than shown (p. 45).
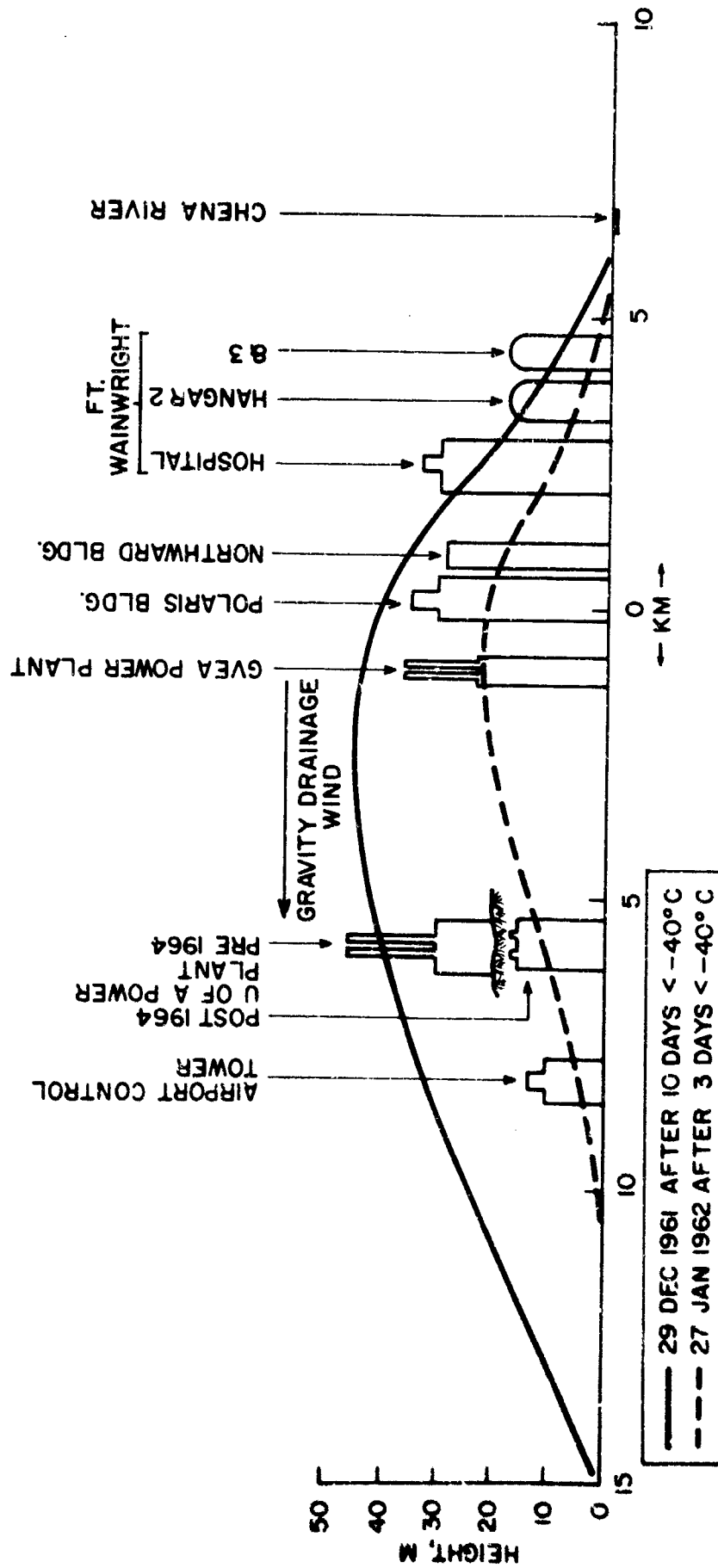
Fig. 27. Cross sections of ice fog thickness across Fairbanks from Chena River east of Ft. Wainwright to the junction of the Chena and Tanana Rivers SW of the Fairbanks airport. These cross sections were based on visual observations and photos from control points and U.S. Weather Bureau observations, summarized in Table I.

with the Chena River and into the Salchaket Slough area. The area of this extension has been estimated to be about 32 km^2. If this is added to the maximum area listed above, the result is 198 km^2, or approximately 200 km^2.

In summary

	Cumulative Total Area, km^2
(1) the inner core area (approximately)	50
(2) extended area commonly covered (approximately)	100
(3) maximum area commonly covered "	166
(4) maximum area in extreme cases "	200

Thickness

Ice fog is usually thin with a sharply defined upper boundary. This is clear from our observations and photos, and from similar descriptions by Robinson and Bell (1956) and others. It is generally about 10 m thick although it becomes thicker in the heart of town when air temperature remains below -40°C for several consecutive days. The cross sections in Figure 27 were based on visual observations and photos from the above mentioned control points. Some key buildings used for altitude measurements are indicated.*

Ice fog thickness data are recorded by the U.S. Weather Bureau at Fairbanks Airport by comparing visibility observations from the surface and from 12 m above the surface at the control tower (Hanson, 1964). Data covering the two cold spells which are treated in detail in Appendix A, are summarized in Table I The first cold spell began on 15 December 1961, and after a slight warming it was firmly established by 19 December. The table shows that at the Fairbanks airport the fog was thicker than 10 m during most of the time between 22 and 30 December. This is one of the worst cold spells in the U.S. Weather Bureau records at Fairbanks. By contrast, ice fog during the cold spell of 23 to 29 January 1962 was never 10 m thick at the airport. The data in Table I are in good agreement with the cross sections in Figure 27.

*Building altitudes were provided by Mr. John Chapman, Fairbanks City Engineer and Mr. George McGee, Assistant Post Engineer, Ft. Wainwright.

Table I.

U.S. Weather Bureau Comparative Visibility Records at Surface and Control Tower at Fairbanks International Airport

Cold Spell 15-29 December 1961

Date	Time 150°WMT	Visibility (miles)		Comments
		Surface	Tower (12 m above surface)	
20 Dec '61	0155	1	1 1/2	
	0345	1 1/2	4	
	0355	1 1/2	4	
	0555	3/4	15+	
	0610	3/4	15+	
	0625	3/4	15+	
	0643	2	15+	
	0655	2	15+	
	0955	1/2	1	
	1010	1/2	1	
	1025	1/2	i	
	1040	1/2	1	
	1055-1155	3/4	15+	
	1210-1540	1	15	
	1555-	1/2	1/2	
21 Dec	1225	1/4	3/8	Tower visibility SW 3.
	1440	1/2	1	Higher toward west.
	1555-1625	1/4	1	
	1930-1945	1/2	1	
	2310	1	4	
22 Dec	No significant differences			Less than 3/4 mi all day.
23 Dec	1512-1540	1/2	1	
24 Dec	No significant differences			Less than 3/4 mi all day.
25 Dec	"			"
26 Dec	"			"
27 Dec	"			"
28 Dec	"			"
29 Dec	0408	1 1/2	1 1/2 variable	Tower visibility NE 7
	1540-1740	1/2	1	
30 Dec	No significant differences - fog broke 0555			

Table I. (Cont'd)

Cold Spell 23-29 January 1962

Date	Time 150°WMT	Surface	Tower (12 m)	Comments
25 Jan '62	0828	2	4	
	1031	3/4	5	
	1230	3/8	1 1/2	
	1328	1/2	15+	
	1340	1 1/2	15+	
	1355	1 1/2	15+	
	1455	1	5 ·	
26 Jan	0415	2	15+	
	0455-0555	2	7	
	0735	1	4	
	1210-1240	1/4	7	
	1306-1345	1/2	7	
	1355	1/2	15+	
	1410	1/2	7	
	1555-1610	1/2	15+	
	1655-2355	1/2-1	4	
27 Jan	0055	2	7	
	0228	2	5	
	0255	2	7	
	0355	2	4	
	0455	2	5	
	1021-1140	3/8	15+	
	1155	1/2	15+	
	1205-1255	2 1/2	15+	
	1555-1640	5/8	6	
	1655-1740	3/4	5	
	1755-1810	3/4	4	
	1825	3/4	6	
	1835-1855	2	6	
	1955	1	6	
	2055-2355	2	6	
28 Jan	0055-0355	3	7	
	0455-0655	2 variable	7-15+	
	0810-0955	1 variable	15+	
	1008-1021	1/2	15+	
	1034-1046	1	15+	
	1055-1110	1 1/2 variable	15+	

Fog broke 1115

Estimates of Volume

The majority of cases can be covered by three estimates: (1) an extreme maximum volume, after 10 or more consecutive days with temperatures always below -40°C, (2) widespread ice fog, after several days with ice fog conditions, and (3) common, or minimum ice fog volume which can be expected whenever ice fog is present. In each case a thickness of 10 m is assumed for the entire area, with increased thickness added in the inner areas. For the most extreme case assume a maximum area of 200 km^2. Assume cumulative thicknesses of 20 m for the inner 50 km^2, 30 m for an inner core area of 10 km^2, and 40 m for 5 km^2 directly over the city center. By proceeding in this manner the following volume estimates are obtained:

(1) Extreme ice fog

Area (km^2)	x	Thickness (m)	=	Volume (m^3)
200	x	10	=	200×10^7
50	x	10	=	50
10	x	10	=	10
5	x	10	=	5
Cumulative Volume			=	265×10^7 m^3

(2) Widespread ice fog

Area (km^2)	x	thickness (m)	=	Volume (m^3)
165	x	10	=	165×10^7
50	x	10	=	50×10^7
Cumulative Volume			=	215×10^7 m^3

(3) Common ice fog

Area (km^2)	x	thickness (m)	=	Volume (m^3)
100	x	10	=	100×10^7
50	x	10	=	50×10^7
Cumulative Volume			=	150×10^7 m^3

These estimates are especially important when we attempt to calculate the concentration of pollutants in ice fog. In summary, it is unlikely that the

49

volume occupied by ice crystals and other pollutants will exceed 300×10^7 m^3, whereas a minimum volume of 100×10^7 m^3 can probably always be counted on when ice fog is present.

Temperature Distribution and Convection in Fairbanks Air

The network of meteorological stations (Fig. 2) provided information on the air structure near the ground which could not be obtained from radiosonde records such as shown in Figure 3. Thermograph records from the 2 m level at points from the Chena River up the ski-slope to the top of Birch Hill are shown in Figure 28. The two bottom traces are from points only 3 m apart in altitude; yet their temperatures differ by the same amount as the next two points which are vertically separated by 36 m. If these differences of temperature and altitude were expressed as air temperature gradients, in the usual units, they would be equivalent to 167 and 14°C per 100 m respectively. However, care must be exercised in making such comparisons because of topographic features. Tower 3 is near the bottom of the small valley of the Chena River (Fig. 2). This topographic depression of only 3 m further reduces the slight turbulence existing in the flats, and permits more effective heat loss by radiation. Thus, the river channel is essentially a heat sink compared to the surrounding flats and temperatures measured 2 m above the surface on towers 2, 3, and 4 show variations of 5°C (Figs. 29, 30).

When traverses are run across Fairbanks a heat source is encountered. This should be expected since "heat islands" are measured over cities in general[*]. The heat island across Fairbanks has been measured during the past 3 winters by mounting a thermistor 2 m above ground on a vehicle and making continuous readings along selected traverses. The temperature in the city exceeds that of the surrounding flats by 5 to 6°C when the air temperature is

[*]Examples where accurate measurements have been made include: Leicester (Dobson, 1948), London (Chandler, 1962), Rotterdam (Schmidt and Boer, 1963) and Washington D.C. (Woolum, 1964).
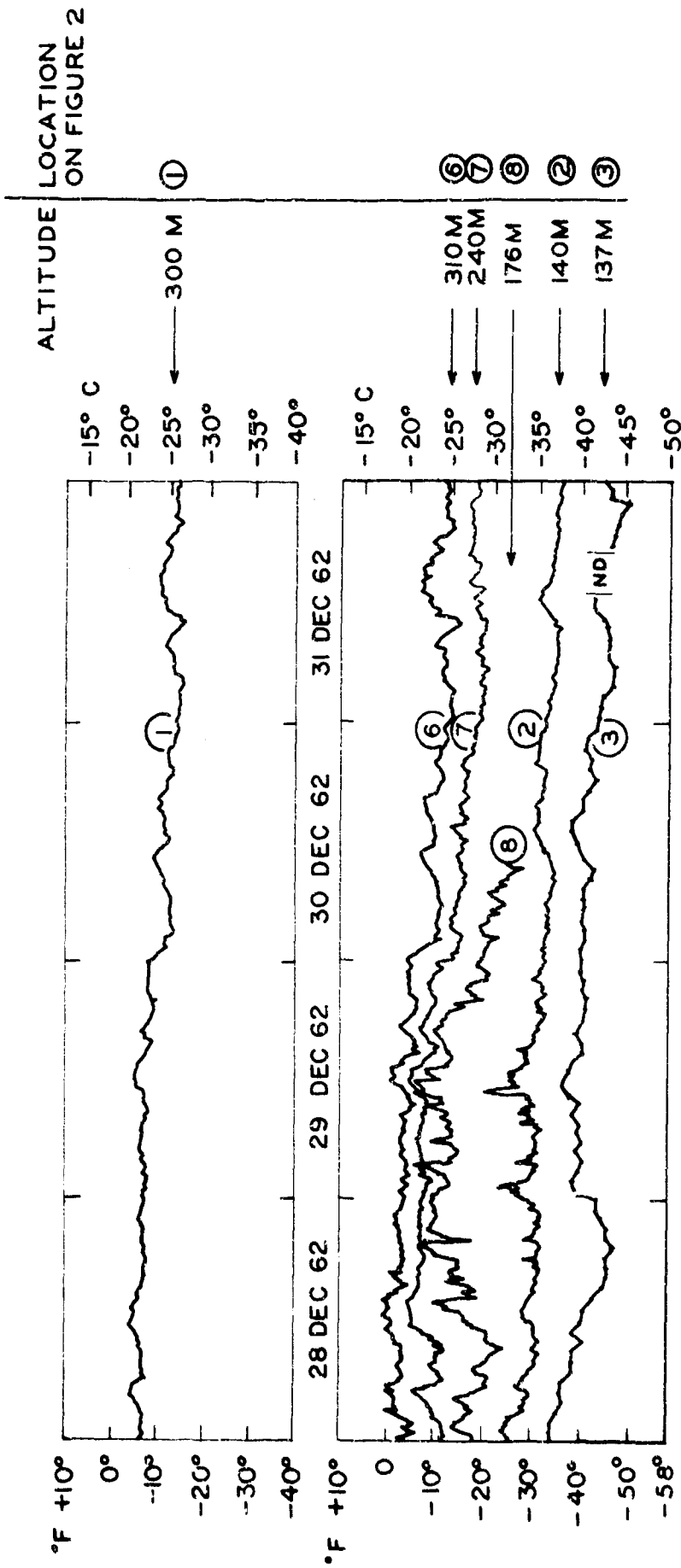
Fig. 28. Thermograph records obtained 2 m above the ground along the slope of Birch Hill from 137 to 310 m. The individual traces are numbered here according to their location on Figure 2. No thermograph record was available at Tower 3 so the 2 m thermocouple record was used. The temperature differences between points 2 and 3 which are only 3 m apart in altitude, are nearly the same as those between points 2 and 8 which differ in altitude by 36 m. Oscillations in temperature with amplitudes about 1 to 2°C and with periods of less than an hour, appear frequently on thermograph records obtained near the base of Birch Hill (points 2 and 8) but are less pronounced near the top of the hill (points 1, 6 and 7). See Figure 33.
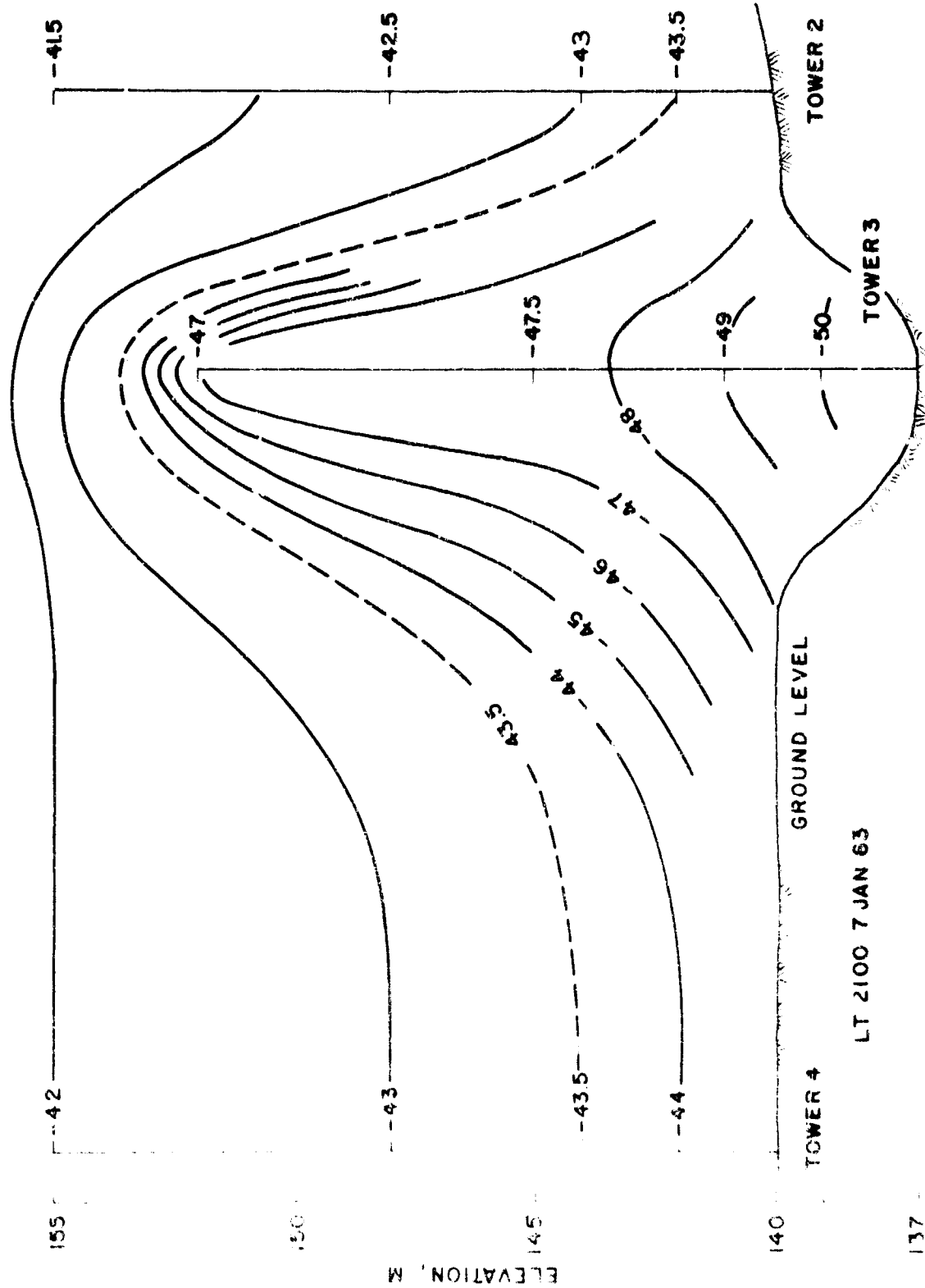
Fig. 39. Temperature (°C) cross section at 21:00 (150 WMT) 7 Jan. 1963 along lines connecting meteorological towers 2, 3 and 4 (see Fig. 2). The vertical dimension is exaggerated by 300 X for clarity. Towers 2 and 4 are at the same altitude (140 m), tower 3 is lower by only 3 m but there produces a difference in temperature between towers 3 and 4 of 6°C at the 2 m level and less at the 15 m level; the differences are greater between towers 2 and 3.
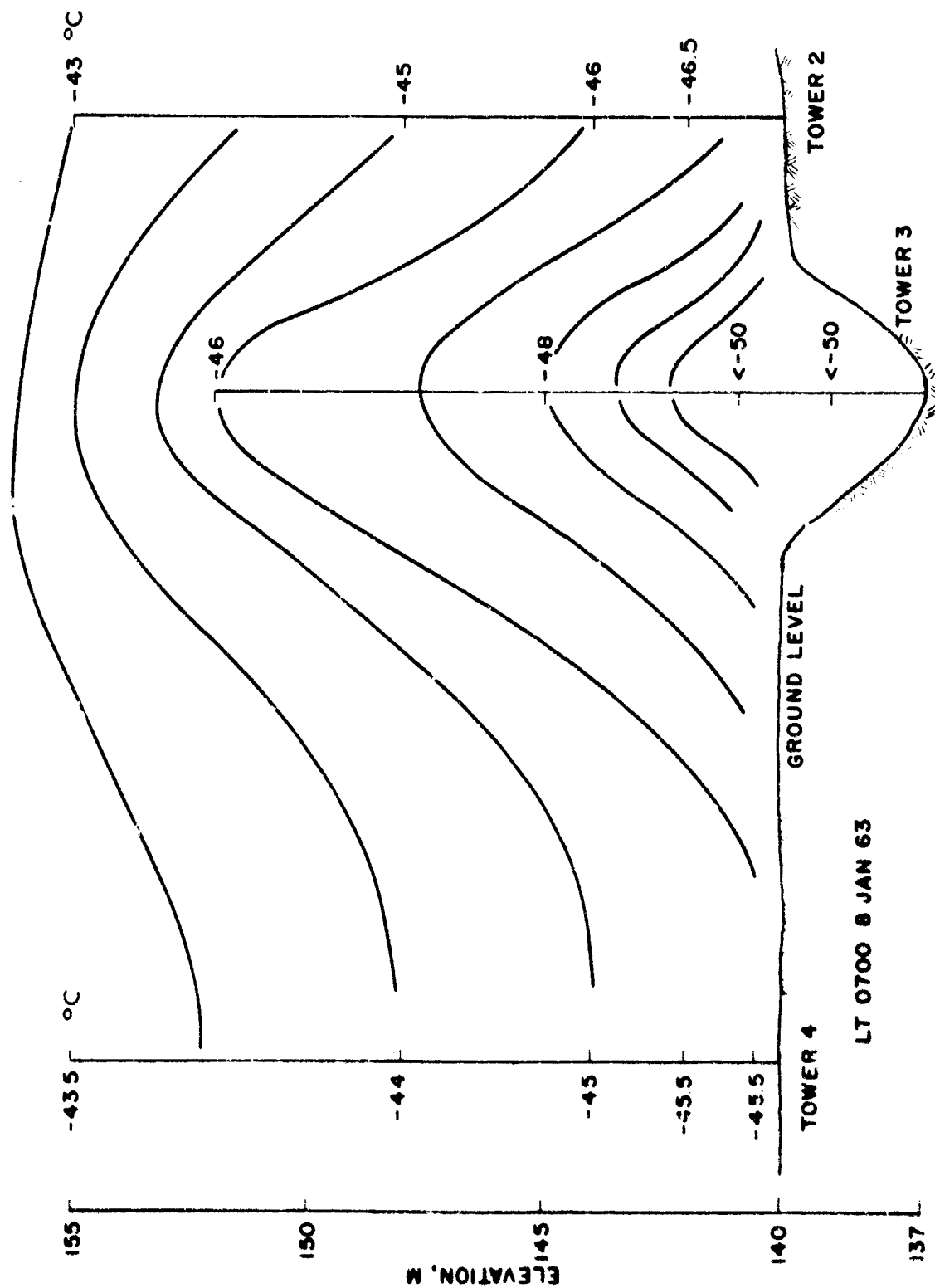
Fig. 30. Temperature (°C) cross section at 07:00 150 WMT 8 Jan. 1963 along same lines as shown in Figure 29. The 2 m and 4 m thermocouples on tower 3 were off the scale of the recorder below -50°C. Thus the temperature difference between towers 3 and 4 is greater than 4.5°C at 2 m and about 2.5°C at 15 m. The corresponding differences at towers 2 and 3 are 3.5°C and 3°C respectively.

in the -40 to -45°C range, and by about 3°C in the -20°C range. A similar increase in the heat island effect with decreasing temperature was noted in Washington, D.C. (Wollum, 1964). Figures 31 and 32 show a well developed heat island over Fairbanks. Note the low temperature about 1 mile from the USWB station; it occurs at the point where the road comes close to the river, so it is influenced by the heat sink effect described above.

Regardless of horizontal variations in temperature, the strength of inversions is greatest at the lowest levels; this shows clearly in Figures 33 and 34. In particular, temperature gradients between the 15 and 2 m levels on tower 1 (top of Birch Hill) and tower 3 (in Chena River cut) are equivalent to 8 and 40°C per 100 m respectively. The weaker inversion on top of Birch Hill is due to increased turbulence at that height. The opposite case of calmer air in the lower levels, permits radiative cooling to form strong inversions, with an extreme case being in the protected wooded area of the Chena River valley (Figs. 29, 30, 33, and 34). Increased stability with decreased turbulence in the first few mm above the snow surface, allows gradients to form, which are three orders of magnitude greater than those mentioned above. Nyberg's (1938) measurements, made very close to a snow surface during clear weather with winds less than 1 m sec^{-1}, may be summarized as follows:

Height above Snow Surface (mm)	Average temperature Difference (°C)	Equivalent gradient °C/100 m
0-5	1.6	3.2×10^4
0-20	3.8	1.9×10^4
0-1400	7.5	5.4×10^2

The relatively weak surface inversions on top of Birch Hill allows use of the 2 m thermograph record as an approximation to the free air temperature at that level (see pp 2-3 Appendix A).

51
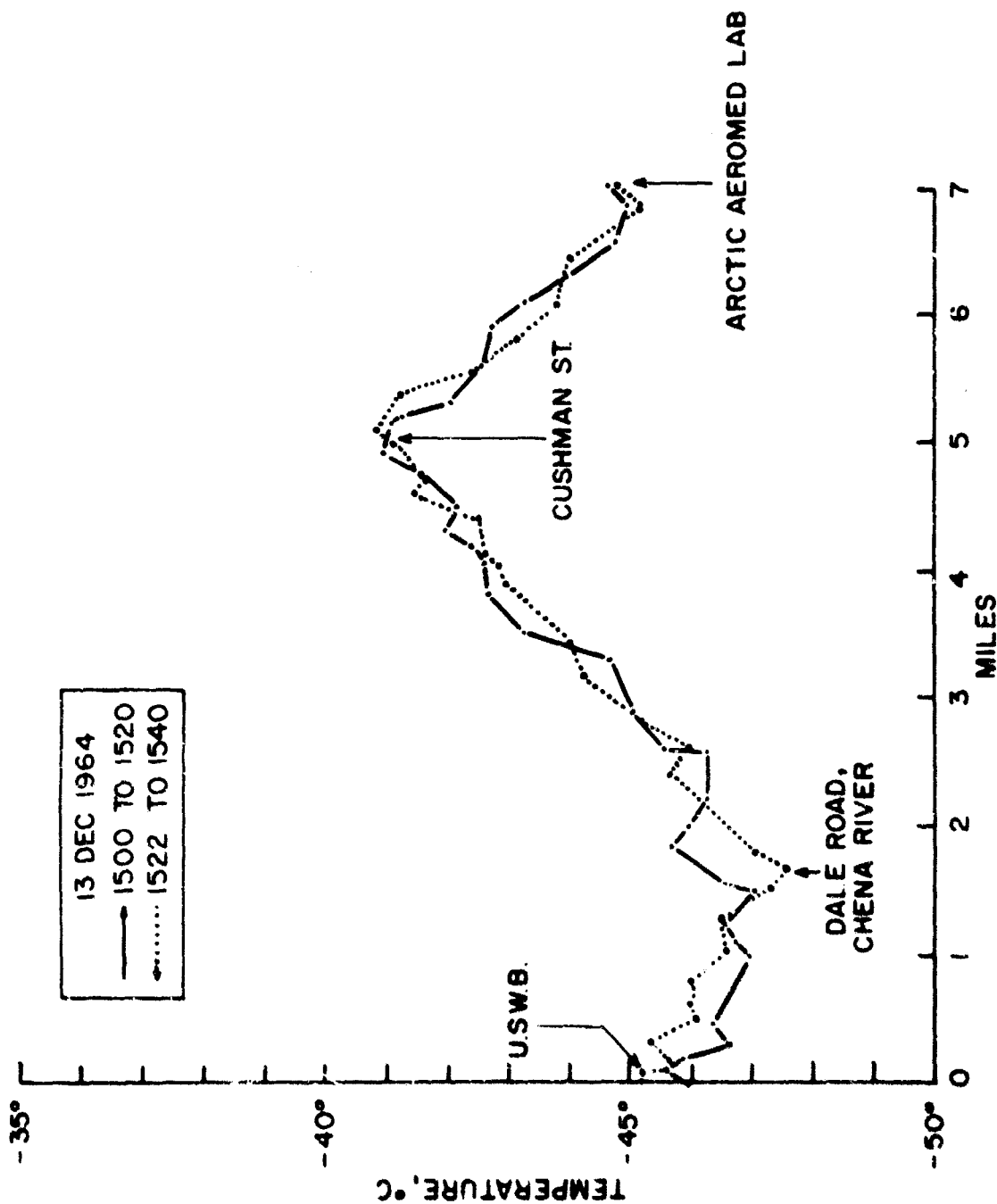
Fig. 31. East-west temperature traverse through Fairbanks on 13 Dec. 1964. This temperature traverse was run from the U.S. Weather Bureau Station at Fairbanks Airport to the Arctic Aeromedical Laboratory, Ft. Wainwright and back to the Weather Bureau. A thermistor probe mounted 2 m above the road on the front of an automobile was read inside the vehicle at frequent intervals along the traverse. The round trip traverse consisted of two independent runs in different directions along the same line during a total elapsed time of 40 minutes. This double run insures that the observed temperature differences are not caused by local short-time changes in temperature.
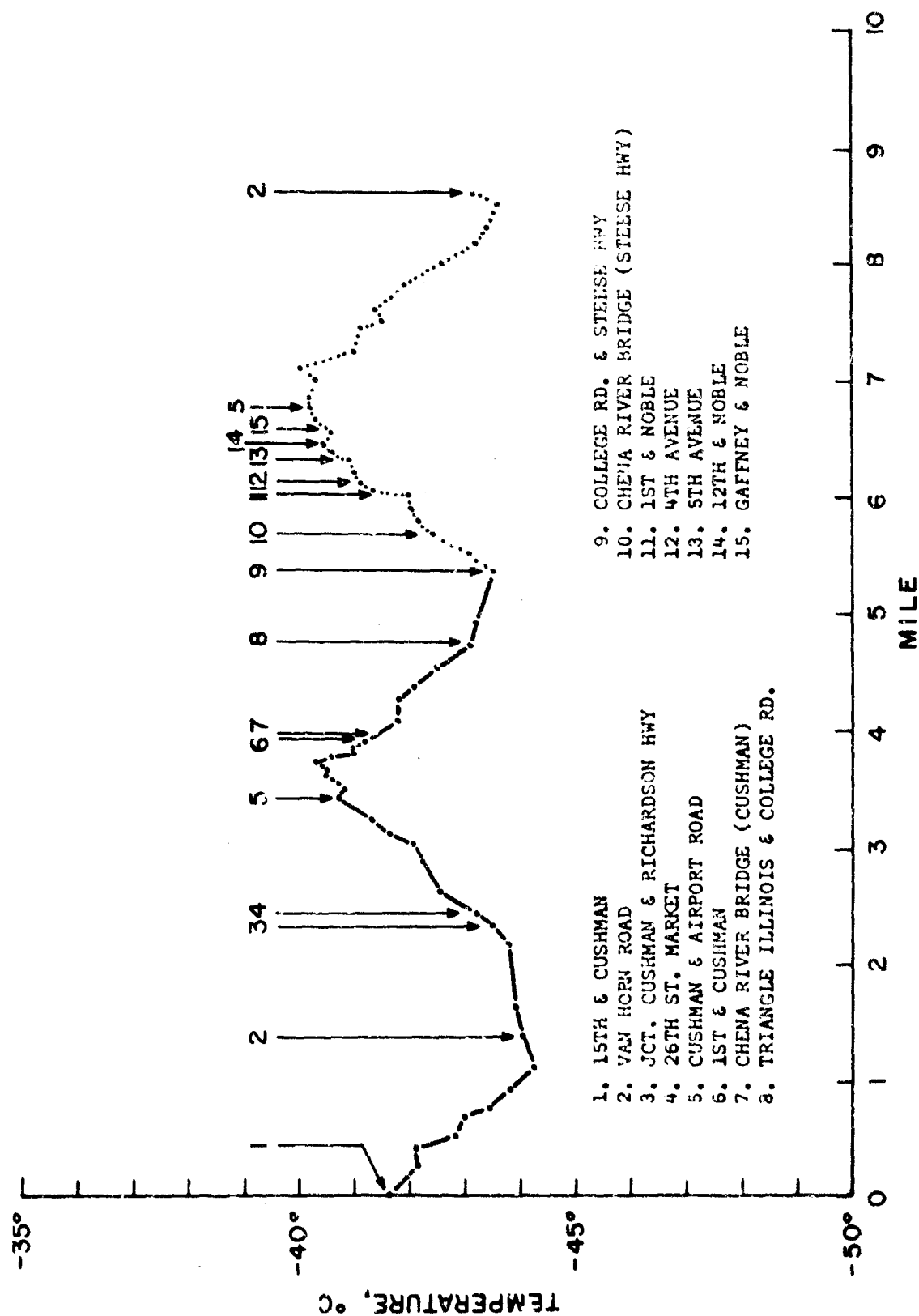
Fig. 32. North-south temperature traverse through Fairbanks. This temperature traverse was also run on 13 Dec. 1964. It began at 15th and Cushman St. (point 1) and went south on Cushman to Van Horn Road (point 2), then north again through Fairbanks on Cushman St. to point 8. The traverse followed a parallel return route from point 8 to point 9 and then back along Noble St. to point 5 where Cushman was again followed to Van Horn Road (point 2). The return part of the traverse from point 9 to point 2 is dotted. The total time was about 30 minutes.

1. 15TH & CUSHMAN
2. VAN HORN ROAD
3. JCT. CUSHMAN & RICHARDSON HWY
4. 26TH ST. MARKET
5. CUSHMAN & AIRPORT ROAD
6. 1ST & CUSHMAN
7. CHENA RIVER BRIDGE (CUSHMAN)
8. TRIANGLE ILLINOIS & COLLEGE RD.

9. COLLEGE RD. & STEESE HWY
10. CHENA RIVER BRIDGE (STEESE HWY)
11. 1ST & NOBLE
12. 4TH AVENUE
13. 5TH AVENUE
14. 12TH & NOBLE
15. GAFFNEY & NOBLE
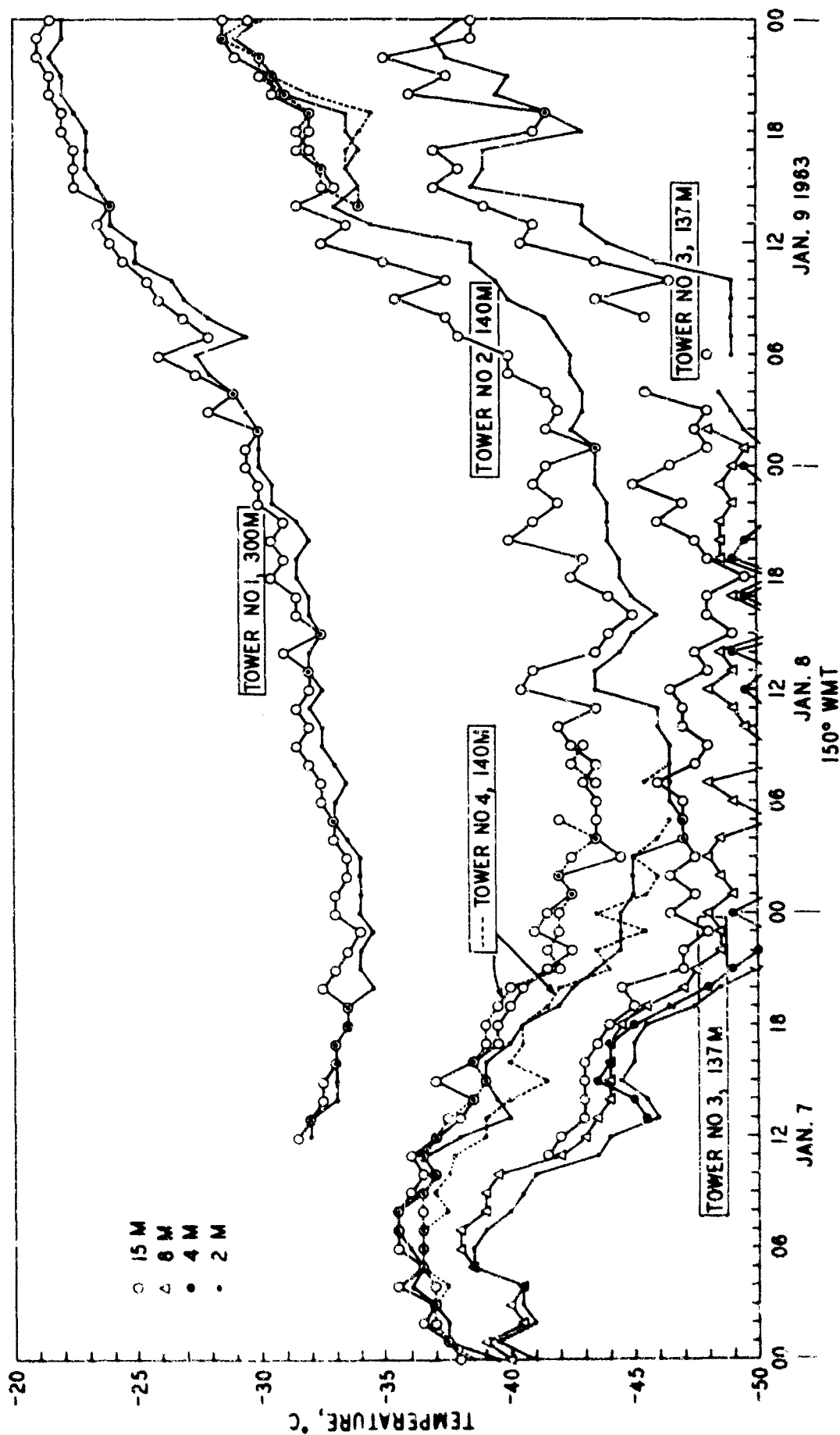
Fig. 33. Hourly temperature values at 2 and 15 m above ground on towers 1, 2, 3 and 4 during the cold spell of 7 to 9 January 1963. The 2 m thermocouple on tower 3 was off scale (below -50°C) during most of 8 January so the 8 m and 4 m values are included. The temperature differences between the 2 and 15 m levels are greater at the lower altitudes. For example at tower 3 this temperature difference exceeds 5°C whereas it never exceeds 2°C at tower 1. Towers 2 and 4 are at the same altitude and their temperature records are very similar.
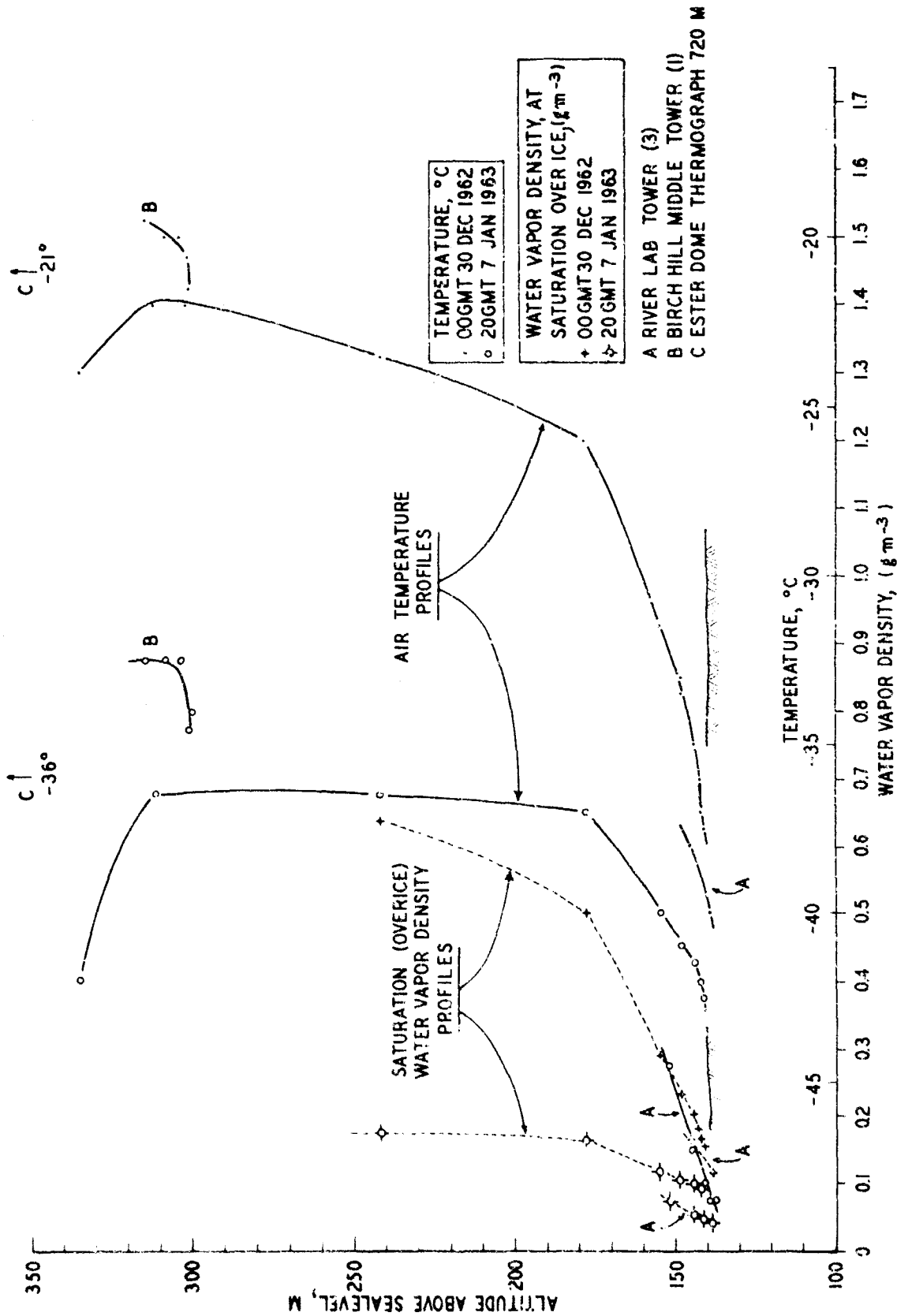
Fig. 34. Temperature and saturation water vapor density profiles based on data from meteorological towers at top and bottom of Birch Hill and thermographs along the slope. The Ski Lodge Tower (2) was used for the lowest temperature data on the main curves. The River Lab Tower (3) shows separately because the temperature over it is lower than over the adjacent area on the flats (Fig. 28, 29, 30 and 35). The increased ability of air to hold moisture at increasing altitudes shows clearly. For example: air 40 m above ground was able to dissolve more water than air 10 m above ground by a factor of 1.5 on 7 Jan 1963, and by a factor of 2.0 on 30 Dec. 1962.

The heat source in the city sets up circulation cells. However, this circulation remains under, the top of the inversion because the heat island effect is not sufficient to destroy the inversion (see p.16). City heat sources combined with the heat sink along the river, produce complex cells because of the way the river meanders through the city.

In addition to circulation forced by the above situation, wave motions exist in the low-level dense air similar to a seiche on a lake, or a bay open at one end. The first evidence indicating the presence of such waves was obtained from thermograph records on the slope of Birch Hill such as shown in Figure 28. The records at the lower levels on the slope frequently show temperature variations with amplitude of about $2^{\circ}C$ and periods of less than an hour. Although these variations are most pronounced at lower levels, they exist at all levels. The temperature variations are clearly not the result of adiabatic heating and cooling of the air, for this would require vertical motions of 200 m. However, wave motion of 3 m amplitude would produce these temperature variations at a fixed point because of the steep temperature gradients in the air.

These oscillations are most pronounced at low temperatures and especially during times when temperature is fairly constant. Figure 35 shows this in the evening part of records from the Ski Lodge (Point 2) at the base of Birch Hill during a time of strong diurnal cycles. Also shown in Figure 35 is a temperature record presumably produced by seiche-type oscillations in the steep-walled valley of Wild Lake in the Brooks Range.[*] Wave motions extending to significant heights within an inversion layer were recently described by Grant (1965).

Several attempts have been made to photograph the waves which are frequently observed on top of the ice fog layer. One of the best examples is shown in Figure 25c; it is the complex net result of seiche and thermally forced oscillations.

[*]Record taken by Mr. Frederick Meader at Wild Lake, Alaska.

WILDLAKE

F +10° 0° -10° -20° -30° -40° -50°

18 JAN 1963   19 JAN   20 JAN   21 JAN   22 JAN

-15° C -20° -25° -30° -35° -40° -45°

SKI LODGE

F +20° +10° 0 -10° -20° -30° -40°

13 MAR 1963   14 MAR   15 MAR   16 MAR   17 MAR

-5° C -10° -15° -20° -25° -30° -35° -40°
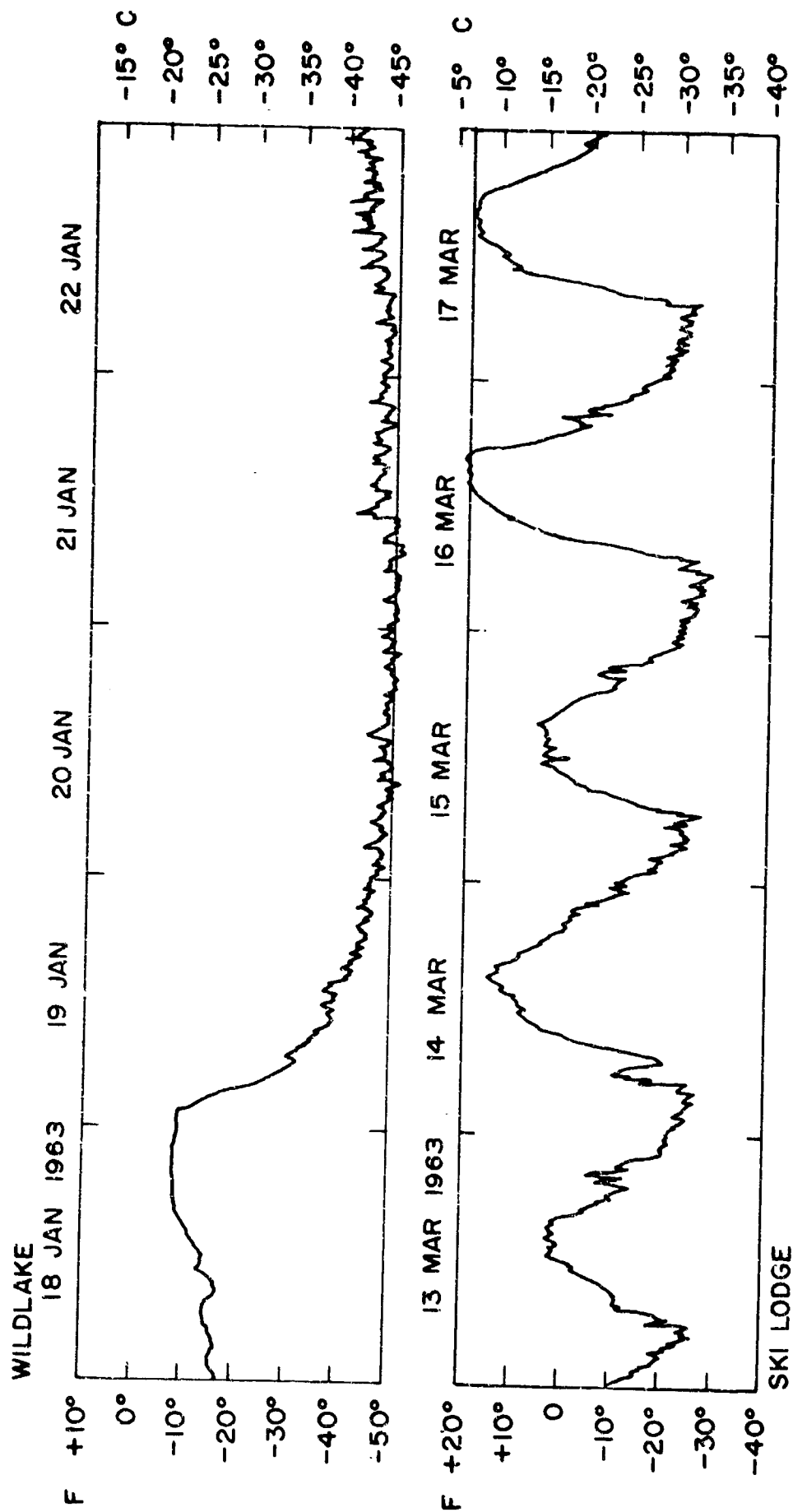
Fig. 35. Temperature oscillations on thermograph records. Wildlake lies in a steep-walled valley in the Brooks Range; during prolonged cold spells, temperature variations similar to those shown in Figure 28, but more pronounced, are frequently found on thermo-graph records taken here. Such temperature oscillations occur with strong inversions. However, they do not require prolonged cold spells in order to develop, as shown in the record from the Ski Lodge Tower (point 2 on Fig. 2) between 13 and 17 March 1963. In this example, the oscillations appear with stable air every night even though a strong diurnal temperature cycle exists.

Once ice fog is well established the base of the inversion shifts upward. This effect is observed in water droplet fogs also, in particular, Dines (1931) shows that the base of the inversion coincides with the top of the fog. Sometimes a negative lapse rate forms within the fog, and rarely it approaches the dry adiabatic rate. Dines (1931, p. 280) cites an extreme example where the dry adiabatic rate was approximated throughout a 60 m thickness of fog. Examples of weak inversions, isothermal and even negative lapse rates in ice fog are given by Robinson and Bell (1956, p. 511-512). Negative lapse rates in the ice fog layer show clearly in the soundings at Fairbanks on 26 and 27 December 1961 (Fig. 3, see also Fig. 2 of Appendix A). The latter example is especially pertinent since it occurred near the end of almost two weeks of ice fog. This agrees with the expected and observed case in "old" water droplet fogs (Dines, 1931; Dobson 1948).

When the base of the inversion is shifted upward the main outward radiation of heat taken place from the upper surface of the fog. This has little effect on calculations dealing with the net outgoing radiation (see p. 6 Appendix A); however, within the fog it enhances the upward air flow in the heat island area. Upward air velocities were not measured in Fairbanks, but such measurements from the industrial area of Rotterdam (Schmidt and Boer, 1963, especially p. 29) show maximum upward velocities of 15 cm sec^{-1} in localized areas and large areas with upward velocities of 5 cm sec^{-1}. In Fairbanks the 5 to 6°C heat island, compared to the surrounding flats, combined with 5 to 6°C heat sinks, also compared to the surrounding flats, gives rise to local convection cells driven by temperature differences of 10 to 12°C. These horizontal temperature differences were not exceeded in the above mentioned measurements in and around Rotterdam; therefore, it is reasonable to expect that upward velocities of 5 cm sec^{-1} would apply to much of the area covered by the heat island in Fairbanks, and that maximum velocities of 15 cm sec^{-1} would prevail locally.

53

Such upward velocities exceed the fall velocities of most ice fog crystals.
These crystals are less than 30 μ diameter (pp. 40-41) so Stokes law applies to
them giving terminal velocities as follows:

| Sphere | | Terminal falling |
Radius, μ	Diameter μ	speed, cm sec^{-1}
1	2	0.0117
10	20	1.2
20	40	4.8
30	60	10.8

The net effect is to retard precipitation of the ice fog crystals and to
increase the height of the ice fog over the city center (Fig. 27).

Within the ice fog layer of downtown Fairbanks the heat source from com-
bustion processes, combined with radiative and other heat losses from buildings
will in itself cause upward movement of the crystals. If a negative lapse rate
develops in fog, mixing becomes more active and the air pollution problem is
intensified in the fog whether it consists of water droplets or ice crystals.
However, the situation is worst for the case of ice fog as illustrated by the
following simple comparison.

(1) Water droplet log: from Dobson (1948, p. 142)

> "...It seems probable, ...that once a lapse of temperature is
> formed in the lower foggy air, there will be more active mixing,
> and the saturated surface air will be carried up and cooled by
> expansion or mixed with colder saturated air unt''   super-
> saturated and fog formed. In this way, given a   heat
> to the surface of the ground either by conducti<   elow or
> by absorption of daylight, and loss of heat by   radiation
> from the upper part of the fog, the fog particles ы , o on
> falling out and other fog particles may be formed indefinitely.
> Hygroscopic nuclei will be removed continually, but there is
> usually no lack of these, and in a city the combustion of fuel
> will produce plenty of them."

(2) Ice Fog:

In ice fog the process of condensation as the moisture is carried aloft by upward air currents does not exist because the moisture is already in the form of crystals even at street level. Crystals caught in upward air currents don't readily precipitate out because the particle sizes are so small that the upward air speed exceeds their fall speeds. When a negative lapse rate exists the crystals will be able to grow by sublimation as they move upward, but there is a limit to this, especially as they reach the upper level of the fog because the crystals enter a desicating environment. The primary sources of heat and moisture are combined in the form of combustion products; and since the input rate is greater than the precipitation rate (p. 68) the vertical thickness and the density of the fog continually increase. As long as ice fog conditions prevail the process perpetuates itself (Fig. 27). However, the process of condensation and production of fog at the upper level as in the case of water droplet fogs, is reversed in ice fogs. The upward moving crystals are constantly moving into a region which tends to dissolve them. This will be treated in more detail below.

MASS BUDGET OF ICE FOG

Ice fog forms a lens-like blob, 10-40 m thick, over a maximum area of about 200 km^2 around Fairbanks and Ft. Wainwright. The ice crystals in this fog layer are produced by sources of moisture discussed in Chapter III which provide slightly over 4×10^9 g H_2O per day. While these crystals are temporaril. suspended within the ice fog layer they may grow or evaporate by sublimation. Individual crystals also collide and form twinned aggregates as evidenced by the many twinned crystals seen in microscope collections. However, regardless of the physical history of individual crystals or groups of crystals, eventually they either precipitate out through the bottom of the ice fog layer - or

55

sublimate into the air, primarily through the fairly well-defined top of the ice fog layer. The mass budget deals with rates of input and removal of ice crystals to and from the ice fog layer and the concentration of suspended ice crystals within it.

The mass budget is most easily expressed in the form of an equation of rates as follows:

$$I = PA_B + EA_T + \rho \frac{dv}{dt} \tag{5}$$

where,   I is the rate of input: $g\ H_2O\ day^{-1}$,

P is the rate of precipitation: $g\ H_2O\ cm^{-2}\ day^{-1}$,

E is the rate of evaporation: $g\ H_2O\ cm^{-2}\ day^{-1}$,

A_B is the bottom area of the ice fog layer: km^2,

A_T is the top area of the ice fog layer: km^2,

ρ is the density of ice crystals in the air: $g\ H_2O\ cm^{-3}$,

and $\frac{dv}{dt}$ is the rate of change in volume of ice fog with time: $m^3\ day^{-1}$

Equation 5 allows one to consider the ice fog as contained in a bag-like membrane with a source of ice crystals inside. Crystals are lost through the bottom by precipitation and through the top by sublimation. There is a limit to the value of ρ so that the volume occupied will increase while ice fog conditions prevail. However, since the value of I is essentially constant and the values of P and E are bounded, there is also a maximum to the volume which can be occupied by the ice fog. When this maximum is reached, $\frac{dv}{dt}$ becomes zero and the ice fog will be in steady-state equilibrium. This condition will prevail until changes occur in the values of I, E, or P. Consider some examples:

(1) At the beginning of an ice fog event the area covered is small and I exceeds the sum of PA_B and EA_T, ie,

$$I > PA_B + EA_T$$

so that $\frac{dv}{dt} > 0$ and the ice fog layer grows.

56

(2) As the area covered by ice fog expands the sum $PA_B + EA_T$ will approach

the limiting value I, at which time $\frac{dv}{dt}$ approaches zero. If the source is

limited to a given rate of input I, there will be a maximum to the area which

can be occupied by the ice fog and $\frac{dv}{dt}$ will remain zero until the equilibrium

between input and output is disturbed.

(3) When air temperature rises so does the vapor pressure of the air and

the value of E with the result that $\frac{dv}{dt}$ becomes negative and the ice fog

begins to dissipate. Increased air temperature may also increase the rate of

aggregation of suspended crystals into groups which fall faster. This would

effectively produce an increase in the value of P as well as E.

(4) Another cause for negative values of $\frac{dv}{dt}$ may occur during prolonged

ice fog events by a reduction in the value of I caused by a reduction in the

number of vehicles operating as the cold weather continues.

Equation 5 provides a useful base for estimating the values of some

parameters once measurements are available for others. As a starting point the

input rate I, determined in Chapter III, is 4100×10^6 g H_2O day^{-1}. Values of

A_B and A_T, taken as equal, together with estimates of $\frac{dv}{dt}$ may be derived from

the observations and photos discussed in Chapter VII. Measurements of P,

together with estimates for ρ will be presented next. Once reasonable values

are available for I, P, ρ , and $\frac{dv}{dt}$, equation 5 will provide a value for E.

Internal consistency between the terms of equation 5 guides the following

discussion.

Ice Fog Precipitation Rates

Precipitation rates, based on the number of crystals landing on microscope

slides were calculated by Kumai (1964, p. 11).

> "The rate of precipitation and the size and mass distribution
> of ice-fog crystals observed at a temperature of -39C in the
> city of Fairbanks and at a temperature -41C at Fairbanks
> International Airport are shown in Figures 14 and 15 (of
> Kumai's (1964) paper). At -39C, the rate of precipitation of
> ice-fog crystals was 2302 crystals/cm^2-min, and the mass was
> 6.91×10^{-7} g/cm^2-min. At -41C, the precipitation rate was
> 832 crystals/cm^2-min and the mass was 2.87×10^{-8} g/cm^2-min."

57

It is especially significant that the two values cited were measured in different places as well as at different temperatures. The areal distribution of ice fog is such that the distance between these points of measurement is undoubtedly more important to the precipitation rate than is the 2°C difference in temperature. Indeed, larger temperature differences than this, up to 5°C, exist simultaneously between downtown Fairbanks and the airport (Fig. 31).

Independent measurements on precipitation rates were made with the 1 m^2 collector described on p. 34. The two most successful tests were:

(A) Test number 3, 09:45 3 Feb. to 13:30 6 Feb. 1965

Total ice fog residue collected = 98 g

Total number of hours = 75.25

Hours with temperature below -30°C = 71.0

Hours with temperature below -35°C = 51.0

(B) Test number 5, 23:15 16 Feb. to 19:29 19 Feb. 1965

Total ice fog residue collected = 80 g

Total number of hours = 68.25

Hours with temperature below -30°C = 65.0

Hours with temperature below -35°C = 50.0

The above tests give the following rates of precipitation:

		Precipitation Rates	
		g H_2O cm^{-2} min^{-1}	g H_2O cm^{-2} day^{-1}
Test A	Total hours	2.17×10^{-6}	3.12×10^{-3}
	hours below -30°C	2.30×10^{-6}	3.31×10^{-3}
	hours below -35°C	3.20×10^{-6}	4.60×10^{-3}
Test B	Total hours	1.95×10^{-6}	2.80×10^{-3}
	hours below -30°C	2.05×10^{-6}	2.95×10^{-3}
	hours below -35°C	2.67×10^{-6}	3.84×10^{-3}

These precipitation rates measured downtown, are in the range of 2 to 3×10^{-6} g H_2O cm^{-2} min^{-1} which is the same order of magnitude as Kumai's (1964) downtown value, ie, 0.69×10^{-6} g cm^{-2} min^{-1}. They are slightly higher, but that may be due to the different method of collection, ie, a large area exposed for many hours compared with a microscope slide for several minutes. Kumai's lower precipitation rate, measured outside the core of the fog area, is two orders of magnitude less. For purposes of calculating the input-output balance of ice fog, maximum precipitation rates will be used. The value 3×10^{-6} g H_2O cm^{-2} min^{-1} based on the above conside .tions will be used for the core area. Kumai's measurements, showing that the outlying areas have rates about two orders of magnitude less, will be used to assign values to the outlying areas. Thus the rate used here for the outlying areas is the same, to one significant figure, as that used by Kumai (3×10^{-8} as compared with 2.87×10^{-8}).

In summary, the rates used in this paper are:

Area	Precipitation Rates	
	g H_2O cm^{-2} min^{-1}	g H_2O cm^{-2} day^{-1}
Inner 50 km^2 core	3×10^{-6}	4.3×10^{-3}
Outlying areas	3×10^{-8}	4.3×10^{-5}

These are probably maximum values.

Density of Ice Fog

Consider a unit cube at a point within the ice fog but removed from any "source" or "sink" of ice crystals. Ice crystals of variable size and velocity pass through the cube. Since sources or sinks are eliminated, the flux is equal across each pair of parallel faces. If a wind prevails, even though slight, the problem can be simplified by taking one axis of the cube parallel to the wind to eliminate the flux across one pair of planes. Each ice crystal will fall in a <u>direction</u> determined by the wind force and gravity. The <u>speed</u> of fall will be constant when the resultant of these forces is equal and opposite to the viscous drag force as determined by Stokes law, ie,

$$\vec{mg} + \vec{W} = - 6\pi \, \eta \, r \, \vec{v} \qquad (6)$$

where m is the mass of the crystal

$\vec{g}$ is acceleration of gravity

$\vec{W}$ is the wind force

η is the viscosity of air

r is the crystal radius, and

$\vec{v}$ is the terminal velocity

If the flux of crystals across the horizontal plane and the vertical plane, which is not parallel to the wind, could be absolutely determined one could calculate the volume density of crystals in the air. An approximation to this can be made by assuming that all crystals have a net downward component of velocity. Then, if the unit cube is imagined to be distorted parallel to the fall direction of a given size range, only the horizontal flux need be considered. In this case the precipitation rate can be taken as an approximation of the flux across the horizontal plane. When precipitation rates for each size range are determined and divided by their respective terminal velocities and summed over all size ranges one obtains the density of crystals in the air. Kumai (1964, pp. 11-13) has done this for his two precipitation measurements referred to above. He calculates the mass of ice crystals in the air to be 0.07 g m^{-3} for the -39°C case and 0.02 g m^{-3} for the -41°C case. Actually, these cases are not temperature dependent as is pointed out on p. 58 above, instead the situation should read: 0.07 g m^{-3} downtown and 0.02 g m^{-3} for the outlying areas according to this approximation.

The above approximations give minimum values because some of the crystals have a net upward velocity (pp. 53-54) and are therefore not included in the precipitation measurements. This can be demonstrated by a simple calculation based on the fact that thick ice fog at -50°C did not completely dissolve when

60

air temperature increased to -40°C. It is reasonable to assume that the air in thick fog is saturated (see pp 12-15 Appendix A). Also, as air warms its capacity to hold moisture increases, so some of the ice crystals suspended in it will dissolve. At saturation relative to ice the air can hold: 0.038, 0.119, and 0.338 g m^{-3}, at temperatures of -50, -40, and -30°C respectively. Thus, when the air warms from -50 to -40°C it can dissolve 0.073 g m^{-3} of ice and still be saturated; since this amount of warming reduced the density but did not completely dissolve the ice fog at the airport, where density is less than it is downtown, it is reasonable to expect 0.07 g m^{-3} to be a minimum value. On the other hand, ice fog always disappears when the temperature arises to -30°C. If the initial air temperature was -50°C the original water content of ice crystals could have been as high as 0.30 g m^{-3}; or 0.22 g m^{-3} if the initial temperature was -40°C. These are probably not maximum values, since when air temperature rises at the end of an ice fog event there is usually some advection of unsaturated air which would assist in dissolving the fog. The above calculation is simply based on a direct warming of the air with no advection.

Kumai's measurements indicate that ice fog density in downtown Fairbanks is 3 times greater than in the outlying areas. His method of measurement was the same in both places. However, the prevailing conditions were not the same in both places since there is more upward movement of air in the city than in the outlying areas. Therefore, his 3-fold difference in density represents a minimum difference between the core area and the outlying areas. Based on the above considerations we assume two conservative density values:

$$0.21 \text{ g m}^{-3} \text{ for the } 50 \text{ km}^2 \text{ core area, and}$$

$$0.07 \text{ g m}^{-3} \text{ for the outlying areas.}$$

Ice Fog Evaporation Rates

The daily input rate exceeds the precipitation rate by about 2000 x 10^6 g H$_2$O. It is instinctive to speculate on what would happen to this excess if no

evaporation took place. If ice fog with an average density of 0.10 g m^{-3} covered the extended area of 200 km^2 with no evaporation, it would increase in thickness by about 100 m day^{-1}. This is two orders of magnitude greater than the rate of increase in thickness seen in Figure 27. If a lower density value is assumed for the ice fog the calculated rate of thickening will increase. Such an order of magnitude calculation effectively demonstrates that a significant amount of ice fog is dissolved by the overlying warmer air. Temperature and water vapor density profiles measured during ice fog conditions (Fig. 34) show that air near the top of the ice fog layer can dissolve 1.5 to 3 times more ice than air near the bottom. This process is especially important over the city center where upward movement of ice crystals continually brings them into air which is more able to dissolve them.

The difference between calculated rates of increase in volume of the ice fog layer, which ignore evaporation, and its true rate of increase may be attributed to evaporation. To calculate an evaporation rate it remains to calculate a reasonable approximation for the actual rate of volume increase. To do this it is now only necessary to obtain some measure of the rate of increase in thickness of the ice fog layer since the other required parameters are already available, ie, the rates of input and precipitation, the areal extent covered by ice fog and its density. Thickening rates for ice fog when air temperature remains below -40°C can be estimated from Figure 27 to be about:

3.5 m day^{-1} for the downtown core area,

2 m day^{-1} for the leeward side of city center,

and   1 m day^{-1} for the windward side.

Leeward and windward as used here refer to the gravity drainage wind which exists during times of ice fog.

For our present purpose equation 5 may be rewritten as follows:

$$I = P_1 A_1 + P_2 A_2 + \rho_1 A_1 \frac{dz_1}{dt} + \rho_2 A_2 \frac{dz_2}{dt} + EA \qquad (5a)$$

where E is the average rate of evaporation for the entire area $A = A_1 + A_2$,

A_1 is the core area,

A_2 is the outlying area,

ρ_1 is the density of ice crystals in the air over the core area,

ρ_2 is the density of ice crystals in the air over the outlying area,

$\frac{dz_1}{dt}$ is the rate of thickening over the core area,

and $\frac{dz_2}{dt}$ is the rate of thickening over the outlying area.

The best estimates for these values available so far from the above discussions are:

$I = 4100 \times 10^6$ g H_2O day^{-1}

$P_1 = 4.3 \times 10^{-3}$ g H_2O cm^{-2} day^{-1}

$P_2 = 4.3 \times 10^{-5}$ g H_2O cm^{-2} day^{-1}

$\rho_1 = 0.21$ g m^{-3}

$\rho_2 = 0.07$ g m^{-3}

$A_1 = 50$ km^2 $= 50 \times 10^6$ m^2 $= 50 \times 10^{10}$ cm^2

$A_2 = 150$ km^2 $= 150 \times 10^6$ m^2 $= 150 \times 10^{10}$ cm^2

Three approximations to thickening rates will be considered, guided by the values from Figure 27, together with a fourth case involving negligible thickening rates.

Case 1. $\frac{dz_1}{dt} = 3.5$ m day^{-1}, $\frac{dz_2}{dt} = 1.5$ m day^{-1}

Case 2. $\frac{dz_1}{dt} = 3.0$ m day^{-1}, $\frac{dz_2}{dt} = 1.0$ m day^{-1}

Case 3. When an area of about 200 km^2 has been occupied, the thickening rate is markedly reduced at the outer perimeter. Assume that the outer perimeter

63

has a negligibly slow thickening rate and subdivide A_2 into an intermediate area A_2i of 100 km^2 and an outer perimeter A_2p of 50 km^2, assume growth rates of: $\dfrac{dz_1}{dt} = 3$ m day^{-1} $\dfrac{dz_{2i}}{dt} = 1$ m day^{-1} and $\dfrac{dz_{2p}}{dt} = 0$.

Case 4. Assume an extreme case of no thickening of the ice fog layer.

For each case a value of EA can be obtained from equation 5 as follows:

$$EA = I - P_1 A_1 - P_2 A_2 - \rho_1 A_1 \frac{dz_1}{dt} - \rho_2 A_2 \frac{dz_2}{dt} \qquad (5b)$$

The values I, $P_1 A_1$ and $P_2 A_2$ are common to all cases, ie

$$I = 4100 \times 10^6 \text{ g H}_2\text{O day}^{-1},$$

$$P_1A_1 = 2150 \times 10^6 \text{ g H}_2\text{O day}^{-1},$$

$$\text{and } P_2A_2 = 65 \times 10^6 \text{ g H}_2\text{O day}^{-1},$$

So equation (5b) becomes:

$$EA = \left(1885 \times 10^6 - \rho_1 A_1 \frac{dz_1}{dt} - \rho_2 A_2 \frac{dz_2}{dt}\right) \text{ g H}_2\text{O day}^{-1}.$$

The values of $\rho A \dfrac{dz}{dt}$ for the four cases are:

	Total	$\rho_1 A_1 \frac{dz_1}{dt}$	$\rho_2 A_2 \frac{dz_2}{dt}$	$\rho_2 A_{zi} \frac{dz_{2i}}{dt}$	$\rho_2 A_{2p} \frac{dz_{2p}}{dt}$
		All values x 10^6 g H$_2$O day^{-1}			
Case 1	52	36.75	15.75	—	—
Case 2	42	31.50	10.50	—	—
Case 3	38	31.50	--	7	0
Case 4	0	0	0	0	0

The resultant values of EA are:

Case 1   1833 x 10^6 g H_2O day^{-1},

Case 2   1843 "   "   ,

Case 3   1847 "   "   ,

and Case 4   1885 "   "   .

Since the total area covered, A, is about 200 km^2, we obtain the following evaporation rates:

Case 1   9.15 x 10^{-4} g H_2O cm^{-2} day^{-1},

Case 2   9.20 "   "   ,

Case 3   9.23 "   "   ,

Case 4   9.42 "   "   .

An average value of E can be used for several general calculations. The value E = 9.2 x 10^{-4} g H_2O cm^{-2} day^{-1} will be used here. It is within 0.5% of the three estimates involving calculated thickening rates, and within 2.5% of the extreme estimate based on no thickening.

Use of the Mass Budget Equation

An interesting use of equation 5 is in calculating the growth rate of volume occupied by ice fog. Assume that air temperature remains below -40°C that the core area of 50 km^2 is completely covered by a 3 m thick blanket of ice fog on the first day, and that the ice fog outside the core area is 1 m thick; calculate the extent of the outlying area. The amount of material available is:

$$I = 4100 \times 10^6 \text{ g } H_2O \text{ day}^{-1}.$$

The amount of material needed to form the 3 m thick layer of ice fog in the 50 km^2 core area is:

$$P_1 A_1 + E_1 A_1 + \rho_1 A_1 \frac{dz_1}{dt}$$

$$= \left(4.3 \times 10^{-3} \times 50 \times 10^{10} + 9.2 \times 10^{-4} \times 50 \times 10^{10} + 0.21 \times 50 \times 10^6 \times 3 \right) g\, H_2O\, day^{-1}$$

$$= 2672 \times 10^6\, g\, H_2O\, day^{-1}$$

Therefore $1428\, g\, H_2O\, day^{-1}$ is available for growth of the outer area, so

$$1428\, g\, H_2O\, day^{-1} = P_2 A_2 + E A_2 + \rho_2 \frac{dz_2}{dt} A_2 = A_2 \left(P_2 + E + \rho_2 \frac{dz_2}{dt} \right),$$

and $A_2 = \dfrac{1428\, g\, H_2O\, day^{-1}}{(0.43 + 9.2 + 0.07) \times 10^{-4}\, g\, H_2O\, day^{-1} cm^{-2}} = 147 \times 10^{10}\, cm^2 = 147\, km^2.$

Thus, after 1 day our ice fog layer is 3 m thick over the 50 km^2 core area and 1 m thick over an extended area of 147 km^2. In reality the thickness varies gradually and the ice fog is patchy (Fig. 25b). Notice that the majority of the input is lost by precipitation and evaporation and that only a small fraction actually remains suspended in the air.

As the area covered by ice fog increases there will be a balance between input and output. If we assume the core area to be 50 km^2 we can calculate the total area covered when this balance is achieved by setting $\frac{dv}{dt} = 0$.

$$I = P_1 A_1 + E A_1 + [P_2 + E] A_2$$

$$41' \qquad 640 + [0.43 + 9.2] \times 10^{-4}$$

$$\text{or } A_2 = \frac{4100 - 2640 \times 10^6}{(0.43 + 9.2) \times 10^{-4}} = 152 \times 10^{10}\, cm^2 = 152\, km^2$$

So that $A_1 + A_2 = 202\, km^2$ when equilibrium exists between input and output.

The mass budget as presented above is rough and can be revised as more accurate information is obtained for the parameters I, P, E, ρ and $\frac{dv}{dt}$. However, the order of magnitudes are probably well in hand. One refinement which immediately comes to mind is a breakdown of evaporation rates according to area just as was done for the precipitation rates, density values and growth rates. It is reasonable to expect that the evaporation rate is greater over

the city center than over the outlying areas for several interrelated reasons.
First, there is an active upward movement of crystals over the city. This
brings more crystals to the top of the ice fog over the city than over the out-
lying area. It also contributes to the fact that the top of the ice fog is at
a higher altitude over the city. The higher altitude in turn places the
crystals in warmer air which can dissolve more ice. From Figures 27 and 34 it
may be seen that air in contact with the ice fog top over the city can hold
at least twice as much water vapor as air at the ice fog top in outlying areas.
Also, it is important that wind increases with altitude, this means that the
water vapor dissolved into the air over the city center will be removed more
rapidly, this further increases the evaporation rate. From these consider-
ations it is reasonable to assume that the evaporation rate over the city is
more than twice that over the outlying areas.

One may experiment with values of the various parameters in equation 5 to
obtain upper and lower limits for them. For example accept the values for pre-
cipitation rates and densities and assume several sets of values for the
evaporation rates in the 50 km^2 core area and the extended area and calculate
the total area covered by ice fog at equilibrium between input and output,
ie. when $\frac{dv}{dt} = 0$.

	g H_2O cm^{-2} day^{-1}		g m^{-3}		g H_2O cm^{-2} day^{-1}		Total Area (km^2)
	P_1	P_2	ρ_1	ρ_2	E_1	E_2	
Case 1	4.3×10^{-3}	4.3×10^{-5}	0.21	0.07	9.2×10^{-4}	9.2×10^{-4}	202
Case 2	4.3×10^{-3}	4.3×10^{-5}	0.21	0.07	15×10^{-4}	7×10^{-4}	212
Case 3	4.3×10^{-3}	4.3×10^{-5}	0.21	0.07	20×10^{-4}	10×10^{-4}	141

In this example cases 1 and 2 are reasonable but case 3 obviously has exces-
sive evaporation rates for the equilibrium condition because the total area
covered is observably too small.

In summary the mass budget equation for Fairbanks ice fog and estimates for the parameters involved are as follows:

$$I = P_1 A_1 + P_2 A_2 + E_1 A_1 + E_2 A_2 + \rho_1 A_1 \frac{dz_1}{dt} + \rho_2 A_2 \frac{dz_2}{dt}$$

where I = rate of input $\approx 4100 \times 10^6$ g H_2O day^{-1}

A_1 = core area of ice fog ≈ 50 km^2

A_2 = area of outlying area ≈ 150 km^2

P_1 = precipitation rate in core area $\approx 4.3 \times 10^{-3}$ g H_2O cm^{-2} day^{-1}

P_2 = precipitation rate in outlying area $\approx 4.3 \times 10^{-5}$ g H_2O cm^{-2} day^{-1}

ρ_1 = density of ice fog crystals in core area $= 0.21$ g m^{-3}

ρ_2 = density of ice fog crystals in outlying area $= 0.07$ g m^{-3}

E = average evaporation rate for entire area $\approx 9.2 \times 10^{-4}$ g H_2O cm^{-2} day^{-1}

$\left.\begin{array}{l} E_1 = \text{evaporation rate in core area} \\ E_2 = \text{evaporation rate in outlying area} \end{array}\right\}$ $E_1 > 2 E_2$

Estimated values of E_1 and E_2 considered separately should be the subject of additional research. Values consistent with present information are:

$E_1 = 15 \times 10^{-4}$ g H_2O cm^{-2} day^{-1}

$E_2 = 7 \times 10^{-4}$ g H_2O cm^{-2} day^{-1}

Air Pollution

Many people seek comfort in comments such as: "Ice fog is not really harmful since it merely consists of ice crystals"-or "photochemical reactions which are so important in Los Angeles smog are unimportant here because of negligible sunlight during Fairbanks ice fog conditions." To be sure photochemical action is less important in Fairbanks during ice fog than in Los Angeles but one can't completely dismiss its importance without further investigation. Also, it is important to point out several prominent problems of ice fog, some of which are unique.

The small ice crystals suspended in ice fog constitute air pollutants even in the absence of other material; but they also play an important role in more popular aspects of air pollution by providing an extensive surface area capable of adsorbing and thereby concentrating pollutants. The fact that particulate material does adsorb to these crystals is shown by the tests described on pages 34-35. Also, the air-cleaning action of precipitation in general is a matter of common experience. This phenomenon is especially noticeable in the Los Angeles area when smoggy air becomes strikingly clean and transparent following a rainstorm. The amount of surface area per unit mass increases with decreasing particle size as summarized in the following table which assumes spherical shapes for simplicity; actual ice fog crystals have more complex shapes, so their specific surfaces will be greater than indicated here.

Diameter (μ)	Volume (X 10^{-10} cm^3)	Mass (X 10^{-10} g)	Area (X 10^{-8} cm^2)	Specific Surface cm^2 g^{-1}
1	0.005	.0046	3.14	68,295
5	0.65	0.596	78.54	13,178
10	5.23	4.796	314.16	6,550
20	41.9	38.42	1256.64	3,271
30	141.4	129.66	2827.43	2,181
40	335.1	307.29	5026.54	1,636
50	654.5	600.18	7853.98	1,309
60	1131.0	1037.13	11309.72	1,090

The specific surface area on ice fog crystals is about 10,000 cm^2 g^{-1}, and since their concentration is about 0.21 g m^{-3} in the core area, they provide an adsorption surface of about 2000 cm^2 per cubic meter of air. As the crystals gather up pollutants they serve as local concentration points suspended in the air with 0.5% of their mass being foreign matter. When crystals precipitate out of the air they take pollutants out with them. However, as crystals evaporate near the top of the ice fog layer some of the particulate matter may fall back into the polluted layer to increase the concentration of pollutants.

Compounds like lead, chlorine bromine, and SO_2 will not dissolve in the air like ice does. If half of these products were precipitated, as is the case for ice crystals, there would be a net increase of 30 kg Pb, 23 kg Br and 10 kg Cl suspended in the air each day. Consider the case for lead. If it could be dispersed uniformly throughout the entire 300×10^7 m^3 (it is more likely that it would be locally concentrated see Figs. 9, 10, 11) there would be an increased concentration of 10 μg Pb m^{-3} day^{-1}; at the end of ten consecutive days of ice fog the concentration could approach 100 μg m^{-3} in parts of the core area. The average atmospheric Pb concentration for the northern hemisphere is 0.005 μg m^{-3} (Patterson, 1964). The value for urban areas reaches 2 or 3 μg m^{-3} (Junge, 1963, p. 361) and Patterson (1964) has measured 10 to 20 μg m^{-3} in Pasadena, California. The above calculations may be excessive but they indicate that the lead concentration in downtown Fairbanks could easily double the high Los Angeles values. Samples of the lead content of Fairbanks air were measured during inversion conditions in 1965 by Drs. Winchester and Duce of MIT but results are not yet available.

Samples of soil taken in and around Fairbanks (Chapman and Benson, 1965) have been analyzed spectroscopically. First results indicate higher concentration of lead in the soil within the city of Fairbanks than in the adjacent outlying area. Additional sampling and analysis is underway including analyses of

70

particulate matter collected fi ice fog. This work will be presented in a separate paper. Lead seems to be the best trace element for ice fog because it has the widest range of variation, and it can be traced to the tetraethyl lead (TEL) added to gasoline. Direct measurement of lead in the air by fast portable techniques are available (Koppius, 1949). Rapid clinical tests of lead absorbed by people breathing polluted air are also available (Forman and Garvin, 1965) and physiological experiments in ice fog, both with people and test animals are in order and under consideration.

As shown on page 37 all of the halogens in TEL fluid don't combine with lead. The presence of halogens in the air raises questions of possible chemical reactions. Among them, the formation of methyl chloride is only one of many which comes to mind; in the presence of methane a simple reaction would be:

$$CH_4 \quad + \quad Cl_2 \underset{\longleftarrow}{\overset{\longrightarrow}{\quad\quad}} CH_3 Cl \quad + \quad HCl$$
Methane   Methyl Chloride

The concentration of CO_2 undoubtedly becomes high during ice fog. The daily input by weight is the same as that for water, ie, 4100×10^6 g CO_2day^{-1}; but, CO_2 does not precipitate out the bottom nor evaporate from the top of the ice fog as water does. Therefore, one days input of CO_2 into the maximum of $300 \times 10^7 m^3$ of air available to ice fog would give a concentration of 0.1% compared to the normal amount of CO_2 in the atmosphere which is 0.046% by weight. After 10 days of ice fog conditions the CO_2 content of the air could exceed 1% in parts of the core area. The concentration of CO may also achieve high values in parts of the downtown area and CO measurements must be made.

An interesting case arises in connection with the sulfur which is added to low-temperature ice fog. The daily input of SO_2 is 8.6×10^6 g SO_2 day^{-1}. Some of the SO_2 is oxidized to SO_3 and reacts with H_2O to form H_2SO_4 droplets in the air. Droplets of H_2SO_4 exist in polluted fog as shown by Costes and

71

Courtier (1936). They were able to measure concentrations of H_2SO_4 in London, but only when fog was present; fog-free air was also free from H_2SO_4 althoug' it contained ample SO_2. The H_2SO_4 - SO_3 - H_2O reaction is more active at temperatures below, than above, 0°C (Mellor, 1930); this is one example of a chemical reaction which is more likely to be a problem in the low temperatures of ice fog than in the high-temperature smogs of Los Angeles. The reduction of vapor pressure over droplets of H_2SO_4 may be one of the reasons that fog persists in cities longer than in open country (Dobson, 1948, p. 143). This interpretation is also in agreement with observations on ice fog.

In addition to the products listed on p. 38, dry cleaning establishments in Fairbanks and Ft. Wainwright use 500 liters of solvents per day. These heavy molecules are toxic[*] but it is not known what concentrations occur locally in the stagnant ice fog air of Fairbanks. The concentrations of all pollutants increase in Fairbanks air during ice fog conditions, and research is clearly needed on the air chemistry of ice fog.

Remedial Action

One of the best remedial actions for ice fog is to concentrate on eliminating low altitude sources of water vapor. During strong inversions which prevail during ice fog events it is especially important to discharge pollutants at the highest possible altitude. The exhaust plumes from power plants provide an excellent example. As shown by Barad (1951) the diffusion of stack gases in very stable atmospheres should be treated as coming from a planar source of finite concentration rather than as from a point of infinite concentration. Barad's treatment agrees well with observations on power plant plumes which remain aloft and move with the wind, rarely joining the main ice fog before they dissolve (Figs. 20, 25a, 25c). Thus, the exhaust products from coal burned in power plants are separated from those derived from

[*]Consumer Reports, July 1964, p. 317 sites toxic effects of Perchloroethylene, the solvent used in Coin-op establishments.

domestic coal on pages 19 and 30. As a source of ice fog one could probably neglect the entire output of power plant exhaust gases which go above the inversion layer, even though they are so dramatic in appearance.

The lower the level of a pollutant source the more it contributes to the ice fog. Cooling waters from power plants are the largest single source (64%), and they are at ground level. However, automobile exhausts although they contribute only 3% of the total moisture are next in importance as a water vapor source because of their low altitude. Also, they are probably the most dangerous of all sources because of products other than water which accompany them.

Fig. 36. Ice Fog Probability. The ice fog probability is defined here as the fraction of total hours, at or below the indicated temperature, which have visibilities below the indicated value. In each of the three cases shown here the limiting visibility is 5 miles. When temperatures are below -30°C there is a good probability of ice fog; this increases to more than 50% when we consider only temperatures at or below -35°C and is nearly always 100% for temperatures at and below -40°C. The exceptionally mild winter of 1960-1961 had negligible ice fog whereas the subsequent winters had severe ice fog during each cold spell. The data are from U.S. Weather Bureau Station at the Fairbanks Airport.

A summary of ice fog probability for each degree (F) from -25 to -60°F (Politte 1965, Johnson 1965) shows a steady increase from 10% at -30F to 74% at -43°F, followed by a slight decrease between -50 and -54°F and an increase at still lower temperatures.
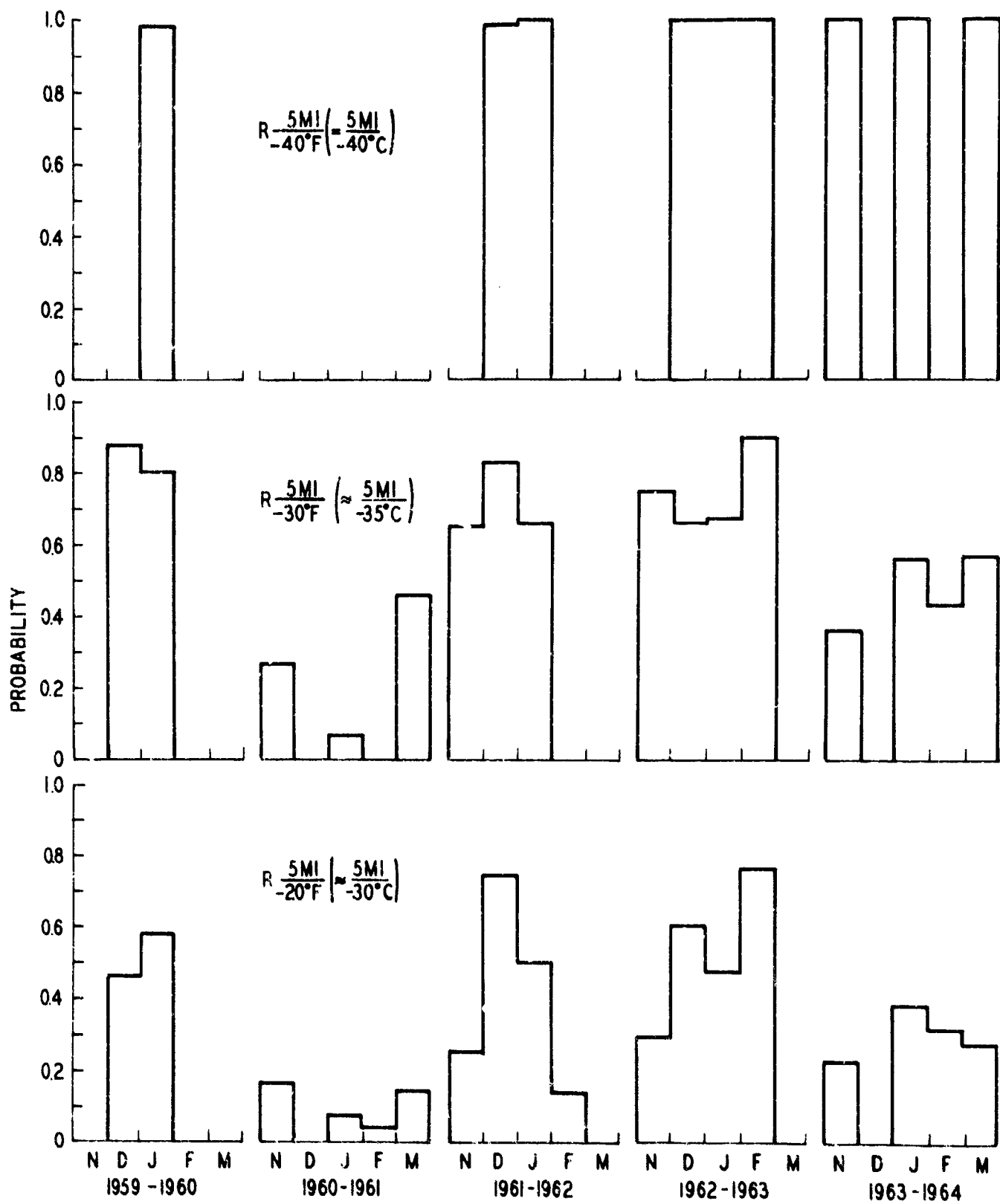
Figure 36

Fig. 37. Ice Fog Probability, 1947 to 1964 at Eielson AFB and 1959 to 1964 at Fairbanks. Richardson (1964) selected the temperature (-20°F, $\simeq$ -30°C) and visibility conditions (3 miles $\sim$ 5 km) and summarized these probability data for Eielson AFB. Corrections were applied to the values from 1961 to 1964 by Johnson (1964). The Fairbanks values were computed from U.S. Weather Bureau data. The mild winter of 1960-1961 shows clearly in this figure as in figure 36.

The apparent reduction in amount of ice fog at Eielson AFB since 1958 coincides with two events: (1) movement of the transmissometer away from ice fog produced by activities in the housing and commissary areas of the base; (2) the B-36 aircraft terminated their operations at Eielson AFB in 1958. These aircraft with six propeller and four jet engines had long warm up periods (in excess of 45 minutes). They produced more ice fog than do the jet aircraft which have very short warm-up and checkout procedures.
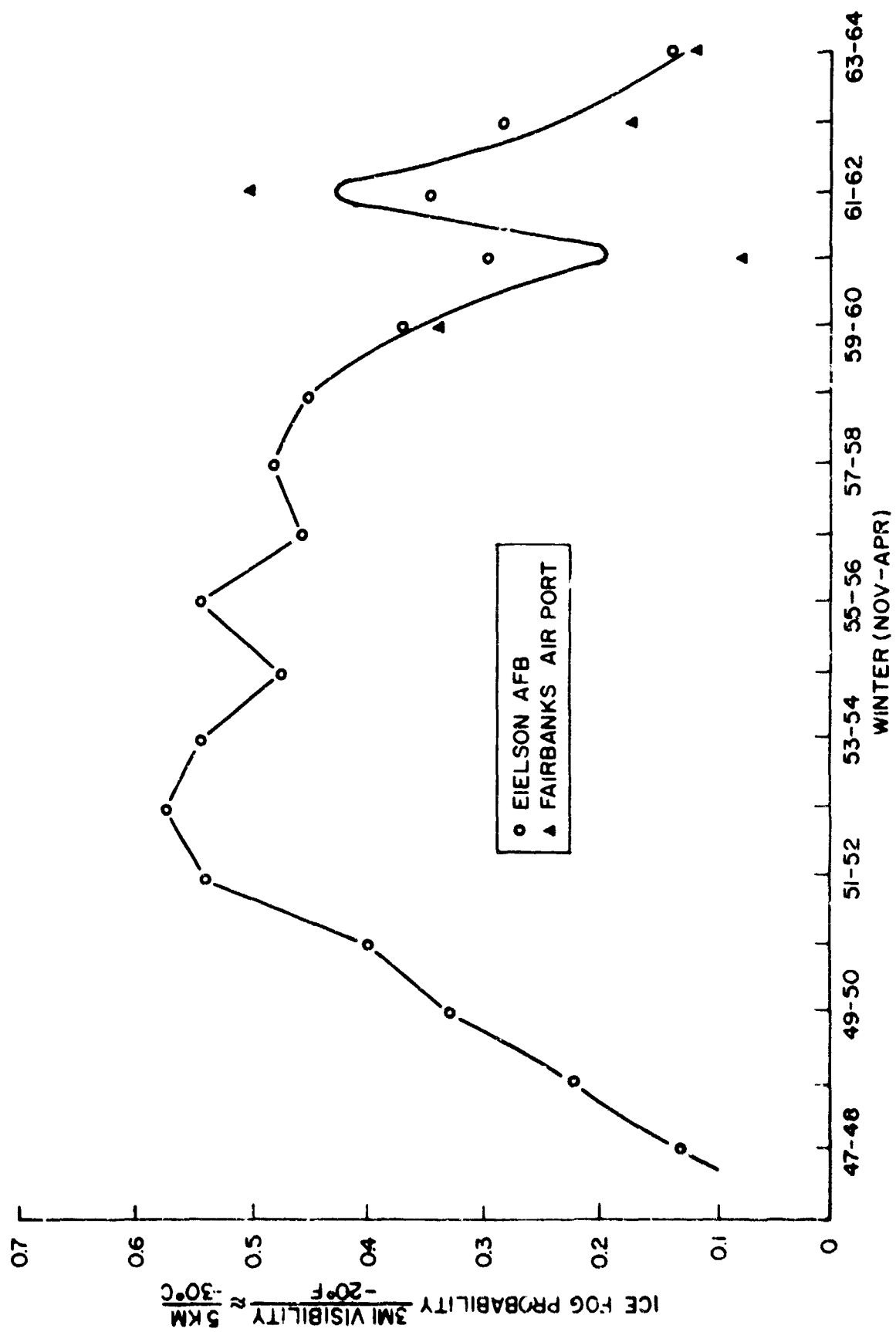
Figure 37

REFERENCES CITED

Altman, P. L. and D. S. Dittmer (1964, Compilers and Editors of <u>Biology Data</u> <u>Book</u>, Federation of American Society of Experimental Biology, Washington,D.C.

Ball, F. K. (1960), Winds on the Ice Slopes of Antarctica, <u>Antarctic Meteorology</u>: Proceedings of the Symposium held in Melbourne, Feb. 1959, pp. 9-16.

Barad, Morton L. (1951), Diffusion of Stack Gases in very Stable Atmospheres, <u>Meteorological Monographs</u>, (4):9-14.

Benson, Carl S., Yngvar Gotaas, Karl E. Francis and Wallace B. Murcray (1964), Ice Fog Studies in the Fairbanks Area 1961-1963. <u>Proceedings of the 15th</u> <u>Alaskan Science Conference</u>, p. 89.

Best, C. H. and N. B. Taylor (1952), <u>The Living Body</u>, A Text in Human Physiology 3rd Ed. Henry Holt & Co. N.Y. (792 pp).

Carey, Fabian (1964), Personal Communication, 17 July 1964.

Carlson, John (1964), North Star Borough Tax Assessor, Personal Communication.

Chambers, Leslie A. (1962), Classification and Extent of Air Pollution Problems Chapter I, Vol. I of <u>Air Pollution</u> Edited by Arthur C. Stern, Academic Press, N.Y.

Chandler, T. J. (1962), London's Urban Climate, <u>Geographical Journal</u> Vol.128, pp. 279-302.

Chapman, John (1963), Fairbanks City Engineer, Personal Communication.

Chapman, R. and C. Benson (1965), Unpublished Results of Preliminary Studies during Summer 1965.

Clark, J. P. (1963), The Effect of Combustion upon the Formation of Ice Fog in the Greater Fairbanks Area, Unpublished term paper for course in Arctic Engineering at University of Alaska.

Coste, J. H. and G. B. Courtier (1936), Sulphuric Acid as a Disperse Phase in Town Air, <u>Transactions of the Faraday Society</u>, Vol. 32, Part 8, pp 1198-1202.

Dalrymple, P. (1964), Personal Communication of data on strongest temperature inversion observed at S. Pole.

Dines, L. H. G. (1931), Temperature Observations in Fog at Kew Observatory, <u>The</u> <u>Meteorological Magazine</u>, Vol. 65, No. 780, pp. 277-280.

Dobson, G. M. B. (1948), Some Meteorological Aspects of Air Pollution, <u>Quarterly</u> <u>Jour. Roy. Met. Soc</u>. Vol. 74, No. 320, pp. 133-143.

Dorsch, R. G. and B. Boyd (1951), X-ray Diffraction Study of the Internal Structure of Supercooled Water, <u>U.S.N.A.C.A. Washington, Tech. Note No. 2532</u>.

Dorsch, R. G. and P. T. Hacker (1950), "Photomicrographic Investigation of Spontaneous Freezing Temperature of Supercooled Water Droplets", <u>U.S.N.A.C.A.</u> <u>Tech. Note 2142</u>.

Dorsch, R. G. and J. Levine (1952), "A Photographic Study of Freezing of Water Droplets Falling Freely in Air." <u>N.A.C.A. Res. Memo</u>. E51217, Feb. 25, 1952.

Elkin, H. F. (1962), Petroleum Refinery Emissions, Chapter 23, Air Pollution Vol. II, Edited by Stern, A.C.

Forman, Donald T. and James E. Garvin (1965) Rapid Determination of Lead in Urine by Ion Exchange, Clinical Chemistry, Vol. 11, No. 1 pp 1-9.

Fuoss, Raymond M. and Filippo Accascina, (1959) Electrolytic Conductance 279 pp. Interscience Publishers, Inc., N.Y.

Gorai, M. (1951), Petrological Studies on Plagioclase Twins, Am. Mineralogist, Vol. 36, pp 884-901.

Gordon, Mack (1965), Air Pollution Control, Science, Vol. 148, No. 3672, p.894.

Grant, D. R. (1965), Waves in an Inversion Layer, Met. Mag., Vol. 94, pp 34-37.

Haagen-Smit, A. J. (1952), Chemistry and Physiology of Los Angeles Smog, Ind. Eng. Chem. Vol. 44 pp 1342-1346.

Haagen-Smit, A. J. (1959), Urban Air Pollution, Advances in Geophysics, Vol. 6, pp 1-17, Academic Press, N.Y.

Haagen-Smit (1962), Reactions in the Atmosphere, Chapter 3 of AIR POLLUTION, Vol. I, Edited by Arthur C. Stern, Academic Press, N.Y.

Hallet, J. (1965), Field and Laboratory Observations of Ice Crystal Growth from the Vapor, Jour. Atmospheric Sciences, Vol. 23, pp 64-69.

Haltiner, George J. and Frank L. Martin, (1957) Dynamical and Physical Meteorology, 470 pp. McGraw-Hill Book Co., N.Y.

Hankinson, F. (1964), Personal Communication, Department of Mining and Metallurgy, University of Alaska.

Hanson J. (1964), Personal Communication of U.S.W.B. data shown in Table I.

Johnson, Wm. R. (1953), The Diurnal Height Variation of the Temperature Inversion in Southern California, Technical Bulletin Vol. 1, No. 2, March 1953, 3rd Weather Group Pub. Norton AFB, California.

Johnson, W. R. (1964) Major, USAF, Air Weather Service, Eielson, AFB, Personal Communication on Ice Fog Probability calculations.

Johnson, W. R. (1965) Ice Fog at Eielson AFB, Alaska with Statistical Analysis of Ice Fog Visibility and Temperature, U.S. Air Force Technical Report, Eielson Air Force Base, Alaska.

Junge, C. E. (1963) Air Chemistry and Radioactivity, Academic Press, N.Y., (382 pp)

Karabelinkoff, W. (1963) Personal Communication, Foreman, Ft. Wainwright Power Plants.

Koppius, O. G. (1949), Detection of Lead in Air with the Aid of a Geiger-Müller Counter, Journal of the Optical Society of America, Vol. 39, No. 4, pp 294-297.

Kumai, Motoi, (1964), A study of Ice Fog and Ice-Fog Nuclei at Fairbanks, Alaska, Part I. CRREL Research Report 150.

Kuno, Yas (1956), Human Perspiration (416 pp.) C. C. Thomas, Publisher, Springfield, Ill.

Magill, P. L. and R. W. Benoliel, (1952) Air Pollution in Los Angeles County: Contribution of Combustion Products, Ind. Eng. Chem. Vol. 44, No. 6, pp 1347-1351.

Magono, Choji (1954), On the Falling Velocity of Solid Precipitation Elements, Science Reports of the Yokohama National University, Sec. 1, No. 3, pp 33-40.

McGee, George (1963, Deputy Post Engineer, Ft. Wainwright, Personal Communication

Mellor, J. W. (1930), Comprehensive Treatise on Inorganic and Theoretical Chemistry, Vol. 10, Sulfur and Selenium, Longmans Green & Co. Inc., N.Y.

Merryman, T. (1964), Personal Communication, Foreman South Power Plant, Ft. Wainwright, Alaska.

Midgley, Thomas (1925), Tetraethyl Lead Poison Hazards, Ind. Eng. Chem. Vol. 17, No. 8, pp 827-828.

Nelson, W. L. (1958), Petroleum Refinery Engineering 960 pp. McGraw-Hill Book Co.

Nyberg, A. (1938), Temperature Measurements in an Air Layer very Close to a Snow Surface: Geografiska Annaler Vol. 20, pp 234-275.

Obert, E. F. (1950), Internal Combustion Engines, 2nd Edition 596 pp. plus appendicies. International Text Book Co., Scranton, Pa.

Pack, Donald H. (1964), Meteorology of Air Pollution, Science, Vol. 146, No. 3648, pp. 1119-1128.

Patterson, C. C. (1964), Personal Communication.

Politte, F. E. (1965), Minimum Ice Fog Visibility at Low Temperatures at Eielson AFB, Alaska, U.S. Air Force Technical Report, Eielson Air Force Base.

Plyler, E. K. (1924) The Infrared Absorption of Ice, Journal of the Optical Society of America and Review of Scientific Instruments, Vol. 9, pp. 545-555.

Plyler, E. K. (1926), "The Growth of Ice Crystals", Journ. of Geol. Vol. 34, pp. 58-64.

Reimer, Harry (1964), Municipal Utilities System of Fairbanks, Personal Communication.

Richardson, Gary L., (1964) Ice Fog Pollution at Eielson Air Force Base, A project presented to the Faculty of the University of Alaska in Partial Fulfillment of the requirements for the M.S. Degree.

Robertson, George W. (1955), Low-Temperature Fog at Edmonton Airport as Influenced by Moisture from Natural Gas, Quart. Jour. Royal Met. Soc. Vol. 81, No. 348, pp. 190-197.

Robinson, E., G. B. Bell, W. C. Thuman, G. A. St. John and E. J. Wiggins (1955), An Investigation of the Ice Fog Phenomena in the Alaskan Area, Final Report, Contract No. AF 19(122)-634, Stanford Research Institute, Stanford, Calif.

Robinson, E. and G. B. Bell, Jr. (1956) Low-Level Temperature Structure under Alaskan Ice Fog Conditions, Bull. Am. Met. Soc. Vol. 37, No. 10, pp 506-513.

Robinson, E., W. C. Thuman, and E. J. Wiggins, (1957) Ice Fog as a Problem of Air Pollution in the Arctic, Arctic Vol. 10, pp.89-104.

Ross, J. V. (1957), Combination Twinning in Plagioclase Feldspars, Am. Jour.Sci. Vol. 255, pp 650-655.

Schmidt, F. H. and J. H. Boer (1963), Local Circulation Around an Industrial Area, Berichte des Deutschen Wetterdienstes, Band 12 Nr. 91 pp 28-31.

Schaefer, V. J. (1941), A Method for Making Snowflake Replicas, Sci.Vol. 93, No.2410,pp 239-240.

Selvig, W. A. and W. H. Ode (1957), Low-temperature Carbonization Assays of North American Coals, Bulletin 571, U.S. Bureau of Mines.

Smith, V. M. (1963), Personal Communication.

Smithsonian Meteorological Tables (6th Ed.) Prepared by R. J. List, Smithsonian Miscellaneous Collections, Volume 114, Publication 4014 Washington, D.C.

Stefansson, Vilhajalmur (1913), My Life with the Eskimo, MacMillan & Co. See p. 235 for reference to ice fog produced by Caribou.

Swinbank, W. C. (1947) "Collisions of Cloud Droplets", Nature, Vol 159, pp 849-850.

Thuman, Wm. C., and E. Robinson (1954), Studies of Alaskan Ice-Fog Particles, Journal of Meteorology, Vol. 11, pp. 151-156.

Vance, J. A. (1961), Polysynthetic Twinning in Plagioclase, Am. Mineralogist, Vol. 46, pp 1097-1119.

Vance, Joseph A. (1962), Zoning in Igneous Plagioclase: Normal and Oscillatory Zoning, Am. Jour. Sci. Vol. 260, pp 746-760.

Van Krevelen, D. W. (1961), Coal, Typology-Chemistry-Physics-Constitution 514 pp. Elsevier Pub. Co.; Amsterdam, London, N.Y.

Went, F. W. (1955), Air Pollution, Scientific American, May 1955, Vol. 192, No. 5, pp. 62-72.

Wexler, H. (1941), Observations of Nocturnal Radiation at Fairbanks, Alaska and Fargo, N. Dak. Mon. Wea. Rev., Suppl. No. 46.

Woolum, Clarence A. (1964), Notes from a Study of the Microclimatology of the Washington, D.C. Area for the Winter and Spring Seasons, Weatherwise, Vol. 17, No. 6, pp. 262-271.

APPENDIX A

The Effect of Suspended Ice Crystals on Radiative Cooling[*]

by

Yrgvar Gotaas[**]and Carl S. Benson

Geophysical Institute
University of Alaska
College, Alaska

Weyl, W. A. (1951), Transitions in Glass, from Phase Transformations in Solids by Smoluchowski, Mayer & Weyl. Published by John Wiley & Sons, Inc. New York, N.Y., pp. 296-334.

Williams, G. P. (1959), Frazil Ice, A Review of its Properties with a Selected Bibliography, The Engineering Journal, Vol. 42, No. 11, pp. 55-60.

Workman, E. J., and S. E. Reynolds, (1949), Electrical Phenomena Resulting from the Freezing of Dilute Solutions, Phys. Rev., Vol. 75, Ser. 2, pp. 347-348

Workman, E. J., and S. E. Reynolds (1950), Electrical Phenomena Occurring during the Freezing of Dilute Aqueous Solutions and their Possible Relationship to Thunderstorm Electricity, Phys. Rev. Vol. 78, No. 3, p. 254-259.

Young, S. W. (1910), Mechanical Stimulus to Crystallization in Supercooled Liquids, Journ. Am. Chem. Soc. Vol. 33, pp. 148-162.

Young, S. W. and W. J. Van Sicklen (1913), The Mechanical Stimulus to Crystallization, Journ. Am. Chem. Soc. Vol. 35, pp. 1067-1078.

CONTENTS

LIST OF FIGURES

i

ABSTRACT

Two periods of very low (below -40C) surface temperature at Fairbanks, Alaska were studied in detail as part of ice fog investigations during the 1961-1962 winter. The observed cooling rates from the snow surface up to 3000 m were too large to be satisfactorily explained by advection and/or by radiative heat losses from the air and from the snow surface. The excess is shown to be due to radiation from ice crystals suspended in the air.

The ice crystals, formed by overall cooling of the air, act as heat sinks. Heat flows from the air to the crystals and is radiated away. This process results in strong temperature gradients in the air immediately adjacent to the crystals. It also accounts for the fact that humidity measurements show less than saturation values during occurrences of ice fog, light snowfall, or "diamond dust" crystal displays. The air temperature values used in determining humidity pertain to ambient air between the ice crystals, whereas the air in contact with crystals has a lower temperature and is saturated with respect to ice.

1. Introduction

As part of an investigation on ice fog in and around Fairbanks, Alaska, two prolonged, extreme (below -40 C) cold spells were studied in detail. The first one, from 15 to 29 December 1961, set an all time Fairbanks record for the month of December with 231 consecutive hours below -40 C, including an officially recorded minimum of -52 C (-61.6 F). The second cold spell lasted from 23 to 29 January 1962.

The mechanism of heat loss by radiation from the snow surface outlined by Wexler (1936) does not seem sufficient to explain the rapid cooling of the air in these cases. This is especially so because the cooling does not start at the surface and spread upward but occurs simultaneously at all levels up to 3 km. Advection must be considered as indicated by Wexler. However, in addition to advection, the radiative heat losses from ice crystals formed, and suspended, in the cooling air appear to play a major role. This will be demonstrated by outlining the physical history of the two cold spells and comparing observed and calculated cooling rates with, and without, allowance for radiation from suspended ice crystals.

The surface and upper air data used in this paper were obtained from the U.S. Weather Bureau station at Fairbanks International Airport, situated 6 km southwest of the city of Fairbanks (in the Tanana River Flats, 130 m above sea level).

It is not the purpose of this paper to discuss ice fog. However, since this study grew out of ice fog investigations, a general description of the phenomenon is in order. Ice fog is primarily a man-made air pollution problem which becomes a nuisance at temperatures below -30 C in the Fairbanks - Ft. Wainwright area of interior Alaska. It is produced by water vapor output from automobile exhaust, power plant stacks, household chimneys and other sources

associated with urban environments. The reduction of visibility by ice fog, although serious in itself, is only one of the more obvious manifestations. Aside from local sources of water vapor, such as hot springs and caribou herds, ice fog is restricted to populated areas. It rarely exceeds 30 m in thickness, although it exceeded 50 m over Fairbanks during the cold spell of 15-29 December 1961. The most detailed published work on ice fog to date is that by Robinson et al (1955). Research associated with the study described here will be published in another paper; a preliminary account was presented at the 15th Alaskan Science Conference (Benson, Gotaas, Francis, and Murcray, 1964).

2. The Period 14-30 December 1961.

On 14 December high surface pressure started building up over Northern Alaska and during the following days gradually spread over the interior. Simultaneously, a low pressure center was situated over the Gulf of Alaska. This situation persisted until 29 December, when a new and stronger low pressure center moved into the Gulf and the high pressure system rapidly moved into Canada. During the whole period, 15 to 30 December, the high was centered north of Fairbanks, causing north-easterly winds at low levels.

Fig. 1 shows the temperature variations at different levels. Selected soundings are shown in Fig. 2; the strength and vertical extent of inversions are shown in Fig. 3, and the upper wind data for the period are summarized in Fig. 4.

Temperatures from a hill top (Birch Hill) 2.5 km northeast of the city and 200 meters above the flat, are available, but are not shown in Fig. 1. Only occasionally do they differ more than a few degrees from the free air temperatures at the 200 meter level. Thus it appears that a local strong surface inversion over the hill top does not form. This inference is supported by measurements made on micrometeorological towers during the 1962-63 winter. For

Fig. A-1. Temperature variations at selected heights, December 1961, from U.S. Weather Bureau rawinsonde data, Fairbanks.
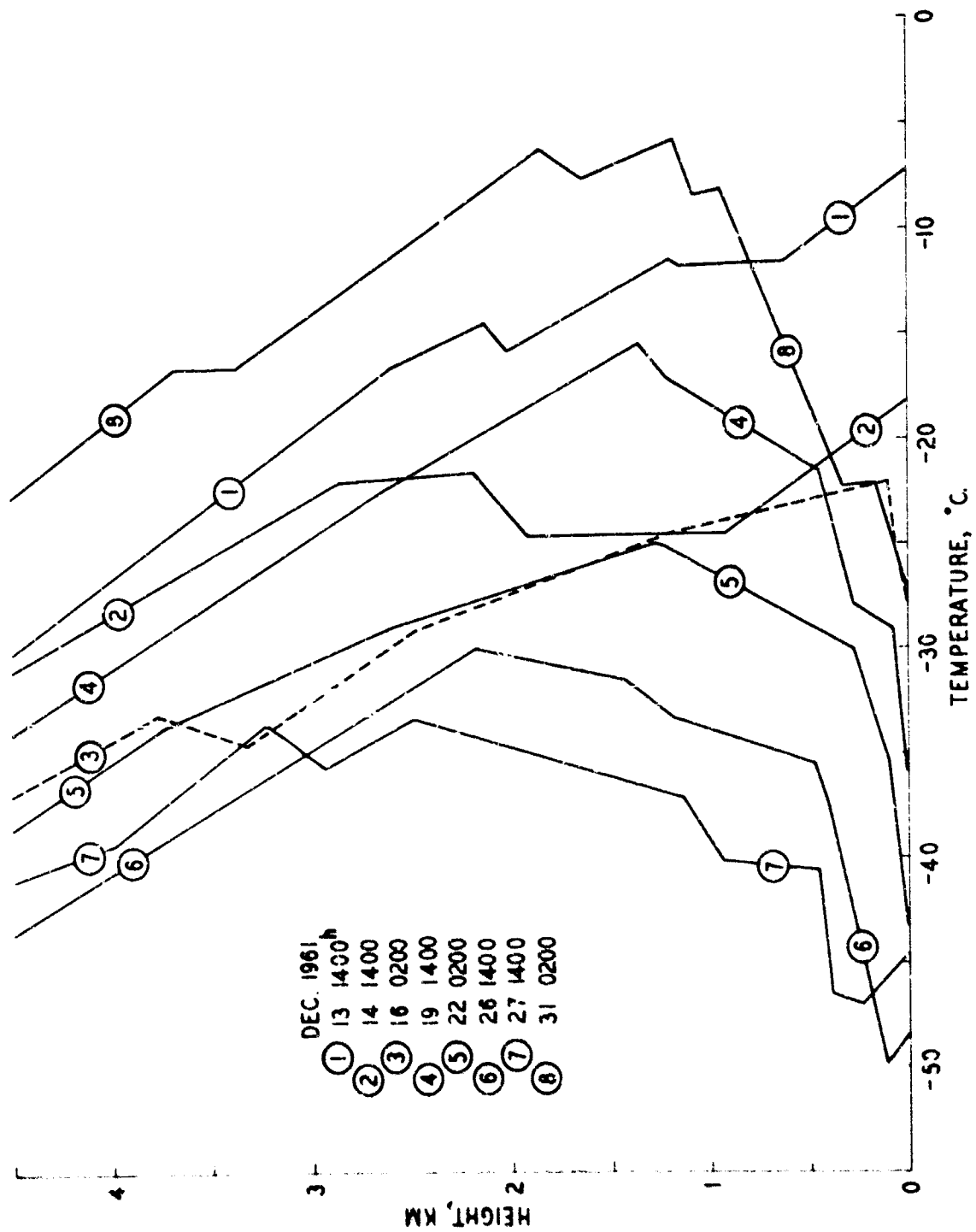
Fig. A-2. Temperature profiles, December 1961, from U.S. Weather Bureau rawinsonde data Fairbanks.
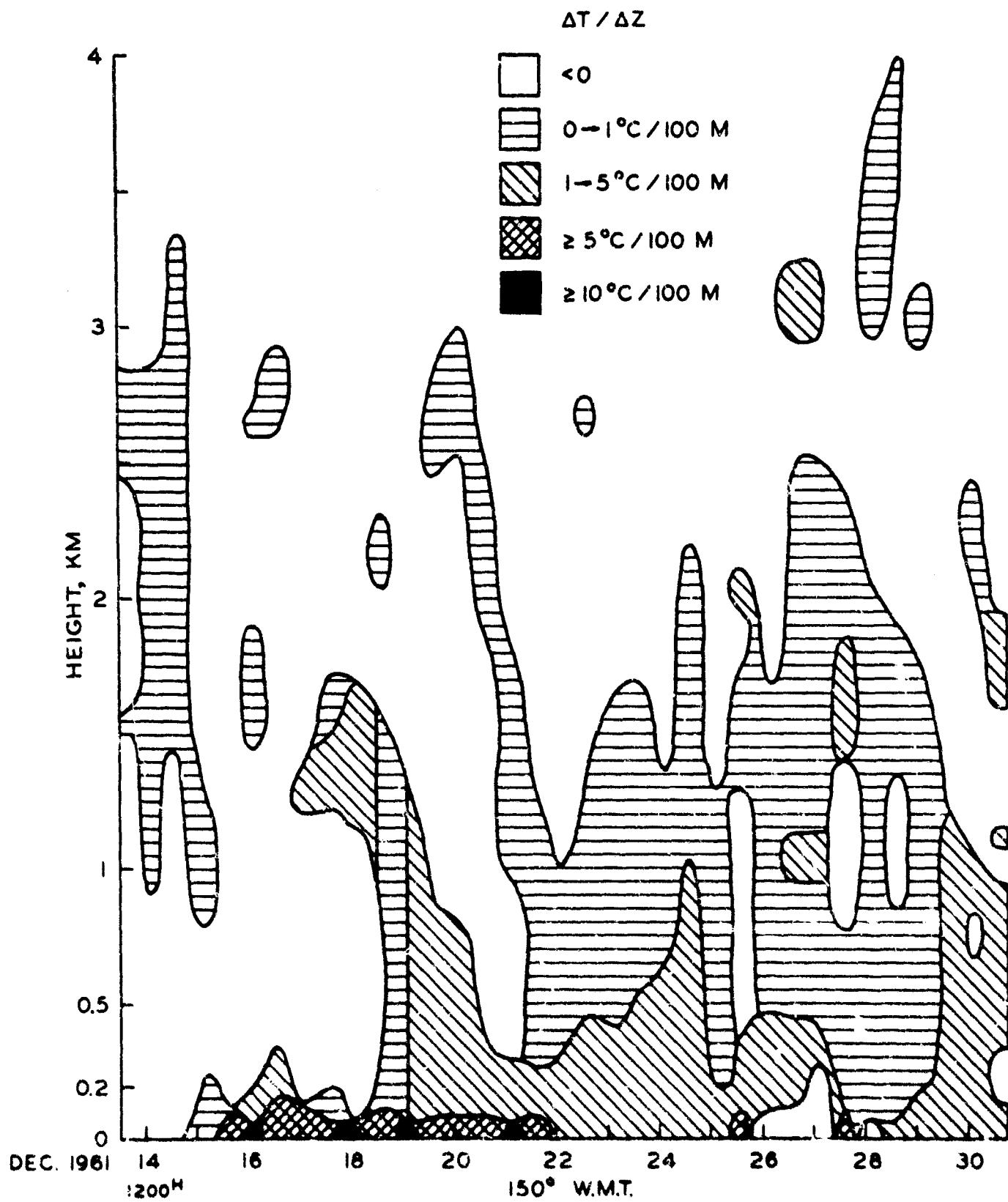
Fig. A-3. Strength and vertical extent of inversions based on rawinsonde data from U.S. Weather Bureau, Fairbanks.
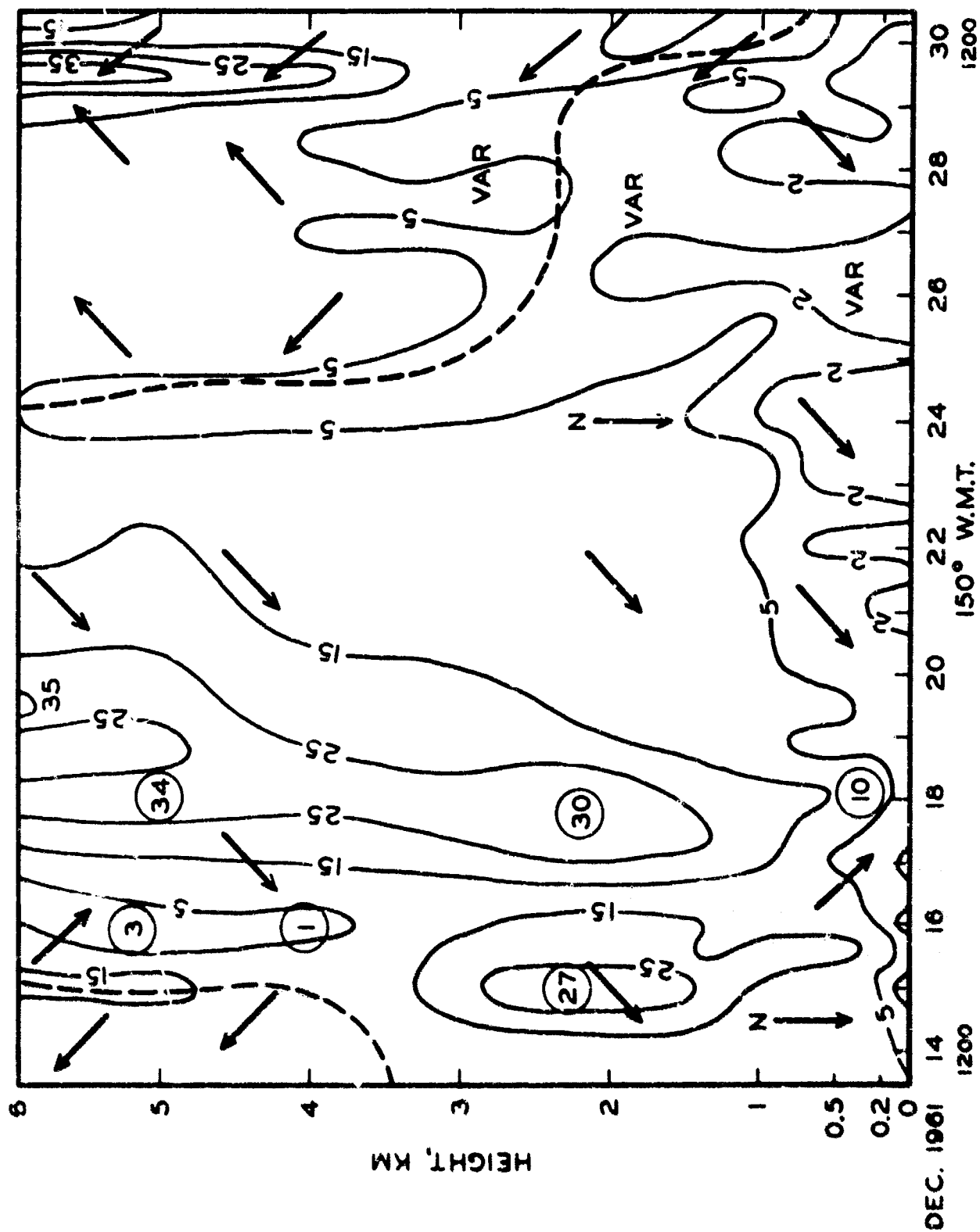
Fig. A-4. Upper winds, December 1961, U.S. Weather Bureau rawinsonde data, Fairbanks. Isolines are drawn for 2, 5, 15, 25 and 35 meters per second. Wind directions are indicated by arrows, and dashed lines divide northerly from southerly flows. VAR = variable directions.

example, during the cold period 7-9 January 1963 the temperature difference between 2 and 15 m above snow surface on top of Birch Hill rarely exceeded 1 C; during the same time period, similar measurements at the base of the hill, commonly showed differences of 4 to 5 C.

Even though surface winds were low, nearly always less than 2 m sec^{-1}, one could hardly consider the entire airmass to be stagnant. Upper level winds were variable (Fig. 4) and both the depth and strength of the inversions underwent considerable changes. The improved visibilities and higher temperatures between 18 and 19 December are, for instance, correlated to the higher wind speeds at low levels, accompanied by a decreased ground inversion.

On 25 December air started moving in from the south at higher levels, bringing in some high clouds, and weakening the inversion. When clouds appeared at medium altitudes on 27 December, the surface temperatures increased and visibility improved. However, the clouds rapidly dissolved and the surface temperature dropped to a record low for the month of December, -52 C on 28 and 29 December. The tempreature at the 200 meter level (and at Birch Hill) approached the values of the flats on 27 December, thus creating an isothermal layer. The 200 meter temperature started rising on 28 December, about 24 hours before the increase in surface temperature. Not until the southerly flow penetrated to lower levels, accompanied by increasing cloudiness, did the ground inversion break up. Then the cold spell ended and temperatures at all levels rose rapidly.

3. The Period 23-29 January 1962

The weather development was similar to the December case. On 23 January high surface pressure started building up over northern Alaska and slowly intensified. A stationary low was situated in the Gulf of Alaska and, on 26 January, a strong cyclone moved into the Gulf. By 28 January the cold spell ended.

Temperature variations at different levels during this cold spell are shown in Fig. 5. Temperatures at Birch Hill again closely followed those of the free air at the same level and are not shown. Most of the time the surface wind was less than 2 m sec^{-1}. Selected soundings are shown in Fig. 6. Fig. 7 is a photograph taken 27 January from Birch Hill overlooking the south eastern Fairbanks area. The smoke plume from a power plant is clearly visible, drifting with the wind down the valley. The height to which it rises before spreading out horizontally is a function of the outlet temperature and velocity as well as of the lapse rate (negative) in the air. Thus, visual observation or photographs of smoke plumes do not, in themselves, provide reliable information on the increase of windspeed with altitude nor on the inversion.

4. Discussion of data

Wexler (1936 and 1941) has shown how extreme low surface temperatures can be explained theoretically by radiational cooling, and that temperatures at intermediate and higher levels will set a limit to the cooling of the surface air. Not before temperatures at these levels get sufficiently low can the extreme low surface temperatures be obtained. The radiative cooling of polar air during clear weather starts below and spreads upwards in successive stages. A strong surface inversion develops, but decreases in strength with time. Above the ground inversion an isothermal layer should develop and increase in thickness. But subsidence will have a tendency to lower the top of the isothermal layer and create a weaker inversion above the ground inversion. The data presented here agree with Wexler's model; the ground inversion is strongest in the first parts of the cooling periods, and the effect of subsidence can be seen in Fig. 3.

Apart from the warming on 18 December, which can partly be ascribed to advection, increased wind speed, and turbulent mixing, the observed patterns within the cooling periods seem on the whole to agree with Wexler's findings.

A-4
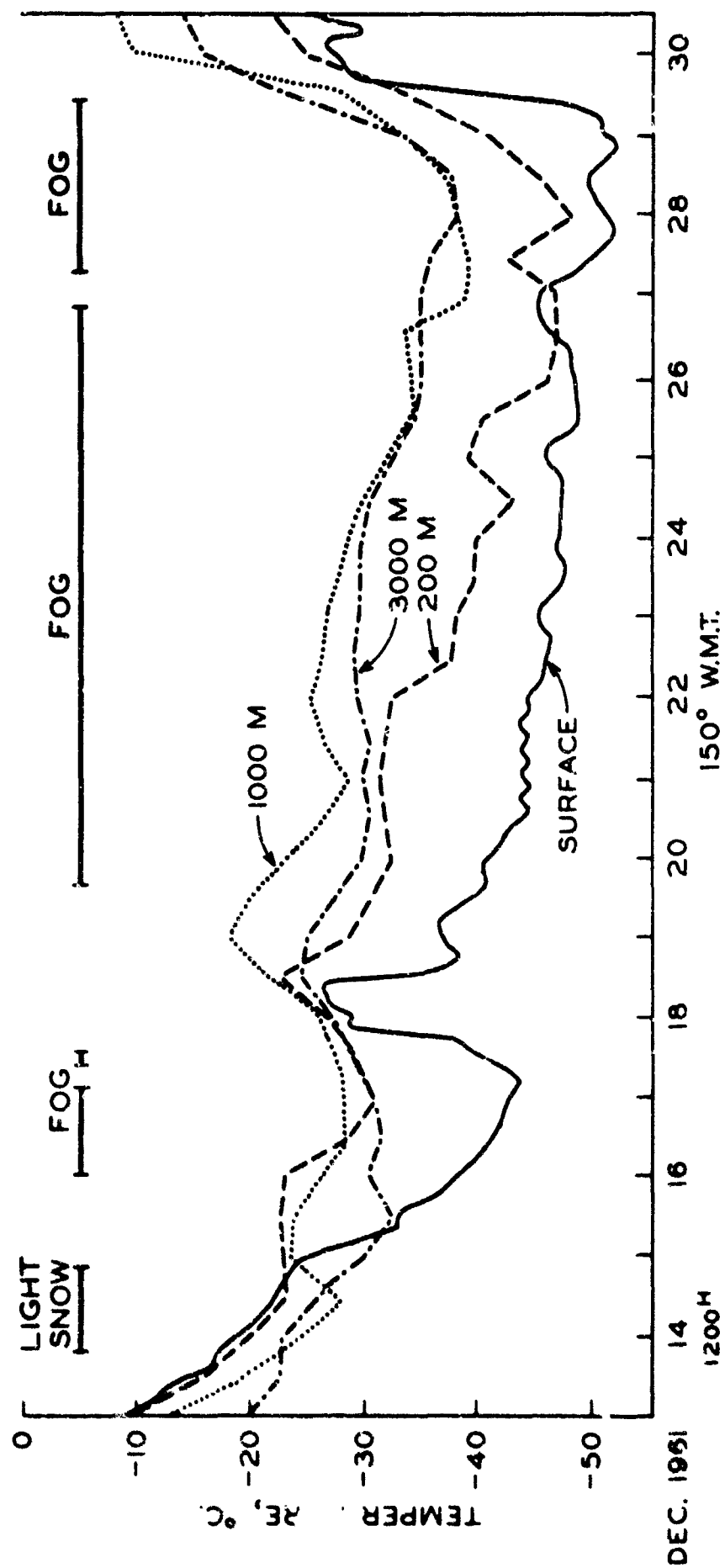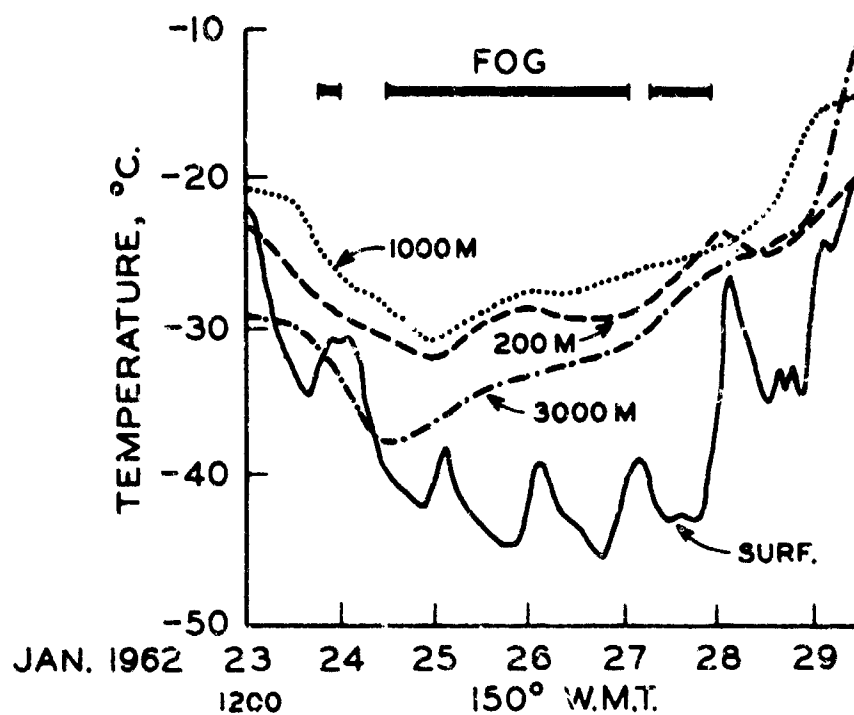
Fig. A-5. Temperature variations at selected heights, January 1962 from U.S. Weather Bureau data, Fairbanks.
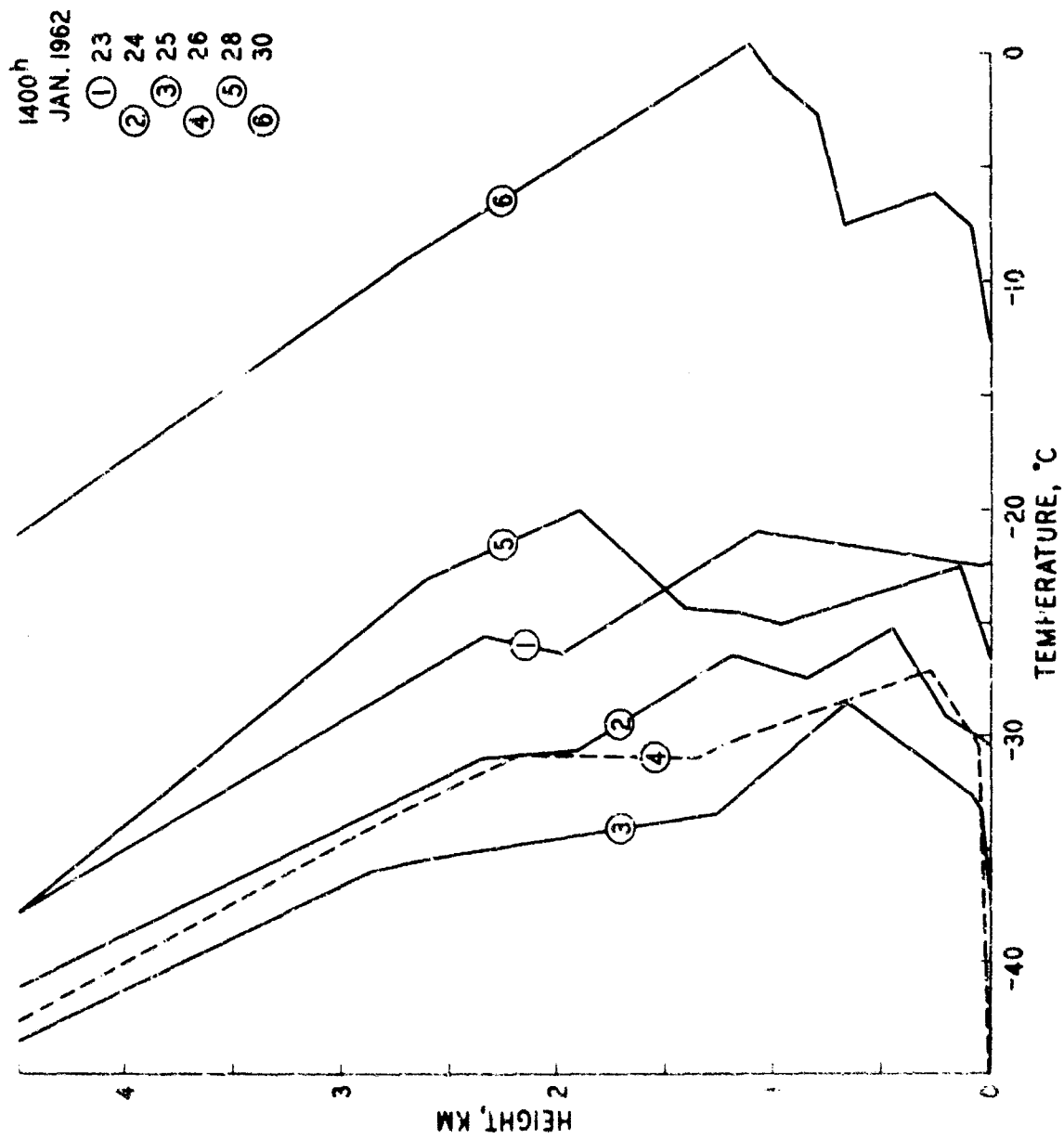
Fig. A-6. Temperature profiles, January 1962 from U.S. Weather Bureau rawinsonde data, Fairbanks.

Fig. A-7. Ice fog over Fairbanks, 1400, 150°W, 27 Jan. 1962, as seen from Birch Hill. Photo: K. Francis.

However, the rapid rate of cooling of the entire airmass (up to 3 km) observed at the start of each period far exceeds that which can be explained solely by radiational cooling from the surface, and as indicated by Wexler (1936, p. 133) advection must also be considered.

From Fig. 1 and 4 it seems reasonable to attribute the cooling from 14 to 15 December to advection. A deep layer from ground to about 5 km was affected. The maximum cooling occurred at a height of 1200 meters. Light snow was falling and the surface wind averaged 9 knots. On 15 December the wind speed decreased to below 5 knots and only then did a ground inversion develop.

An interesting case where the temperature fell simultaneously with the pressure occurred in February 1963, when a cold upper trough moved in and became stationary. From 2 to 3 February the temperature fell from -19 C to -38 C. From then on the minimum temperature gradually decreased to -43 C on 5 February. The pressure (reduced to mean sea level) fell from 1030 mb on 2 February to 1004 mb on 5 February. Clear sky prevailed and "diamond dust" ice crystals[*] were observed during the rapid cooling. The advection of cold, dry air aloft was apparently the main cause of the cooling.

5. Net radiation

With less than 4 hours of sunshine at the end of December, and the sun barely above the horizon, the effect of incoming solar radiation can safely be neglected. The effect of the ice fog on the infrared radiation is difficult to estimate. Ice fog rarely exceeds 30 m in thickness, and contains a low water vapor density because of the overall low temperature. It should have

---

[*] Many terms exist to describe the appearance of small crystals which form in clear air (see Glossary of Meteorology, 1959, p. 164 and p. 295; American Meteorological Society, Boston, Mass.). The terms "diamond dust" or "ice crystals" are used here and the occurrence of such an event is conveniently lumped under the term "ice crystal display". Such occurrences indicate existence of ice in the air which may go unrecorded in the meteorological records. The crystals produce optical effects, such as "sun dogs", halos, etc., which are generally included under "halo phenomena" (Neuberger, 1951).

little effect on the net outgoing radiation heat flux; this is especially so because the top of the inversion, which generally lies well above the ice fog, has the maximum water vapor content. However, within the ice fog itself, radiation heat exchange will weaken the inversion. In time the ice fog may become isothermal, or, if conditions persist, a layer with negative lapse rate may form near the ground. Thus, the presence of ice fog should decrease the rate of surface cooling. This shows in the temperature and radiation data in the first 29 meters as presented by Robinson et al. (1955). Their discussion refers to an upward displacement of the black-body reference level. Even if this occurs it should have negligible effect on values of net outgoing radiation obtained by using surface temperatures for the black-body reference level.

During the cold spell in January the effect of the incoming solar radiation shows in the daily surface temperature (Fig. 5). Otherwise the pattern follows the previous one, although the surface temperature continued to fall for 2 days after the temperatures at higher levels began increasing.

Wexler (1941) gives two formulae for the outgoing radiation at Fairbanks during clear weather. They are based on radiometer and temperature measurements alone. The formula for the temperature range -20C to -40C is used here, ie,

$$Q = 0.105 + 0.0018 \ T,$$

where the units of Q are ly min^{-1} and T is temperature (C). Hoinkes (1961), using radiometer and temperature data from Little America finds figures in good agreement with Wexler.

No reliable radiometer data are available from the periods investigated. We are mainly interested in correct order of magnitudes, so Elsasser's radiation chart (2nd revised edition) was used to simplify the calculations (Haltiner and Martin 1957, Elsasser 1942). A linear pressure reduction has been used

throughout in place of the former square-root reduction, in accordance with newer findings (Elsasser 1960).

Table 1 gives the calculated fluxes from the chart as compared to the mean values from Wexler's formula and from Hoinkes's data.

Table 1.

Net outgoing radiation (ly per min) (Calculated from Elsasser's radiation chart and compared with values taken from Wexler's formula and Hoinkes's table.

Date	Time	Temp C	Elsasser	Wexler	Hoinkes	Remarks
14 Dec	1400	-18.2	0.112	0.072	0.064	No inversion, light snow
16 Dec	0200	-27.9	0.129	0.055	0.052	Shallow inversion, clear
19 Dec	1400	-36.0	0.053	0.040	0.042	Strong inversion, clear
24 Jan	0200	-33.8	0.078	0.044	0.045	Weak inversion, light snow

On 14 December and 25 January light snow was falling, but so light that the vertical visibility was unlimited. The correction to the calculated fluxes should be negligible when we consider the very low concentration of the snow particles. As there was no inversion on 14 December and only a rather weak one on 24 January it is reasonable that the values calculated from Elsasser's chart are higher than the mean values taken from observations by Wexler and Hoinkes. With the strong inversion on 19 December the agreement between values is better. The use of Elsasser's radiation chart seems justified. The measurements of water vapor are inaccurate at low temperatures, but the main effect of the water vapor comes from the warmer layers aloft where the values are more trust-worthy. Although the chart may give slightly high values it will at least give the correct order of magnitude.

When comparing the calculated fluxes (Elsasser) with those derived from observations (Wexler, Hoinkes) it is necessary to keep in mind the wide scatter-ing of the values obtained from the radiometers. For example, at -30C Wexler (1941) observed variations from 0.03 to 0.08 Ly min^{-1}. Also, the calculated values are based on temperature measurements from a standard instrument shelter

which, under these conditions, may be several degrees higher than the temperature of the snow surface, or even of a low placed radiometer. This may contribute to the difference between calculated and empirical values in Table 1, because Wexler used the air temperature measured near the radiometer and Hoinkes used the temperature of the radiometer itself.

6. Cooling rates

Table 2 shows calculated cooling rates using the radiation chart by Elsasser. In two cases the radiation chart by Yamamoto (1953) has also been used as a check. Yamamoto's chart is especially practical for calculating cooling rates at specific levels. The effect of carbon dioxide was neglected in the latter case, as its effect on the temperature changes is relatively small near the ground. Yamamoto finds his chart to give somewhat higher cooling rates than the chart by Elsasser (Yamamoto 1953).

Table 2.

Observed cooling rates compared with rates
calculated from radiation charts

Date	Time	Radiation Chart	Height (m)	Temperature change (C) per 12 hrs for period starting on given date		
				Calculated	Observed	Average observed over next 3 days
14 Dec	1400	Elsasser	915-1915	0.02	4	
		Yamamoto	915	0.2	2.8	
19 Dec	1400	Elsasser	ground-1105	0.8	1.1	1
		Yamamoto	1105	1.6	3	2
24 Jan	1400	Elsasser	1025-1245	0.3	2.7	

Yamamoto's method refers to a specific level, whereas Elsasser's radiation chart refers to a layer of air. The calculated and observed cooling rates agree reasonably well on 19 December, at least they are of the same order of magnitude; this is not the case on 14 December and 24 January.

The initial rapid cooling occurs not only at the surface but at higher levels as well. This is not in agreement with the cooling model of Wexler where the cooling starts at the surface and gradually spreads upwards. At first sight the explanation for this would be advection of colder air. Undoubtedly advection plays an important part. However, another effect mentioned by Wexler but not seriously considered, is the effect of radiation from ice surfaces in the very light snowfall or in ice crystal displays accompanying the cooling of the air. In most cases this effect appears to be of primary importance.

7. Effect of ice crystals in the air.

Both periods started after or at the end of a light snowfall which ended in an ice crystal display. The record for Fairbanks, 1959 to 1963, shows that all the cold spells, when the surface temperature dropped below -34.4C (-30F) started during a snowfall or an ice crystal display. During observations made from 1961 through 1964 rapid coolings were not observed without associated formation of ice crystals in the air. Crystal displays during cooling were observed on a hill 600 m above the flats as well as in the flats. There were 12 such cases during these 4 winters each of which showed the rapid rate of cooling. This relationship is also noted in the data compiled by Byers (1940) for the Fairbanks winters 1936-1938. His data show 10 similar cold spells, 6 of which started with snowfall or snowflurries reported. In two cases thin "stratus" clouds were reported. At the low temperatures involved, they must have been pure ice clouds from which ice crystals would precipitate out without being reported. Often this type of low "cloud" has no definite base or top and, according to our usage, would be referred to as a crystal display. Only in one case were no clouds or snowflurries reported. Ice crystal displays were not noted in the 1936-1938 data, yet may well have occurred without affecting

unlimited vertical visibility. In general, the occurrence of crystal displays,
or light snowfall associated with sudden onset of cold spells seems to be the
rule for interior Alaska, not the exception, even in the extreme case of no
advection.

The formation and growth of ice crystals from vapor will release latent
heat to the air; on the other hand, an ice crystal radiates essentially like a
black body in the infrared. It receives radiation from the ground as well as
from water vapor and carbon dioxide. Water vapor densities calculated from
observed relative humidity values during the rapid coolings are shown in
Table 3. Very light snow was falling on 14 December and ice crystals were
reported on 15 December and 24 January.

Table 3.

Water Vapor Densities

(Relative humidity and air temperature values taken
from radiosonde records)

Date	Time	Height m	TempC	Observed Relative Humidity (Over water)	(Over Ice)	Water Vapor density (g m^{-3})	12 hrs diff.
14 Dec	1400	915	-24.5	66	84	0.486	0.121
15 Dec	0200	915	-27.3	63	82	0.365	
16 Dec	0200	95	-22.1	59	73	0.532	0.229
16 Dec	1400	95	-25.0	43	55	0.302	
24 Jan	1400	1025	-26.8	64	83	0.386	0.090
25 Jan	0200	1025	-28.7	58	77	0.296	

Table 4.

Heat budget and cooling rates per cm^3 air at the levels given in Table 3.

Date and Time 1961-1962	Height,m	Heat Exchanges (cal x 10^{-4} per cm^3)			Cooling (C)	
		Heat Loss by Radiation	Heat gained by liberation of latent heat	Net heat Loss	Calculated	Observed
14 Dec 1400 to 15 Dec 0200	915	10.25	0.82	9.7	3.1	2.8
16 Dec 0200 to 16 Dec 1400	95	21.50	1.55	19.55	6.0	2.9
24 Jan 1400 to 25 Jan 0200	1025	8.16	0.61	9.55	2.5	1.9[*]

[*]This value was measured at the 1025 m level, the average for the layer 1025 to 1248 m was 2.7 C (see Table 2).

The values in Table 4 were obtained as follows:

(1) The radiative heat loss was found by using Elsasser's radiation chart, including the heat flux resulting from ice crystals treated as black bodies placed at the level concerned. For simplicity the ice crystals are assumed to be plates of radius 25 μ, and with a concentration of 1 per cm^3 at any time.[**]

(2) The heat gain per cm^3 is the heat of sublimation times the water vapor density differences calculated in Table 3.

(3) The calculated rate of cooling (Table 4) is obtained from the formula:

$$dT/dt = dQ/(c_p m_a + c_i m_i)dt$$

Where dQ = net loss of heat, dt = 12 hours, c_p = specific heat of dry air, c_i = specific heat of ice and m_a and m_i = mass of air and of ice crystal in one cm^3 of air. Even if m_i is not well known, the term $c_i m_i$, being several orders of magnitudes smaller than $c_p m_a$, can safely be neglected.

The heat loss by radiation is proportional to the concentration and to the square of the radius of the crystals. Even if the size is smaller, say 10 μ,

[**]These values are consistent with observations by M. Kumai, K. Francis and the authors during typical ice crystal displays in the Fairbanks area.

and the concentration is assumed to be one crystal per cm^3, the radiative heat loss exceeds the heat added. The latter assumption of size and concentration, representing an extreme case unfavorable to the present argument does not alter the direction of heat flow. Influence from neighboring particles is neglected. With the concentrations observed this seems reasonable. The net result will, in any case, be a heat flow from the air to the crystal, as the crystals cool so does the air.

The calculated and observed[*] cooling rates are of the same order of magnitude, even though the calculated values for 16 December are too high. The cooling rates calculated without considering radiation from ice crystals, i.e., considering only water vapor and carbon dioxide, as in Table 2 are obviously too low. Thus, to understand the rapid cooling rates observed at the onset of cold spells, it appears that one must consider radiation from the suspended, growing ice crystals.

8. Crystal temperatures, humidity measurements and cooling mechanism.

In making the above calculations the ice crystals were assumed to have the same temperature as the (surrounding) air. However, this is not strictly correct because as the ice crystals cool by radiation they will be cooler than the air, and strong temperature gradients will form in the air immediately adjacent. Although the differences are small they are of special interest in that they may explain the fact that during light snowfalls and ice crystal displays we generally measure less than 100% relative humidity with respect to ice. These measurements pertain to the air between the ice crystals, whereas the temperature of the air in contact with the ice crystal may be low enough to be saturated. In the examples cited in Table 3 the temperature difference

[*]It is clear from Figs. 2 and 6 that the observed cooling rates entered in the tables are not exceptional. For example, the temperature at 1025 m decreased 5.3 C between 0200 and 1400 on 24 Jan. and 2.8 C between 0200 and 1400 on 25 January.

between the measured air temperature and the temperature corresponding to saturation with respect to ice and water is close to 2C and 5C respectively.

> (The range of values is 1.8C to 2.6C and 4.7C to 6.1C, excluding the dates for 16 December 1400 where the values were 6.1C and 12.3C respectively. In the latter case there is reason to suspect that the crystals, if present, were evaporating.)

Let us follow this point one step further by looking at the temperature distribution in the air around the crystals. The first question that comes to mind is: "how far from the crystal is the air temperature different from ambient, i.e. from the air between the crystals?" For simplicity, assume spherical crystals with diameter of 25 μ, and concentration 1 crystal per cm^3. In keeping with the values in Table 3 consider the relative humidity of the air to be about 80% relative to ice. Assume the surface temperature of the crystal to be 2C lower than the ambient air temperature and that the air in contact with it is saturated with respect to ice. For convenience we use temperatures of 240 K(-33C) for the crystal surface, and 242 K (-31C) for the ambient air; this gives a relative humidity of 81% for the ambient air. Assume further, that the air temperature gradient produced by the cooling crystals extends for such a short distance that heat transfer by convection is negligible, as a first approximation, and consider conduction alone. Then we can equate the outgoing heat flux by radiation from the crystal, to the incoming heat by conduction from the air,

$$F = \sigma T^4 = k \frac{dT}{dn} \tag{1}$$

where F is the heat flux, ly sec^{-1}

σ is the Stefan-Boltzman constant = 13.6 x 10^{-13} ly sec^{-1} K^{-4}

T is degrees Absolute

k is the thermal conductivity of air ~ 57 x 10^{-6} cal sec cm^{-1} C^{-1}

$\frac{dT}{dn}$ is the thermal gradient normal to the surface C cm^{-1}

Since we have assumed the temperature difference between the ice surface and the ambient air to be $dT = 2^\circ C$, we can solve eq. (1) for dn

$$dn = \frac{kdT}{\sigma T^4} = \frac{57 \times 10^{-6}}{4.5 \times 10^{-3}} \times 2 = 0.025 \text{ cm} = 250 \text{ } \mu \text{ .} \qquad (2)$$

Within this short distance from the crystal surface, the computed gradient (80 C cm^{-1}) is about 10^6 greater than normal atmospheric lapse rates. The above assumptions imply a simple linear gradient; however, it is more likely that an exponential decrease of temperature would prevail from the crystal into the air. This would make the gradient even steeper near the crystal and would restrict it to within about 100 μ from the crystal surface. Thus under the assumed conditions, the calculated value of 250 μ represents an extreme maximum distance for the temperature anomaly caused by the crystal to extend into the surrounding air. Two other factors contribute to insure this, they are:

(1) the possibility of some convective heat transfer as the crystal falls through the air, and

(2) the liberation of latent heat of sublimation by the crystal if it is growing.

An order of magnitude for the amount of latent heat transfer may be obtained by assuming a growth rate for our spherical ice crystal whose initial volume and mass are 7.9×10^{-9} cm^3, and 7.25×10^{-9} gm respectively. If, as it falls through the air, this crystal adds 10 per cent to its mass it will liberate

$$\left[678 \text{ cal gm}^{-1} \right] \quad \times \quad \left[0.725 \times 10^{-9} \text{ gm} \right] = 4.92 \times 10^{-7} \text{ cal,}$$

which when spread over the surface area (1.96×10^{-5} cm^2) amounts to 2.5×10^{-2} ly. If this 10 per cent growth occurs in an hour the resultant heat flux would be 6.9×10^{-6} ly sec^{-1}, if it occurs in 1 minute the heat flux would be 4.2×10^{-4} ly sec^{-1}. A faster growth rate would be very unlikely because of

the low water vapor density at the temperatures involved. In these cases the radiative heat flux is orders of magnitude greater than the flux due to liberation of latent heat.

Thus, the ice crystals, formed by overall cooling of the air have lower temperatures than the surrounding air, and act as heat sinks. Heat flows from the air to the crystal and is radiated away. The process results in a net heat loss even though the crystals are growing and releasing latent heat to the air. This cooling mechanism explains how cooling may be as rapid at higher levels as near the ground. At the end of the crystal display the cooling rate should be expected to level off, and again, this agrees well with the observations.

The differences in temperature, between crystals and surrounding air, also accounts for measured values less than 100% relative humidity during occurrences of light snow fall and "diamond dust" crystal displays. The air temperature values used in humidity determinations pertain to ambient air between the ice crystals, whereas the air in contact with the crystals has a lower temperature and is saturated with respect to ice. Spatial relations between the crystals and the localized air temperature gradients produced by them are shown in Figure 8.
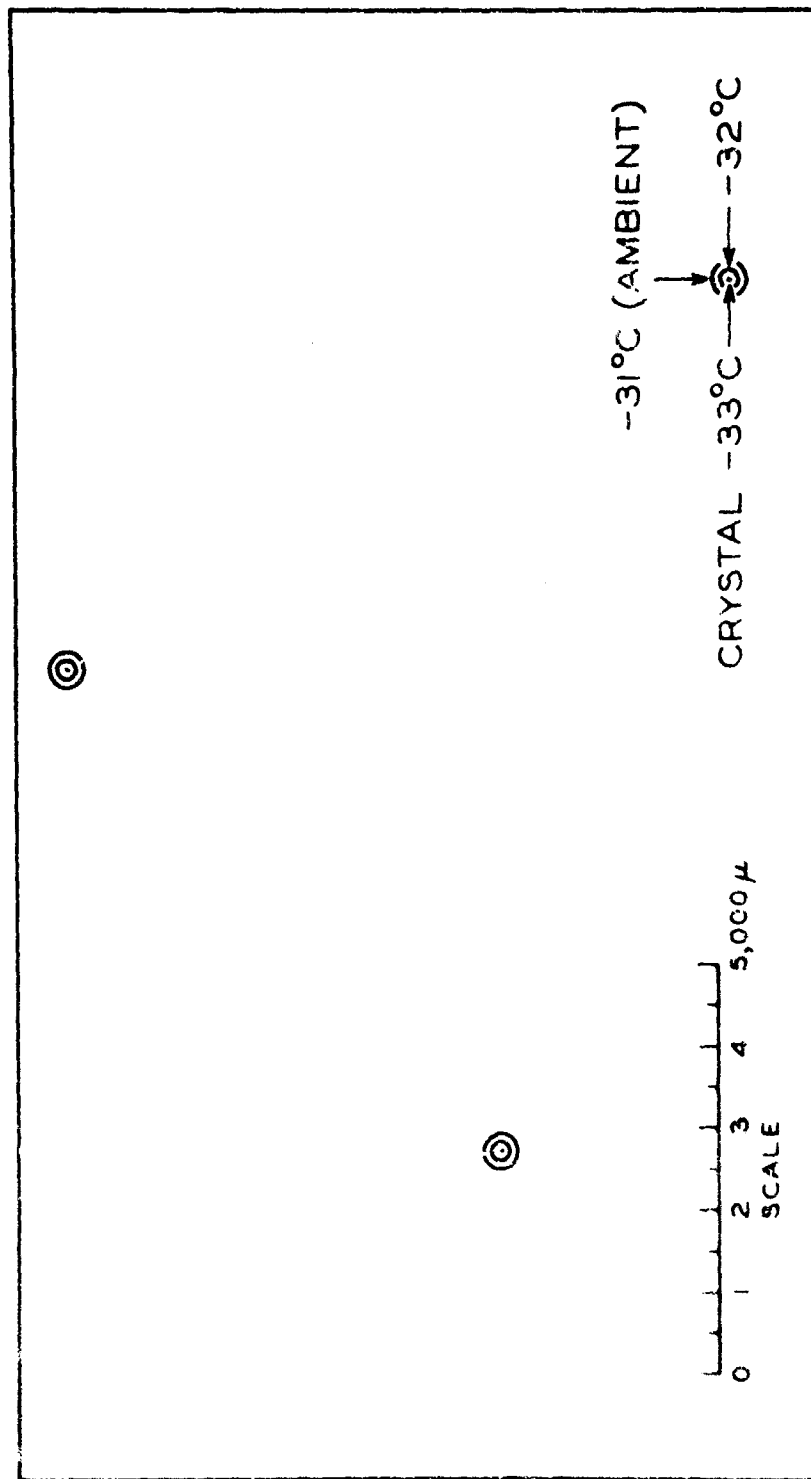
Fig. A-8. Spatial relations between ice crystals and the maximum radius through which they produce local temperature gradients in the air; calculated for spherical crystals 25 μ in diameter. The air in contact with the crystal is saturated, whereas the humidity in the ambient air is 81% relative to ice.

REFERENCES

Benson, Carl S., Yngvar Gotaas, Karl E. Francis and Wallace B. Murcray 1964, Ice Fog studies in the Fairbanks area 1961-1963. Proceedings of the 15th Alaskan Science Conference, p. 89.

Byers, H. R., 1940, Data from aerological soundings at Fairbanks Alaska during the winters 1936-37 and 1937-38. Mon. Wea. Rev., Suppl. No. 40.

Elsasser, W. M., 1942, Heat transfer by infrared radiation in the atmosphere. Harvard Met. Studies, No. 6, Cambridge, Harvard Univ. Press, 107 pp.

Elsasser, W. M., 1960, Atmospheric radiation tables. Met. Mon. 4, No. 23.

Haltiner, G. J. and F. L. Martin, 1957, Dynamical and Physical Meteorology. McGraw-Hill Book Co., New York, Toronto, London, pp. 112-124.

Hoinkes, H. C., 1961, Studies in glacial meteorology at Little America V, Antarctica, Publ. No. 55, I.A.S.H. Sym. Ant. Glac., pp 32-33.

Neuberger, Hans, 1951, General Meteorological Optics, Compendium of Meteorology: published by American Meteorological Society, Boston, Massachusetts, pp. 61-78.

Robinson, E., G. B. Bell, W. C. Thuman, G. A. St. John and E. J. Wiggins, 1955, An investigation of the ice fog phenomena in the Alaskan area, Final Report, Contract No. AF 19(122)-634, Stanford Research Institute, Stanford, California.

Wexler, H., 1936, Cooling in the lower atmosphere and the structure of polar continental air. Mon. Wea. Rev., 64, 122-136.

Wexler, H., 1941, Observations of nocturnal radiation at Faribanks Alaska and Fargo, N. Dak. Mon. Wea. Rev., Suppl. No. 46.

Yamamoto, G. and G. Onishi, 1953, A chart for the calculation of radiative temperature changes. Sci. Rep. Tohoku Univ., Series 5, Geophys. 4, pp. 108-115.

APPENDIX B

NUCLEATION AND FREEZING OF SUPERCOOLED WATER DROPLETS

by

Carl S. Benson

ABSTRACT

This appendix reviews some problems associated with supercooling
and saturation, with special emphasis on freezing supercooled water
droplets. Moisture is continuously condensed out of air as it cools,
but, when supercooled water droplets freeze, at about -40°C, there
is a discontinuous increase in the amount of water condensed, because
the vapor pressure over ice is less than that over water. At -40°C
the excess water produced by freezing is more than 5 times greater
than that produced by one degree of cooling at -40°C. The effect
this has on producing ice fog is illustrated by specific calculations
which show that the water produced in less than 1 hour by freezing is
comparable to twice the daily input from the University of Alaska's
power plant. The sudden and widespread appearance of ice fog at
temperatures of -35 to -40°C is attributed to the freezing of water
droplets.

APPENDIX B

NUCLEATION AND FREEZING OF SUPERCOOLED WATER DROPLETS

Table of Contents

APPENDIX B

NUCLEATION AND FREEZING OF SUPERCOOLED WATER DROPLETS

Introduction

The subject of ice formation in the atmosphere has received much attention because of its fundamental importance to the mechanism of precipitation as well summarized by Mason (1957, pp.199-308) and also because of its long-standing operational importance to aviation (Hallanger, 1938; Stickley, 1938). Ice formation in the atmosphere brings to special attention the effects of small volumes on supercooling.

The term "Supercooled water" refers to water in the liquid state at temperatures below the melting point. Although water can be cooled below its equilibrium freezing point and remain liquid, there is no evidence available to indicate that ice can be "superheated", that is, raised above its melting point and remain solid. Therefore, the point at which ice melts is a constant, whereas the initial point of freezing for water is not. For this reason it is better to use the term "melting point" or "ice point" instead of "freezing point" when describing the equilibrium condition between water and ice.

When a sample of supercooled water begins to crystallize, (at a temperature which may be considerably below 0°C) it experiences a rapid rise in temperature to the ice point (0°C) and additional freezing or melting will take place at this temperature. No further temperature changes will occur until one of the phases disappears.

The temperature at which crystallization begins was termed the "spontaneous freezing point" by Miers and Isaac (1906a, 1906b); it is abbreviated "tsf" (Dorsey, 1938, 1948). Unlike the melting point, or ice point, the spontaneous freezing point, or point of first crystallization, is not an equilibrium point between two phases.

The phenomena of supercooling in melts and supersaturation in solutions are important to understanding the general processes of nucleation in phase transformations. Since the equilibrium point between water and ice is very clearly defined and reproducible, and since ice is thermodynamically more stable than water below 0°C, the very existence of supercooling presents several questions:

(1) Under what conditions may supercooling occur?

(2) How often does supercooling occur?

(3) Once water is supercooled, under what conditions will it freeze?

In partial answer to these questions, present knowledge indicates:

(1) The only condition necessary for producing supercooled water is that no ice is present when the water is cooled down to and below 0°C. In other words, the melt is not "seeded" with the solid phase.

(2) Supercooling always takes place before freezing (not only in water but in all unseeded melts). This is also true for supersaturation of solutions prior to crystallization and precipitation of one of the components.

(3) The third question has been the cause of a great amount of speculation together with theoretical and experimental work.
Some of the theoretical arguments include the phenomenon of supercooling, while others do not, and the literature abounds with pertinent experimental work, leading to various interpretations, in several at-first-sight unrelated disciplines. A brief statement of some research on this subject is given here in place of the simple answer, which does not exist, for this third question.

Theoretical Considerations

Energy relations

A phase change will not occur spontaneously unless it can be accompanied by a decrease in the free energy of the system. The bulk free energy of ice is less than that of water at temperatures below $0°C$.; thus the formation of ice in supercooled water is accompanied by a loss of free energy. But, the initial formation of an ice crystal is also accompanied by the creation of a new surface and this requires energy. It is clear that the amount of energy necessary to form the ice surface must be less than the amount given off or the phase change will not occur. Thus, the problem reduces to nucleating an ice particle which is able to grow.

Ostwald's metastable limit

Some proposed nuclei will be considered after a brief discussion of one of the earliest (about 1900) ideas dealing specifically with supercooling. Ostwald[*] stated that when a liquid is cooled below its normal melting point, it is in an unstable condition, the degree of instability depending upon the amount of supercooling. He suggested that the unstable field is composed of two parts.

(1) The metastable field, or state, which exists at low degrees of super-cooling in which the only way to cause crystallization is by the introduction of a crystalline part of the solid phase. Without such "seeding", it cannot spontaneously crystallize no matter what shaking, stirring, jarring, etc., takes place.

(2) Upon further supercooling, the liquid will transfer abruptly into the labile or simply unstable, state; in this condition it can be crystallized by mechanical disturbance. The point at which the abrupt transfer from the meta-stable to the labile fields occurs is known as the metastable limit.

[*]La Mer (1952, p.1271) has translated and abridged a useful summary of Ostwald's concept from "Kinetik der Phasenbildung" by M. Volmer.

Miers and Isaac (1906a) found supporting evidence for Ostwald's metastable
limit in their work on the refractive indices of crystallizing solutions. They
draw a supersolubility curve in the ordinary phase diagram for $NaNO_3$, which lies
below, and is roughly parallel to, the solubility curve.

Among opponents of Ostwald's metastable limit were deCoppet (1907) and
Tammann (1925). DeCoppet argued that the time required for a solution to
crystallize was simply inversely proportional to supercooling and the volume of
the sample. Tammann found many substances which supercooled slightly and only
for a short time, and many in which supercooling was negligible. He argued
against Ostwald's metastable limit on the grounds that crystallization often
takes place even with slight supercooling after only a few seconds. Young (1910)
pointed out that no experimental evidence exists for dividing the supercooled
range for water into two parts. As the result of a series of experiments,
Young and Van Sicklen (1913) concluded that if there is a metastable limit for
water, it lies within 0.01°C of the true melting point.

Types of Nuclei

Repeated experimental evidence from many sources indicates that freezing
begins at certain discrete points within water. These points must represent
singularities of one kind or another which exist just before freezing starts.
The number of these points is small; its ratio to the number of molecules in an
ordinary beaker of water is of the order of 10^{-23}. Nucleation theories differ
in their assumptions regarding the nature of these singularities but the majority
of ideas can be grouped under two general headings.

Homogeneous Nuclei. It has been proposed that the aggregation of water mole-
cules varies from one physical state to another as follows: The simple water mole-
cule "hydrol", exists only in the vapor phase. The molecular form of liquid water,

"dihydrol" consists of two H_2O molecules, whereas the ice molecule "trihydrol" is composed of three H_2O molecules, (Barnes, 1906, 1926; Bernal and Fowler, 1933; Sutherland, 1900). According to this concept, water is a solution of dihydrol and trihydrol; it becomes saturated with trihydrol at the freezing point and ice precipitates out of solution.

The ice molecules form the homogeneous singularities in the melt, and arise fortuitously and solely from the thermal agitation of the molecules. The ratio of trihydrol to dihydrol is small at high temperatures, but increases as the temperature decreases. The ratio has a fixed value for every temperature when equilibrium exists. There are different estimates for the amount of time required for equilibrium to occur after a change in temperature. But the general tendency of trihydrol molecules to cohere and grow is assumed to be temperature dependent. At the freezing point the trihydrol ice aggregates have grown to such a size that they can annex the adjacent dihydrol water molecules. Once this process has begun, equilibrium is established, and the process goes in either direction depending on whether heat is added to, or taken from, the system. This theoretical model does not specifically include the phenomenon of supercooling; furthermore, if supercooling, or supersaturation occurs it demands that crystallization will occur if enough time passes. Indeed crystallization depends only upon the probability of kinetic molecular collisions producing a crystal embryo which is able to grow. As the volume of a sample increases, its chances for supercooling will decrease; also, large degrees of supercooling are of short duration.

One objection to the concept of a crystal embryo forming solely from favorable kinetic molecular collisions was made by Ostwald. He pointed out that solutions of salts which are only slightly soluble do not undergo supersaturation to the same extent as do solutions of more soluble salts. The reverse situation should be expected from deCoppet's statement, since fewer favorable collisions are possible in more dilute solutions.

B-5

Heterogeneous Nuclei. It has been proposed that the freezing process is initiated by heterogeneous singularities, i.e., foreign particles termed "motes" by Dorsey (1948), in the water. These singularities may be on the container walls, or they may be minute particles freely suspended within the water. They serve as nuclei about which ice is built up until it forms a viable crystal. The specific "catalytic" action of the motes is unclear. Possible ways in which such particles may be effective were listed by Dorsey (1948, p. 303) as:

(1) A purely mechanical action. (It has been suggested that the foreign particles slow down the motion of the molecules sufficiently to enable them to orient themselves as required for crystallization.)

(2) "The particle or spot acts as a base upon which the molecules of the melt are laid down in a crystalline array."

(3) "The occurrence of freezing depends on the action of the adsorbed layer covering the foreign particle or spot." (Richards (1932) suggests a "crystalline adsorbate," which is regarded as being composed of crystals of the melt.)

In 1948 Dorsey proposed a theory of nucleation in water which was based on his experiments with freezing of supercooled water over a span of twelve years. It combines some points of both the homogeneous and heterogeneous theories. He proposes that freezing is initiated by motes but does not demand that they be of any special kind. Their function is solely to serve as a gathering place for molecules of the liquid which are held by adsorptive forces. It is assumed that this adsorbed layer can be disrupted by mechanical means, including kinetic molecular collisions. If this layer is disrupted, a group of molecules with low random velocities may be freed. These molecules would seek the lowest possible energy level, which in supercooled water could be a viable crystal nucleus.

A statement by Daniels in reference to theoretical chemical kinetics is
appropriate to the nucleation problems in water.

> "The attack along theoretical lines has now progressed so rapidly
> that confusion exists and the weakest link in the chain of develop-
> ment now seems to lie in the determination of exact experimental
> facts regarding significant simple reactions" (Daniels, 1938, p.3).

Rather than discuss details of the various theoretical approaches some of the
available experimental data will be considered next.

Experimental Observations

Frequency of Occurrence and Extent of Supercooling

It has frequently been suggested that a small sample volume is necessary
in order that supercooling may occur. This is a misconception. Supercooling
has been observed in every instance of freezing that has been accompanied by
careful measurement (Altberg, 1936, 1938; Devik, 1942, 1944, 1949; Buckley,1951;
Dinger and Gunn, 1946; Dorsch and Hacker, 1950; Dorsey, 1938, 1940, 1948; Hever-
ly, 1949; Kenrick and Martin, 1913; Schaefer, 1949; Smith-Johannsen, 1948; and
others). These observations have been made on water from many sources, including
pure and polluted water, and ranging from tiny droplets to lakes and even turbu-
lent streams.

> "The phenomenon of supercooling of liquids is apparently of universal
> occurrence. It rarely if ever happens that a liquid cannot be cooled
> some distance below its melting point without solidifying"(Young.
> 1910, p. 148).

Barnes (1906) stated that water may be supercooled to -6° C. with caution,
and that below this temperature the instability becomes so great that extreme
precautions must be taken to obtain further cooling. Many recent references,
including textbooks, also claim that water will undergo only a few degrees of
supercooling, and that quiescence is necessary (Buckley, 1951, p. 13). However,
published accounts as long ago as 1837 (Despretz, 1837, 1839) describe experi-
ments in which water was supercooled to -20° C. Pictet (1879) found that a

stoppered flask half full of water at -19° C. could be shaken violently without causing the water to freeze.

At the other extreme from Barnes, Rau (1944) claimed to have supercooled water to -72° C. by a series of repeated freezings. His water samples consisted of droplets up to a few millimeters in diameter which were supported on a highly polished chromium surface. The crystallization took place at a reproducible temperature with a reproducible pattern from a single nucleus. After repeated freezing and thawing, this nucleus lost its activity, and a lower temperature of freezing about a new nucleus was observed. This nucleus, in turn, became inactive after a while and a further degree of supercooling was possible. When the temperature was down to -72° C. the droplets invariably froze, forming many nuclei. There were other curious phenomena reported with these observations, such as cubic forms of ice at low temperatures, variations in surface tension as seen by flattening of the droplets at low temperatures, and several intermediate melting points. Frank (1946) attempted to interpret Rau's results by assuming variations in the molecular structure of such deeply supercooled water.

The results obtained by Rau have been subject to question, and attempts by Cwilong (1947b) to reproduce them have failed. Cwilong suggested that Rau's results were influenced by contamination of the water samples through evaporation of the refrigerant material (an acetone-dry ice mixture). This suggestion was substantiated by Berger and Saffer (1953) who found that Rau's results could be duplicated (including the elongation of droplets at low temperatures and supercooling to -60° C.) if a dry ice and acetone coolant was used, but not when liquid nitrogen was used as the refrigerant. Cohen and Van der Horst (1938) also obtained ice crystals like those of Rau by freezing dilute acetone-water solutions.

Rau implied that the freezing spread from many nuclei. Berger and Saffer (1952) questioned the possibility of making this observation, since the velocity

of crystallization is expected to be very high at this temperature, and Rau's samples were very small.

Experiments on freezing supercooled water have been done on samples spanning a range of sample volume from lakes and rivers to cloud droplets. In general, the extent of supercooling increases as sample volume decreases with an apparent limit in the range of -40 to -50°C for sizes less than 5 μ.

Lakes. Devik (1942) measured the surface temperature of water during freezing by a radiation thermopile. It was observed that the surface layers are supercooled whenever ice forms.

Devik emphasized that the first crystallization occurs at distinct starting places (the initiating "motes"), and that there must be a temperature gradient from the ice to the water in order to carry away the latent heat of fusion. Thus, as ice advances across a pond or any other body of water, there will be a slightly supercooled layer of water preceding it. In open water there are many various-sized foreign particles suspended in the water, and infinite source material on the shore. These suspended particles, together with rocks and other beach material and nucleation from the atmosphere, are very efficient in starting the crystallization. Thus the degree of supercooling in open waters will never be as great as that for laboratory specimens which are contained in glass bulbs and protected from the atmosphere. However, this amount of supercooling is measurable. Devik measured supercooling which varied from a few hundredths of a degree to as low as -1.2°C.

Rivers. The freezing of rapidly-flowing turbulent rivers presents quite a different problem from that of freezing of quiet waters or slowly flowing streams. A phenomenon occurring in rapidly running water is the formation of underwater ice. The terms frazil ice and anchor ice have been applied and widely used in the discussion of underwater formations of ice (Timonoff, 1936).

Frazil ice forms in supercooled running water; the degree of supercooling may be very slight. The structure of frazil ice has been described by Barnes (1906) as small disclike plates, and this observation has been confirmed by Altberg (1936). Excellent photos of these discs and other modifications of early ice crystal forms have been taken (Altberg, 1938; Altberg and Lavrow,1939; Schaefer, 1950). The frazil ice particles are very small fine crystals and discs which are distributed throughout a turbulent flowing stream. These particles also cluster together to form curtain-like spongy masses which move along under water with the current.

Anchor ice forms on the bottom of rivers and on objects under water. It is firmly attached to the bottom and grows outward. Barnes (1906) explained the formation of anchor ice by radiation from the river beds at night which permits cooling of the river bed to the point where anchor ice would form and grow continuously from the bottom outward. Altberg (1936), however, produced anchor ice under laboratory conditions which completely eliminated any possibility of radiation from the bottom. It has been conclusively proved that the formation of underwater ice is entirely independent of radiation from stream beds (Altberg, 1936; Nybrant, 1943; Gerdel, 1952). Apparently some of the recent references have been neglected since Parsons (1942) accepted the radiation theory and Schaefer (1950) mentioned that it was a possibility.

Altberg does not make any distinction between frazil and anchor ice, but classes them together as underwater ice,[*] which will form when the water temperature falls below 0°C. He found that the water temperature remains fairly constant throughout the river from top to bottom, because of turbulence. The more turbulent the water is, the closer is the temperature at any point to the mean temperature (Altberg, 1923). Measurements showed that the supercooling exists

[*]Altberg's work was started as an investigation of ice formation on water intake pipes in 1914, when the whole bottom of the River Neva was found to be covered with a thick (one meter) crust of porous anchor ice. This left the city of Leningrad without water. Many measurements were made on the temperatures of river waters in the Neva and also several rivers in eastern and north-central Russia (Angara, Amur, Enisey, etc.).

in these streams for long periods--hours, and even days--even in the presence of ice. Altberg (1936) proposed that flowing supercooled water provides a vehicle for removing latent heat and this allows the formation of underwater ice. Furthermore, irregularities on the bottom are accentuated because heat is removed from sharp points or edges faster than from flat or rounded shapes.

Some research on these problems is underway at the University of Alaska (Anderson, et al, 1964), and a comprehensive review paper on the subject was prepared by Williams (1959).

Laboratory samples. Smith-Johannsen (1948) employed an experimental technique in which the sample was completely protected from nucleation by the atmosphere, and crystallization was observed through polarized lenses. For chemically pure water he consistently obtained a spontaneous freezing point of about -20°C. The average crystallization temperature of pure water in these experiments was -19.2°C, with a maximum of -18.0°C, and a minimum of -20.5°C.

> "The normal temperature at which water freezes is, therefore, in the absence of any known foreign nucleating materials, very close to -20°C, and not as is commonly believed, at 0°C." (Smith-Johannsen,1948,p.653).

Berger and Saffer (1953) modified Smith-Johannsen's apparatus so that it would accommodate larger volumes. They obtained data which were in good accord with those of Smith-Johannsen, and in addition observed spontaneous freezing points as low as -35°C.

Dorsey (1948) performed many experiments with water from various sources. He protected the samples from the atmosphere, which might introduce freezing nuclei, by sealing them in glass bulbs (volume about 8 cc.). These bulbs were placed in cooling baths of alcohol, the temperature of which could be varied at will. The spontaneous freezing points varied from -5° to -22°C, but an average figure of -14°C would apply to the overall results. In no case was the spontaneous freezing point of 0°C observed.

Reproducibility of the Extent of Supercooling

In many cases a particular water sample has been observed to undergo approximately the same amount of supercooling when subjected to a series of freeze and thaw cycles. Smith-Johannsen's (1948) results show a remarkable reproducibility of the spontaneous freezing point for a given sample. Similar results have also been observed in the freezing of small water droplets by Cwilong (1947a), Schaefer (1948), Dorsch and Hacker (1950), and others.

Dorsey (1938, 1948) systematically investigated the reproducibility of the tsf for a series of water samples. Table I illustrated some of his results. The tsf varied greatly from one sample to another, even in nominally identical samples drawn from the same source. However, the tsf of a given sample often remained constant throughout many tests (Table I) even with wide variations in rate of cooling. In some cases a sample was rapidly cooled to a temperature barely above its previously determined tsf and then very slowly cooled to its tsf where freezing began. In some cases the tsf changed as the sample aged. The change was generally a progressive downward shift, which Dorsey termed a "secular variation of the tsf". In some cases the shifting in tsf was quite irregular, with certain temperatures occasionally being repeated. Dorsey called the repeated temperatures "preferred temperatures". A greater number of preferred temperatures was observed in samples "which were relatively free of motes".

Dorsey considered these results to be most easily explained by assuming heterogeneous rather than homogeneous singularities. He explained the secular variations by assuming that the size of the motes in the water may undergo changes resulting from the repeated freezing and thawing, or simply from aging. Another bit of evidence supporting the concepts of heterogeneous nucleation is the effect of purity on the extent of supercooling. Water does not have to be chemically pure to undergo supercooling. Both Dorsey (1948) and Heverly (1949) included many samples from random sources in their experiments on supercooling. Also,

TABLE I .

Reproducibility of the observed temperatures of spontaneous freezing
Dorsey (1948, p. 257)

C38 Brook		P10 Vac. Dist.		CIII Vac. Dist.		C12 Dist.		C5 Dist.	
Date	-t	Date	-t	Date	-t	Date	-t	Date	-t
1943	10.8	1943	16.1	1943	17.2	1936	6.8	1943	11.6
Apr.9	10.3	Apr.14	16.0	Apr.12	17.1	Dec.22	6.3	J1.6	12.0
	10.5		16.2		17.4		6.0		12.0
	10.1		16.1		17.7		6.1		12.0
	10.3		12.9[a]		17.0		6.6		12.1
	10.6		16.8		17.6		6.5	J1.9	12.0
	10.7		16.9		17.8		6.8		12.1
	10.4	Apr.15	16.2		17.2		6.9	J1.16	12.2
	10.5		16.6		17.6		6.3		12.1
	10.8		16.5	Apr.13	17.8		6.9		12.2
	10.6		16.2		17.7		6.8		
			16.2		17.6				
			16.0		17.6	1937	7.0		
			16.2		17.6	Jan.5	6.7		
			16.0		17.3		6.4		
					17.4				
					17.2				

C23 Snow		C40 Pool		P25 Dist.		P2 Conductivity		C10 Conductivity	
Date	-t	Date	-t	Date	-t	Date	-t	Date	-t
1937	5.8	1937	6.0	1943	9.7	1937	13.4	1937	16.0
Feb.17	6.0	Mar.4	6.0	J1.5	9.8	Jan.19	13.3	Feb.25	16.0
	6.0	Mar.6	6.9[b]		9.8	Jan.28	13.8		16.0
	6.0		6.0	J1.6	9.6		13.6	Mar.10	16.0
	7.5[b]	Mar.8	6.0		10.0		13.5		15.9
	6.0		6.0		9.5	Feb.24	13.4	Apr.14	16.0
Feb.24	6.1	Mar.22	5.6	J1.9	9.6		13.0[c]		16.0
	6.1		6.0		9.9		13.1		
Mar.9	6.0	Apr.23	6.0		9.7	Mar.10	13.2		
	5.9		6.0	J1.16	9.9		13.2		
	6.0				10.1				
					9.9				

(The water was observed to freeze spontaneously when the temperature of the bath was t°C. No value of t observed during any of these intervals has been omitted from the table.)

Figures such as C38, P10, etc., refer to specific samples. The notations below the numbers indicate the source of the water.

[a]P10. Cannot account for this high reading.

[b]C23, C40. The temperature of the bath when the bulb was placed in it was below the tsf of the bulb.

[c]P2. The water froze within 2½ minutes after the bulb was placed in the -13.0° bath.

the lakes (Devik, 1942) and rivers (Altberg, 1936) which supercool are certainly

not chemically pure. However, in general the degree of supercooling increases

with the purity of the sample, as shown by experiments with filtered (Richards,

Kirkpatrick and Hutz, 1936), distilled (Meyer and Pfaff, 1935), and

centrifuged (Dorsey, 1938, 1948) water.

Duration of Supercooling

Dorsey (1948) maintained a water sample at temperatures between -8.0 and

-13.3°C., i.e. at temperatures slightly above its tsf, for a period of 312 days

continuously without its freezing. He interpreted this to indicate the impor-

tance of motes within the liquid as the controlling agents in nucleating the

solid phase. Therefore, the temperature at which freezing occurs in a given

water sample is the important thing, and the manner in which that temperature

is reached is inconsequential. Berger and Saffer (1953) are in accord with

this view, but from statistical considerations, they point out that nucleation

may occur at a temperature higher than the tsf for a given sample especially

when cooling rates are very slow.

The homogeneous theory demands that a certain number of singularities are

forming in the liquid at every temperature. Below the freezing point these

singularities form crystal nuclei, and, in general, a supercooled melt or super-

saturated solution will crystallize if given enough time. Most work along this

line has been done on substances other than water; nevertheless it is instructive

to briefly consider some of the results.

Tammann (1925) found that the tendency for nucleus formation in supercooled

solutions increased as the temperature decreased. In his experiments he encoun-

tered difficulties in seeing the newly formed embryos because of their minute

size; so, to render them visible he first cooled the melt down to the experi-

mental temperature for a few minutes and then raised it to the point of optimum

B-14

linear growth. At this point the crystal nuclei were growing and of sufficient size to be visible.

Bergman (1943) and Mikhnevich and Browko (1938) have pointed out a possible source of serious error in Tammann's treatment. They maintain that a crystal nucleus must be of a certain size in order to grow at a specified temperature. The temperature changes in Tammann's experimental procedure may exercise control over the observed number of growing crystal embryos. At any rate, Tamman's increased rate of nucleation was not a linear function of temperature, but reached a maximum value after which it decreased with a further decrease in temperature. The maximum and subsequent decrease was attributed to the effect of increasing viscosity with decreasing temperature. According to Tammann's results a substance could possibly reach a high degree of supercooling with practically no tendency to crystallize. This leads to solidification without crystallization and is of importance in the formation of glassy materials. Buckley (1951) cites cases of high degrees of supercooling in several organic substances which were followed by transformation into the glassy state.

In an attempt to measure the "crystallization frequency" (f) Richards (1932) produced some interesting evidence for the stability of supercooled material. A large number of tubes containing samples of the substances investigated was prepared and set in a freezing bath. Two organic materials were used which had freezing points of 42° and 48°C. These were held at a temperature of 130°C for several hours and then placed in a cooling bath at 25°C. They were kept at this temperature, 17 and 23 degrees below their respective freezing points, for several months. During this time none of the samples crystallized. According to Richards if the total number of tubes is "N_0" and after a time, "t", there remains a number of tubes, "N_t", which are unfrozen, they are related to the total number of tubes by the following relation:

$$N_t = N_0 e^{-ft}.$$

B-15

Richards concluded that "f" was very small for these substances. Actually, for this experiment it was zero.

DeCoppet (1907) argued that the duration of supersaturation was inversely proportional to the amount of supersaturation. His experimental results (Table II) seem to lend support to Tammann's conclusions. They also indicate that the volume of the sample is an important factor.

TABLE II

Supersaturation in large and small tubes
(A solution of $Na_2SO_4 \cdot 7H_2O$, saturated at 19.3°C.)

DeCoppet (1907), Table 13, p. 506

| Minimum temp. °C. | Duration of Supersaturation in Days | | |
	Large tubes 180.1 Cm.	Small tubes 89.5 Cm.	Average
5 - 5.9	1	1	1
6 - 6.9	1	1	1
7 - 7.9	1	1	1
8 - 8.9	1	1.1	1
9 - 9.9	1.1	1.3	1.2
10 - 10.9	2.1	3.5	2.6
11 - 11.9	7.8	29.1	12.3
12 - 12.9	24.2	157.5	42.0

The variation in experimental techniques is responsible for some of the disharmony in results presented here. Also, the mechanism of nucleation in multicomponent solutions is different from that in single component melts such as water. However, the general experimental results clearly indicate that crystallization is not initiated merely by lowering the temperature to the melting point, or point of saturation as the case may be.

Effect of Volume on Supercooling

Experiments on bulk water. Dorsey (1948) found that the sample with the most effective mote froze at the higher temperature, regardless of its volume. However, it must be pointed out that he worked with a limited range of sample volumes (about 8 cm^3) and that the literature supports the contention that the degree of supercooling is dependent upon volume.

The summary of deCoppet's work on supersaturation (Table II) is an example of the influence of volume on supercooling. Also, Smith-Johannson (1948) measured a greater average amount of supercooling than did Dorsey, and the volumes of his samples (less than 1 cm^3) were much smaller than those used by Dorsey. By the same token, Dorsey's values of supercooling are far in excess of those obtained in lakes (Devik, 1942) and in rivers (Altberg, 1936). These comparisons leave much to be desired because of the variation in observational techniques, but they do indicate a relationship between volume and degree of supercooling.

Experiments on small droplets. The volume-dependency of the degree of supercooling becomes more pronounced as the volume decreases to droplet size. This is at least partly a manifestation of the realtive increase in surface area, and the consequent increase of surface energy relative to total energy.

Small water droplets can be supercooled to the -30 to -35°C range with ease (Dorsch and Hacker, 1950; Dorsch and Levine, 1952; Fournier D'Albe, 1948; Heverly, 1949; Schaefer, 1946, 1948, 1949; Vonnegut, 1948, 1949; etc.) and values as low as -40°C have been observed by Lafargue (1950), and -50°C by Cwilong (1945).

The effect of small volumes in producing greater degrees of supercooling is not restricted to water. Prins (1950) points out that bulk mercury is supercooled with great difficulty, but that fine droplets (diameter approximately 20 μ) may be easily supercooled to less than -100°C. The equilibrium

melting point of mercury is -38.89°C. Turnbull and Cech (1950) recorded large

degrees of supercooling in small droplets of many different metals. The

highest values wer~ obtained with cobalt and palladium, which were supercooled

through a range of 330°C. Variations were observed in the degree of super->

cooling of any given metal. However, "...a significant, usually the major

fraction of the droplets, supercool some maximum amount $(\Delta T-)$ max. that is

reproductible and characteristic of the metal" (p. 804). For many metals the

ratio $(\Delta T-)$ max. to absolute melting point temperature was approximately

constant at 0.18. The extreme values of the ratio were 0.140 for Aluminum and

0.206 for Manganese. It is of interest to note that the corresponding ratio

for water is 0.18 if Cwilong's (1945) value of -50°C is accepted as maximum

supercooling, whereas the commonly observed supercooling of -40°C gives a ratio

of 0.15.

   Specific relationship between droplet size and supercooling. Since smaller

volumes produce greater degrees of supercooling, it is reasonable to expect a

specific relationship between droplet size and tsf. The existence of such a

relationship is indicated in the following brief review of some studies which

are especially pertinent to the problems of ice fog. A more complete discus-

sion of research along this line is given by Mason (1957).

   Heverly (1949) experimented with droplets which ranged in size from 60

to 1100 μ. The droplets were placed in a test cell which was slightly

submerged in the rapidly circulating bath of a cryostat. Temperature measure-

ments were rapidly made with thermocouples and a combination potentiometer-

galvanometer method as the test cell was cooled. Freezing was observed

visually, and, in the case of large droplets (over 300 μ), there was a galvan-

ometer deflection caused by the release of latent heat. The results are
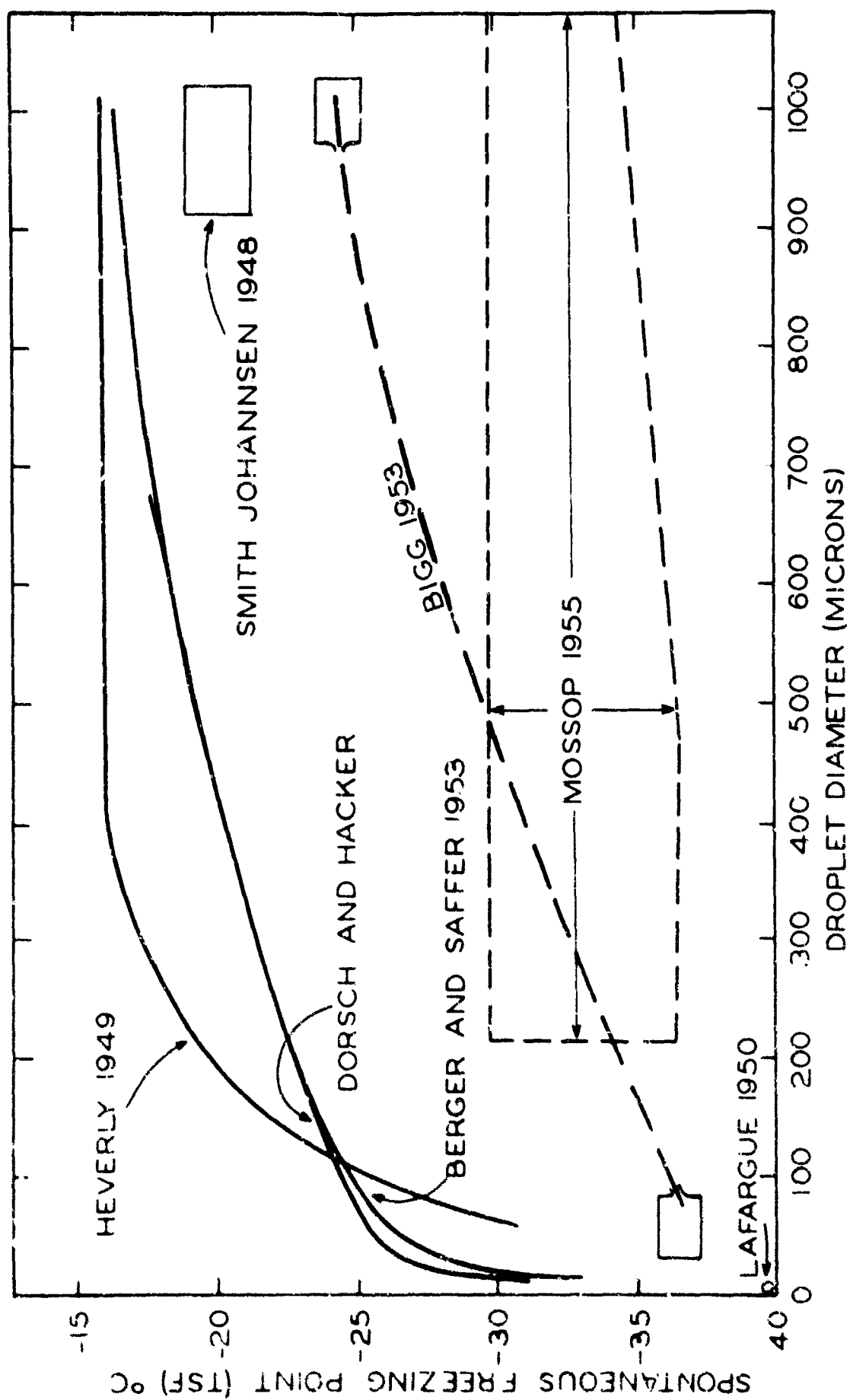
generalized in Figure B-1.

Fig. B-1. Spontaneous freezing point versus droplet diameter.

Dorsch and Hacker (1950) made a quantitative extension of the work on supercooling versus droplet size, and the experimental technique which they developed is extremely well suited for this purpose. The droplets which they investigated ranged in size from 8.75 to 1000 μ in diameter; this brackets the size range of droplets found in the atmosphere. A photomicrographic technique for obtaining a continuous record was developed. Freezing was accompanied by a marked change in appearance of the droplets and easily detected by study of successive frames of the film strip. Cooling was controlled by radio-frequency induction heating of the droplet-supporting surface, which was in thermal contact with a dry-ice bath. The temperature of the droplet-supporting surface was measured by a thermocouple and printed on the chart of a recording potentiometer at one-second intervals. A 16-mm movie camera, which viewed the test surface through a microscope, exposed one frame of film at the same instant that the temperature was printed on the chart. The results are generalized in Figure B-1.

Dorsch and Hacker also noted the same phenomena in the freezing behavior of small droplets that were recorded by Dorsey for larger samples, i.e., the tsf of some droplets was constant through several freezings, but the tsf of other varied. It was assumed that chance nucleation of the droplets by frost particles or other substances from the air may have been responsible for some of the variations in tsf. In order to test this hypothesis, water droplets were placed at the boundary between two oils of different density, but the same randomness was observed in the tsf.

Berger and Saffer (1953a, 1953b) utilized the experimental technique developed by Smith-Johannsen in their work; the original design was modified to accommodate a wider range of sample volumes (10 - 700 μ). Their results were very similar to those of Dorsch and Hacker (Figure B-1).

Lafargue (1950) worked with very fine droplets (1 - 10 μ), which were supported on spider threads of diameter 0.1 to 0.5 μ. Ultramicroscopic techniques were employed to observe the freezing. The spontaneous freezing point for these droplets was observed to be -40.4 ± 1.5°C (Figure B-1). Lafargue's experimental methods were well suited to the examination of droplets below 10 μ in diameter, and they included observations on droplets placed in various media. Exactly the same results were obtained when the droplets were immersed in air, parraffin oil, or silicone.

Bigg (1953) experimented with drops suspended at the interface of two insoluble liquids. He obtained lower values of tsf than previous workers (Fig. B-1) and concluded that the tsf was dependent on cooling rate as well as on volume. He derived a relationship between temperature, volume and time from simple probability considerations which was reasonably consistent with his experimental results. He concluded that spontaneous, or homogeneous nucleation, is an important mechanism for freezing cloud droplets at temperatures below -20°C. Mossop (1955) challenged this conclusion as a result of his experiments which are briefly summarized next.

Mossop (1955) carried out a series of experiments in which extreme care was taken to eliminate impurities. Steam, from which all local air had been eliminated was condensed directly into glass or fused quartz capillaries. The tsf values for his samples were lower than any previously reported for comparable volumes (Fig. B-1). Mossop concluded that all previously reported results in the observed volume range were affected by the presence of impurities in the water. He emphasized that the lowest recorded values are the critical ones to use in an attempt to determine the spontaneous freezing point;this has not always been done. In particular, he pointed out that spontaneous freezing is not as important in freezing droplets as was suggested by Bigg.

Both Bigg and Mossop were unusually careful about eliminating impurities, and the effect of this on increasing the amount of supercooling is clear in Figure B-1.

Freezing of a Supercooled Cloud

In general, it has been observed that freezing may start in a supercooled cloud by (1) cooling it below a certain temperature or by (2) nucleating it with foreign substances.

The Threshold Temperature

From the reports of many observers it is clear that below about $-40^{\circ} \pm 1.5\,^{\circ}C$ clouds are always composed of ice crystals (Cwilong, 1945, 1947a, 1947b, 1948; Schaefer, 1946, 1948, 1949a; Fournier D'Albe, 1948; Oliver and Oliver, 1949; Dobson, 1950; Mason, 1950a).

Cwilong (1945) investigated the formation of supercooled water droplets and ice crystals in a Wilson cloud chamber. When the temperature was above $-35\,^{\circ}C$ at the end of the expansion (i.e., when condensation just begins) no ice crystals were observed; at temperatures below this value, a few ice crystals were formed among a much larger number of water droplets. As the minimum temperature decreased more and more ice crystals appeared until at $-41.2\,^{\circ}C \pm 0.05\,^{\circ}C$ the cloud was composed entirely of ice crystals. The appearance of the solid phase depended solely on the minimum temperature reached. Cwilong assumed that below this "threshold temperature", where ice crystals and no water droplets formed, sublimation was taking place. On making further measurements with outdoor air in the mountains and over the ocean, Cwilong (1947b, 1948) reported the same threshold temperature $(-41\,^{\circ}C)$. This threshold temperature was observed to be slightly higher in air that was polluted; tobacco smoke in the air gave the highest value, $-23\,^{\circ}C$.

Similar observations were reported by Schaefer (1946, 1948, 1949b), who formed supercooled clouds by introducing moist air into a small commercial freezing unit. In Schaefer's work, water droplet clouds never developed into ice-crystal clouds except when a portion of the cloud was cooled to below -39°C or upon the introduction of certain foreign nuclei, "of specific crystalline form."

Schaefer (1948) concluded that spontaneous freezing occurs below a threshold temperature of -39 ± 0.1°C. He found that introducing solid CO_2 (dry-ice) is a very effective way of cooling local portions of the cloud to a temperature below -39°C. Seeding a cloud of supercooled water droplets with dry ice particles produces many ice crystals, which initiate freezing in other droplets upon contact, thus producing a chain reaction. Schaefer (1946) obtained similar results by cooling a rod in liquid air and rapidly passing it through a supercooled cloud. Once an ice particle is formed, it may undergo a splintering action which adds to the chain reaction (Dobson, 1950; Schaefer, 1950a; Palmer, 1950; Brewer, 1950).

Nucleation by Foreign Particles

Of the various foreign nuclei which have been tested, silver iodide is the most effective (Vonnegut, 1947, 1948, 1949a, 1949b). Vonnegut (1949a) prepared smokes of five substances (PbO, Pb_3O_4, KI, and AgI) in a box with air temperature at -19°C. Moist air was introduced merely by breathing into the box. The concentration of crystals formed was visually estimated. These substances (and the system in which they crystallize) are listed in Table III along with the relative number of ice crystals produced under these conditions.

Vonnegut and Schaefer attributed the freezing activity of silver iodide to its close crystalline similarity to ice, "both dimensions of the unit cell of ice and silver iodide are the same to within about one per cent" (Vonnegut, 1947, p. 594). Because of this similarity they assumed sublimation of water molecules directly on the AgI crystal lattice.

TABLE III

Relative effectiveness of various
substances in producing ice crystals at -19°C
(Prepared from data of Vonnegut, 1949a,
and Handbook of Chemistry and Physics)

SUBSTANCE	CRYSTAL FORM	CONCENTRATION OF ICE CRYSTALS PRODUCED PER cm^3
AgI	Hexagonal	10,000
PbC	Tetragonal and orthorhombic	1
Pb_3O_4	Crystalline scales or amorphous powder	0.1
PbO_2	Tetragonal	No visible results
KI	Cubic	No visible results

Smith-Johannsen (1948) points out that graphite is a more effective crystallization nucleus in bulk water than is silver iodide. However, graphite does not act as a "sublimation nucleus" while silver iodide is a very effective one. Thus, the conclusion was drawn that there is a difference between "sublimation nuclei" and "freezing nuclei".

It is reasonable to expect ice formation to take place spontaneously on silver iodide particles because of the very close similarity of crystal structure. However, Vonnegut's (1949b) measurements show that ice crystals do not form immediately on the silver iodide particles. He also points out that some of the smaller particles of silver iodide may dissolve in the water droplets before they have a chance to initiate the formation of an ice crystal. This is very probable. The electron microscope examination of silver iodide smokes showed a large number of particles of about 30 Å. Since these were the smallest particles observable with the electron microscope it is likely that there will be many particles smaller than 30 Å which cannot be observed.

In view of the evidence, Vonnegut (1949b, p.277) states that

".....the presence of silver iodide can be regarded as greatly
increasing the probability of ice crystal formation."

This qualified statement is most certainly true, as evidenced by much experimental work. However, the exact action of the silver iodide in producing freezing is still open to question.

Types of Nuclei

The growth of pre-existing crystals by sublimation is an unquestioned fact. However, the role of sublimation in nucleating new ice crystals in the atmosphere is open to question. The change in energy which accompanies the direct transfer from water vapor to ice is about 13% greater than that required to go from vapor to liquid. This difference in energy levels by itself is not so great that one could rule out nucleation of ice crystals from the vapor. However, the problem is not quite so simple because supercooling in water, and the nucleation required to overcome it, have their counterparts in supersaturation of the air prior to appearance of the condensed phase which must be nucleated. A brief comment on condensation nuclei is in order.

Condensation nuclei. Early investigators did not believe that a sufficient quantity of foreign condensation nuclei existed to form the clouds of nature (Barnes, 1926). Recent inquiry, however, especially since the advent of the electron microscope, has shown that sufficient quantities of impurities exist in the atmosphere to completely validate the concept of foreign condensation nuclei (Ohtee, 1949; Mason, 1950b; Kuroiwa, 1951; Junge, 1951; Nakaya, 1951b; Kumai, 1951). According to Hewson and Longley (1944), if these nuclei were not present a region containing water vapor would experience far greater supersaturation than has ever been observed in nature. The possibility that water molecules themselves can coalesce to form colloidal sized particles which can act as nuclei, as suggested by Barnes (1926), is unlikely. It would take approximately 5000 of them to coalesce into a drop of 10^{-6} cm in diameter (Hewson and Longley, 1944), the minimum size for effective condensation nuclei. If such spontaneous condensation took place among water molecules it would be

difficult to account for supersaturation of an air sample. This
would be analogous to what Dorsey (1948) calls a homogeneous singularity in
freezing, and the results of many investigations on supercooling points toward
nucleation by heteorogeneous singularities, i.e., by foreigh particles.

The action of these "condensation nuclei" is perhaps similar to the action
of Dorsey's "motes", i.e., they provide a greater concentration of molecules
in a specific region due to the presence of their adsorption surface.

<u>Freezing nuclei</u>. If the freezing of a droplet is caused by some special
nucleating mote we should expect to find some of them in the resulting ice
crystals. Locating tiny particles in small ice crystals is easier than in
larger samples because of the smaller area to search. Nakaya (1951b) presents
a brief account of some experimental observations on snow crystal nuclei with
an electron microscope. The crystals were obtained on a film of collodion
mounted on the sample holder of the electron microscope. After the crystal
had evaporated (at subfreezing temperatures) the sample was investigated under
the electron microscope. Nakaya states:

> "One solid nucleus is always observed at the central portion of
> each snow crystal. It is proposed to call this the central
> nucleus. The center nuclei are between 0.5 to 8.0 μ in the
> largest extension.

> "In the remainder of the snow crystal numerous small nuclei are
> to be seen. These are nearly the same size as the condensation
> nuclei in the true atmosphere, that is to say, between 0.01 and
> 0.02 μ in diameter..." (Nakaya, 1951b, p. 550).

After an examination of many photographs Nakaya drew up a frequency curve from
1200 data; the condensation nuclei fell into two major size ranges, the
diameters of which are about 0.15 μ and 0.05 μ, respectively.

The nuclei are composed of soil particles, carbon particles, micro-
organisms, various hygroscopic particles and some of unknown origin (Kumai,
1951). Kumai (1964) has discussed electron microscope studies on ice fog
crystals and this work is currently being extended by Ohtake (1965).

Sublimation nuclei. When ice crystals are formed in an expansion chamber below the "threshold temperature," they seem to form directly from the vapor; Cwilong (1945) described this as "sublimation". However, D'Albe (1948) questioned the role of sublimation of ice crystals directly from the vapor state under any conditions. He devised an apparatus which enabled him to observe with an ultramicroscope the individual condensation nuclei in an expansion chamber. His results were similar to those of Cwilong (1945) except that his techniques were more refined, especially in the critical range slightly above and below the threshold temperature.

In experiments with outdoor air he observed that when the temperature after expansion was above -32°C, the cloud was composed almost entirely of water droplets. If any ice crystals were present in these clouds, they did not exceed one per cc. When the temperature at the end of expansion fell between -32 and -35°C, ice crystals were present in the clouds to the extent of about 20 per cc (water droplets were approximately 1000 per cc). As the final expansion temperature decreased to about -40°C, there was no observed increase in the number of ice crystals produced. Increasing the degree of supersaturation of the vapor also showed no effect in increasing the number of ice nuclei. However, between -41°C and -42°C a very sharp increase in the number of ice crystals occurred, and below -42°C the cloud was composed of ice crystals only.

It has been pointed out by several authors that the formation of ice crystals in the atmosphere occurs only when the air is nearly saturated with water, and never when merely saturated with respect to ice. In some instances ice crystals form at a relative humidity of 150% over ice (D'Albe, 1948; Ludlam, 1948, 1951; Dobson, 1950; Krastanow, 1941; Weickmann, 1942). These authors prefer the term "freezing nuclei" over "sublimation nuclei" in all cases. However, Houghton (1951) pointed out that, although no cases of crystal formation near ice saturation are recorded, there are cases where ice crystals form

below water saturation. He prefers the term "sublimation nuclei" for the nuclei in such cases. However, it is not easy to measure humidity with precision in the range of -40°C. Also once crystals are present the humidity measurements themselves are difficult to interpret because strong local temperature gradients may exist around the crystals (see Appendix A). Therefore, it is difficult to determine when crystals form below water saturation. The difference between saturation with respect to ice and water at -40°C is 0.06 mb.

In this paper it is assumed that the initiation of ice crystals results from freezing a water droplet or a water film on a solid nucleus in all cases. Mason (1957 p.127) also considers this to be the mechanism of initial formation of an ice crystal. Once the crystal exists it will grow or decay by sublimation. This assumption simplifies the problem by confining attention to the problem of nucleating the ice phase in water. It also indicates that the difference in behavior between silver iodide and graphite cannot simply be ascribed to their roles as "sublimation" or "freezing" nuclei.

Surface Structure of Water

It is well known that the properties of matter near the boundary of a phase are significantly different from those of the bulk, or interior, of the phase. According to Weyl (1951) the surface free energy of a substance can be reduced by polarization of the ions making up the surface. Water is a highly polar liquid as evidenced by its high dielectric constant. The large size and double valence of the oxygen ions make them highly polarizable especially when compared with the unpolarizable H^+ ion. Using this type of reasoning, in accord with his work on surface structure of other materials, Weyl proposed the following surface structure for water:

"A droplet of water, therefore, has its O^{2-} ions in the exterior layer, followed by a second layer which contains the nonpolarizable H^+ ions. A particle which contains OH^- or O^{2-} ions in the surface, followed by a layer which is preferentially positive, can be considered as being covered with dipoles, the negative parts of which point into space, whereas the positive parts are directed toward the interior" (Weyl, 1951, p.392).

This surface polarization forms an electrical double layer which should give rise to observable phenomena. Several observations will be discussed in the light of Weyl's hypothesis.

The coalescence of small droplets. Small droplets supported on flat surfaces will coalence when brought into contact. The photos of Dorsch and Hacker (1950) illustrate this phenomenon, and Dessens (1950) observed coalescence of water droplets on fine spider's threads whenever they made contact, "at least whenever their radii exceed one or two microns". Dessens does not state specifically if any of the smaller droplets failed to coalesce.

Free falling droplets appear to behave differently. Swinbank (1947) made microscopic observations of the collisions of cloud droplets and reports that they were never seen to coalesce on impact but behaved much like rigid spheres; this has been reported previously by Millikan (1947, p. 67). Millikan's droplets were found to carry both kinds of electric charge, presumably due to their method of production (Milliken, 1947, pp. 47-89). Swinbank investigated liquids of widely varying physical properties, namely pure water, fluess oil, alcohol, alpha-naphthalene, and benzene. One limitation to the experimental setup was that droplets larger than two microns could not be observed. However, he felt that up to $\approx 50\,\mu$ the results would be the same. However, as the droplets become larger their increasing inertia will overcome the repulsive forces. The concept of an electrical double layer is an appealing explanation of this phenomenon, but aerodynamic considerations are also important in preventing collisions between small droplets.

Electrical effects associated with freezing. Dinger and Gunn (1946) designed an experiment in which a water-air surface was at the gap in a circuit which has a voltmeter connected below the water sample. A potential difference was observed across the interface. Since the voltmeter was connected below the

water surface, a

> "positive potential) terpreted as giving indication that the double layer on the water or ice is such that a layer of positive electricity is encountered as a reference point passes from water to air; a negative voltage on the recording indicates a double layer having the reverse polarity."

It was observed that both water and ice surface exhibit a positive po ntial in this setup, i,e., an electrical double layer with the negative layer on the outside. However, during the phase transformation from water to ice, the positive potential changes to a negative potential. This negative potential increases as the phase change progresses until a maximum is reached during the phase change. After the maximum is reached the negative potential drops off exponentially and when freezing is complete the positive potential that was originally observed on the water surface is again present on the ice surface. Thus, it appears that the surface structure of water is disturbed while the phase change is occurring. This phenomenon is apparently important in the production of thunderstorm electricity (Workman and Reynolds, 1949, 1950). It is of interest to note that electrical effects are also observed during snowstorms (Schaefer, 1947). Accurate temperature measurements must be a part of observations during snowstorms in order to distinguish the effects produced by fracture of ice particles from those associated with phase changes.

Adhesion of ice particles. Nakaya and Matsumoto (1953) investigated the adhesive force between two small ice spheres (d = 1 to 4 mm) suspended by cotton filaments, one of which was movable. A slight contact was made between the spheres for a period of less than one minute. Then they were pulled apart by moving the movable filament with a screw motion device at its top. It was observed that the tension caused the spheres to rotate while still in contact; the point of contact shifted approximately 30°. These observations were interpreted as evidence of the existence of a liquid-like film on the ice surface and are compatible with Weyl's postulate.

B-29

ing of small water droplets. Weyl used his surface structure model

of water to explain the relationship between droplet size and the degree of

supercooling as follows:

> "If we assume that the water in the interior of a droplet has its
> normal atomic structure, whereas that of the surface film of the
> same droplet has a basically different structure, then it follows
> that a water droplet has to have a certain minimum size in order to
> be stable. The transition from one type of structure to another
> type having a different geometry, requires a finite distance. This
> distance must be a function of the temperature, because the structure
> of water changes with temperature with respect to geometry and inter-
> nuclear distance. One would also expect that the more rigid structure
> of ice would require a larger transition layer than the more flexible
> structure of liquid water. As a result, at a given temperature below
> the freezing point, a particular size must exist where a droplet
> of water is stable in the liquid state but not as ice..." (Weyl,
> 1951, p.394).

Hosler (1951) applied these ideas to the problem of initiating freezing

in clouds of supercooled water droplets. He investigated the effectiveness of

many substances on the production of ice crystallization. He found that the

crystal structure of the nucleating material is not the controlling factor.

Cwilong (1945) also reported that the degree of supercooling could be decreased

by the presence of dust and smoke, regardless of whether the particles were

crystalline or amorphous.

Hosler used a home freezer (volume 4.1 ft^3) as a cloud chamber. "Aerosols

were introduced into the cold chamber by spraying aqueous solutions from a

commercial atomizer and by vaporiation from a small basket made of resistance

wire" (p.327). Some results of Hosler's work are reproduced in Table IV,

which lists substances observed to be active in freezing the supercooled

clouds. The column headed "partial" lists the temperature at which the first

increase in ice crystals was noted. The column headed "complete" lists the

temperatures at which the cloud was composed entirely of ice crystals (visual

observations, temperatures accurate to $1^\circ C$).

TABLE IV

List of substances tested and found active in freezing supercooled clouds
(Hosler, 1951, p. 328)

Substance	Crystal form	Method of dispersal	T. at which active (°C)	
			Partial	Complete
AgI	Hexagonal	Vapor	- 3	- 4
$AgNO_3$	Rhombic	Vapor & spray	- 3	- 4
Ag_2S	Cubic-rhombic	Vapor	- 4	- 5
PbI_2	Hexagonal	Vapor	- 4	- 5
Nh_4I	Cubic	Vapor & spray	- 9	-12
Cu_2I_2	Cubic	Vapor	- 9	-12
I_2	Rhombic	Vapor	-12	-15
NaI	Cubic-monoclinic	Vapor & spray	-13	-16
KI	Cubic	Vapor	-13	-16
TlI	Rhombic-cubic	Vapor	-13	-17
$HgCl_2$	Rhombic	Vapor	-14	-17
CdI_2	Hexagonal	Vapor	-15	-18
PbO	Tetragonal-rhombic	Vapor	-16	-19
O_3	---	A.C. spark discharge	-14	-20
HgI_2	Tetragonal	Vapor	-18	-21
Sunlight (uncertain)	---	Through open window	(-16?)	?
$PbCl_2$	Rhombic	Vapor	-18	?
$CuSO_4$	Triclinic	Vapor	-20	?
HgO	Rhombic	Vapor	-22	?

Hosler attacks the concept of "sublimation nuclei", and points out that his spraying of aqueous solutions into the cloud chamber did not lead to the formation of free crystalline particles. As mentioned above, Vonnegut (1949b) also pointed out the possibility of silver iodide particles dissolving in the water droplets. These considerations, in addition to the fact that the crystalline structure seems to be unimportant, cast additional doubt on the concept of "sublimation nuclei."

The concept of surface structure proposed by Weyl (1951) is the basis of Hosler's explanation of these results. The addition of silver iodide or of

other effective substances permits freezing at higher temperatures because they

furnish highly polarizable ions which, on introduction to the surface of the

droplet, increase the possible amount of surface polarization. Since an

increase in the surface polarization is assumed to decrease the surface free

energy, the more highly polarized droplet requires less supercooling to freeze.

According to Hosler (1951, p. 330):

> there are "three ways in which a small supercooled drop can
> be made to crystallize: (1) by increasing the size of the
> droplet, (2) by decreasing its temperature, and (3) by the
> addition of foreign molecules or ions that reduce the surface
> free energy of the drop".

The Weyl-Hosler concepts involving surface energy are interesting in that:

(1) they offer a physical explanation for the dependency of tsf on volume, and

(2) they offer an explanation for the effect of foreign nucleating substances

which does not depend upon similarity of crystal structure. However, there are

still some important points which are not adequately explained. Many of the

substances tested by Hosler and found to be inactive contain highly polarizable

ions. Further, there is no explanation of fluctuations in tsf. The specific

differences between individual droplets which influence their freezing proper-

ties seems best explained in terms of the most effective nuclei in the sample,

but the specification of the nuclei is still in question.

Ice Fog

In the Fairbanks-Ft. Wainwright area, ice fog begins at about -35°C and is

always well developed at -40°C. The fact that these temperatures are in the

range of experimentally determined freezing temperatures for droplets, is not

merely a coincidence. In clean air clouds of water droplets do not freeze

until they are supercooled to about -40°C. In polluted air freezing begins at

higher temperatures, i.e., about -35°C in Fairbanks. As seen in Table IV these

pollutants do not have to be of a special type in order to be effective.

The phase change from water droplets to ice crystals at about -35°C has a profound effect on fog formation. This can be demonstrated by a simple example. Assume that the air near the ground is cooling rapidly. Assume further, that some supercooled water-droplet fogs are forming at localized places, such as over open water, as a result of the cooling. This implies that all of the low-level air will be close to saturation with respect to water. At -35°C the capacity of this air to hold water vapor decreases with decreasing temperature at the rate of 0.027 g m^{-3} °C^{-1} (over water). If the air is saturated, this change in vapor pressure with temperature will force excess moisture to condense out of solution. For simplicity, assume that the presence of water droplets prevents any significant supersaturation of the air. Under these conditions one degree of cooling at -35°C would provide 0.027 g m^{-3} of condensed water to the air.

If the droplets freeze at -35°C there will be an additonal reduction in the air's capacity to hold moisture because the saturation vapor pressure must now be reckoned with respect to ice. The excess moisture produced by freezing at -35°C is more than three times greater than that produced by one degree of cooling at -35°C. This is easily seen in the following table:

Air temperature -35°C	Saturation vapor pressure (mb)	Saturation vapor density (g m^{-3})
Over water surfaces	0.314	0.286
Over ice surfaces	0.223	0.203
Differences	0.091 (mb)	0.063 g m^{-3}

The table shows that the excess water vapor produced by simply freezing drop-lets at -35°C is of the same order of magnitude (slightly higher) as the density of ice fog in outlying areas (0.07 g m^{-3}, see p. 66 of main text). If the droplets freeze at -35°C and cool, with the air, to -36°C it is necessary to take into account the 0.027 g H$_2$O m^{-3} produced by 1°C of cooling. This

gives a total of 0.100 g m^{-3} of water condensed between -35 and -36°C, whereas a maximum of 0.027 g m^{-3} can be condensed in cooling from -34 to -35°C. If the droplets do not freeze until a lower temperature is reached, the relative contribution of water vapor provided by freezing increases. For example, at -40°C more than five times more water is condensed by freezing than by one degree of cooling.

In relation to the problem of ice fog in Fairbanks it is instructive to restate the above discussion. The volume of air available to dissolve the daily output of water was estimated to be about 100×10^7 m^3 (p.50). The excess vapor of 0.083 g m^{-3} produced by freezing will put 83×10^6 g H$_2$O into this volume of air. This, in itself, is nearly twice the daily cold-weather output from the University power plant, yet it is added within several hours. If the air continues to cool, say 2°C, immediately after freezing the resultant condensed moisture, which is added in a few hours, exceeds the 124×10^6 g H$_2$O which is the daily input from automobiles.

Two points of special importance to ice fog are: (1) the source of water vapor provided by freezing is diffuse - indeed, it is spread through the entire air mass, and (2) the observed cooling rates (several °C per hour) are such that the water vapor provided by freezing comes into existence within a few hours (Fig. B-1); yet it compares in magnitude with an entire day's output from a power plant, or from all of the automobiles in the area.

The above argument agrees well with the observed sudden onset and widespread distribution of ice fog at -35 to -40°C.

At lower temperatures all of the water vapor put into the saturated air cools rapidly and condenses to tiny droplets. These quickly supercool to the -35 to -40°C range and freeze. Turbulence associated with exhaust outlets quickly removes these crystals from their source areas, and transports them into relatively dry air. This in turn inhibits them from growing to a rapidly precipitable size so they remain in the air as a fog of tiny ice crystals - Ice Fog.

REFERENCES CITED

Altberg, W. J. (1923), On the Cause of the Formation of Ice at the Bottom of Rivers and Lakes, Quart. Journ. Roy. Met. Soc.,Vol. 49, No.205, pp.54-60.

Altberg, W. J. (1936), Twenty Years of Work in the Domain of Underwater Ice Formation (1915-1935), Assoc. Int. D'Hydrologie Sci. Bull. No. 23, pp.373-407.

Altberg, W. J. (1938), Crystallization Nuclei in Water, Acta Physicochimica U.R.S.S. Vol. 8, pp. 677-678.

Altberg, W. J. and Lavrow, W. (1939), Experiments on the Crystallization of Water II, Acta Phys.-Chim. Vol. XI, No. 2, pp. 287-290.

Anderson, G. S., C. Benson, D. Grybeck and J. Stout (1965), A Preliminary Study on Freezing in Turbulent Streams of Interior Alaska, Proceedings, Fifteenth Alaskan Science Conference, College, Alaska, p. 95.

Barnes, H. T. (1906), Ice Formation, John Wiley & Sons, N. Y., 260 pp.

Barnes, H. T. (1926), Colloid Forms of Ice and Water, Colloid Chem. Ed. J. Alexander, Vol. I, pp. 435-444.

Berger, Carl and Chas. M. Saffer , Jr. (1952), Ice Physics Program, W.A.D.C.-AF 33 (616)-127, C-1053.

Berger, Carl and Charles M., Saffer, Jr. (1953), On Some Recent Experiments with Supercooled Water, Science, Vol. 117, No. 3050, p. 665.

Bergman, P. G. (1943), The Formation of Centers of Condensation in Supercooled Phases, Phys. Rev. (2) Vol. 63, p. 456.

Bernal, J. D. and R. H. Fowler (1933), A Theory of Water and Ionic Solution, Particular Reference to Hydrogen and Hydroxyl Ions, Journ. Chem. Phys. Vol. 1, No. 8, pp. 515-548.

Bigg, E. K. (1953), The Supercooling of Water, Proc. Phys. Soc. $^{\sim}$, Vol. 66, pp. 688-694.

Brewer, A. W.(1950) Discussions on Cloud Physics, Cent. Proc. Roy. Met. Soc. pp. 63-65.

Buckley, H. E. (1951), Crystal Growth Wiley, New York, 571 pp.

Cwilong, B. M. (1945), Sublimation in a Wilson Chamber, Nature, Vol. 155, p.361.

Cwilong, B. M. (1947a) Observations on the Incidence of Supercooled Water in Expansion Chambers and on Cooled Solid Surfaces, Jour. Glaciology, Vol. 1, No. 2, 1947a, p. 53.

Cwilong, B. M. (1947b), Sublimation in Outdoor Air, Nature, Vol. 160, p. 198.

Cwilong, B. M. (1948), Sublimation in the Atmosphere over the Oceans, Nature, Vol. 161, p. 62.

D'Albe, Fournier (1948), Condensation of Water Vapor below 0°C, *Nature*, Vol.162, pp. 921-922.

Daniels, F. (1938), *Chemical Kinetics*, Cornell Univ. Press, Ithica, New York.

deCoppet, L. C. (1907), Recherches sur la Surfusion et la Sursaturation, *Ann. Chim, et Phys.*, 8e ser., 10, pp. 437-527.

Despretz, C. (1837), Reference to Despretzs' Experiments of 1837 cited by Dorsey 1948.

Despretz, C. 1839, Recherches sur le maximum de densite de l'eau pure et des disolutions aqueuses, *Ann. Chim. et Phys.* (2) 70, pp. 5-81.

Dessens, H. (1950), Some Remarks on the Study of the Microphysics of Natural Clouds, *Cent. Proc. Roy. Met. Soc.* pp. 59-60.

Devik, Olaf (1942), Supercooling and Ice Formation in Open Waters, *Geofysicke Publikasjoner*, Vol. XIII, No. 8.

Devik, Olaf (1944), Ice Formation in Lakes and Rivers, *Geog. Journ.* Vol. 103, No. 5, p. 193.

Devik, Olaf (1949), Freezing Water and Supercooling, Anchor Ice and Frazil Ice, *J. Glaciology*, Vol. 1, No. 6, pp. 307-309.

Dinger, J. E. and Ross Gunn (1946), Electrical Effects Associated with a Change of State of Water, *Terr. Magnet. and Atm. Electricity.* Vol. 51, No. 4, pp. 477-494.

Dobson, G. M. B. (1950), Introductory Address on Cloud Physics and Precipitation Symposium, *Cent. Proc. Roy. Met. Soc.* pp. 34-36.

Dorsey, N. E. (1938), Supercooling and Freezing of Water, *Nat'l. Bur. Stand. Journ. Res.* Vol. 20, p. 799.

Dorsey, N. E. (1940), *Properties of Ordinary Water-Substance*, Amer. Chem. Soc. Monograph Series, #81, Reinhold Publishing Corp., N.Y.

Dorsey, N. E. (1948), The Freezing of Supercooled Water, *Trans. Am. Phil. Soc.* N.S. Vol. 38, Part 3, pp. 247-328.

Dorsch, R. G. and P. T. Hacker (1950), Photomicrographic Investigation of Spontaneous Freezing Temperature of Supercooled Water Droplets, *U.S.N.A.C.A. Tech. Note 2142.*

Dorsch, R. G. and Levine, J., 1952, A Photographic Study of Freezing of Water Droplets Falling Freely in Air, *N.A.C.A. Res. Memo. E51217*, Feb. 25, 1952.

Frank, F. C. (1946), The Molecular Structure of Deeply Supercooled Water. *Nature*, Vol. 157, p. 267.

Gerdel, R. W. (1952), Discussion of the Formation of Frazil and Anchor Ice in Cold Water by V. J. Schaefer, Trans. V. 31, pp. 885-893, 1950. *Trans. A.G.U.* Vol. 33, pp. 127-128.

Hallanger, N. L. (1938), A Study of Aircraft Icing, Bull Am. Met. Soc. Vol. 19, pp. 377-381.

Heverly, J. Ross (1949), Supercooling and Crystallization, Trans. A.G.U. Vol.30, No. 2, pp. 205-210.

Hewson, E. W. and R. W. Longley 1944, Meteorology, Theoretical and Applied, 468 pp. John Wiley & Sons, Inc.

Hosler, C. L. (1951), On the Crystallization of Supercooled Clouds, Journ. Met. Vol. 8, pp. 326-331.

Houghton, H. G. (1951), On the Physics of Clouds and Precipitation, Compendium of Meteorology. pp. 165-181.

Junge, C. (1951), Nuclei of Atmospheric Condensation, Compendium of Meteorology pp. 182-191. Am. Met. Soc. Boston, Mass. Edited by Thomas F. Malone.

Kenrick, F. B. and W. H. Martin (1913), On Supercooling Water, Trans. Roy. Soc. Canada, Ser. III, Vol. 7, p. 220.

Krastanow, L. (1941), Beitrag zur Theorie der Tropfen-und Kristallbildung in der Atmosphäre", Meteor. Z., 58, pp. 37-45.

Kumai, Motoi (1951), Electron-Microscope Study of Snow-Crystal Nuclei, Journ. of Meteorology, Vol. 8, pp. 151-156.

Kuroiwa, Daisuke (1951), Electron-Microscope Study of Fog Nuclei, Journ. of Meteorology, Vol. 8, pp. 157-160.

La Fargue, C. (1950), On the Freezing of Droplets of Water and of Aqueous Solution, Cent. Proc. Roy. Met. Soc. pp. 61-63.

La Mer, Victor K. (1952), Nucleation in Phase Transitions, Industrial and Engineering Chemistry, Vol. 44, No. 6, pp. 1270-1277.

Ludlam, F. H. (1948), The Forms of Ice Clouds, Quart. Journ. Roy. Met. Soc., Vol. 74, pp. 39-56.

Ludlam, F. H., (1951), The Physics of Ice Clouds and Mixed Clouds, Compendium of Meteorology, pp. 192-198. Edited by Thomas F. Malone, Am. Met. Soc. Boston, Mass.

Mason, B. J. (1950a), The Formation of Ice Crystals and Snowflakes, Cent. Proc. Roy. Met. Soc. pp. 51-58.

Mason, B. J. (1950b) The Nature of Ice-Forming Nuclei in the Atmosphere, Quart. Journ. Roy. Met. Soc. Vol. 76, #327, pp. 59-75.

Mason, B. J. (1957), The Physics of Clouds (481 pp.) Oxford University Press.

Miers, H. A. and Isaac, Miss. F. (1906a) The Refractive Indices of Crystallizing Solutions, with Special Reference to Passage from the Metastable to the Labile Condition, Journ. of the Chemical Soc. Trans., Vol. 89, Part I, pp. 413-454.

Miers, H. A. and Isaac, Miss. F. (1906b), On the Temperature at which Water Freezes in Sealed Tubes, Chem. News. V. 94, pp. 89-90.

Mikhnevich, G. L., and I. F. Browko (1938), Stability of the Crystallization Centers of an Organic Liquid at Various Temperatures and Conclusions to be Drawn Therefrom Concerning Tammann's Method. Phys. Ztschr. Sowjet 13: pp. 113-122.

Millikan, R. A. (1947), Electrons (+ and -), Proton, Photons, Neutrons, Mesotrons and Cosmic Rays. Rev. ed. The University of Chicago Press. 642 pp.

Mossop, S. C. (1955), The Freezing of Supercooled Water, Proc. Phys. Soc. B., Vol. 68, pp. 193-208.

Nakaya, Ukichiro (1951b), Snow Crystal Growth, Journ Glaciology, Vol. 1, No. 10, pp. 550.

Nakaya, U. and A. Matsumoto (1953), Evidence of the Existence of a Liquidlike Film on Ice Surfaces, SIPRE Research Paper No. 4.

Nybrant, G. (1943), Bildning av Bottenis och Soppa i ett Rinnande Vattendrag, Teknisk Tidskrift, Ht. 4, Vag-och Vatten-byggnadskonst samt (text in Swedish). English Abstract in Journ. of Geol. Vol. 1, #10, 1951, p. 588.

Ohtake, Takeshi (1965), Geophysical Institute, University of Alaska, Personal Communication Regarding Electron Microscope Studies on Ice Fog Crystals.

Ohtee, S. (1949), Investigations on Condensation Nuclei, Am. Met. Soc. Bull. 30 (8), pp. 295-296.

Oliver, V. J. and M. B. Oliver 1949, Ice Fogs in the Interior of Alaska, Bull. Am. Met. Soc. Vol. 30, No. 1, pp. 23-26.

Palmer, H. P. (1950), Discussion on Cloud Physics, Cent. Proc. Roy. Met. Soc. p. 63.

Parsons, W. J., Jr. (1942), The Evolution of Ice in Streams, Hydrology, Physics of the Earth-IX, McGraw Hill Book Co., New York, pp. 137-141.

Pictet, (1879) See Dorsey (1948) p. 248.

Prins, J. A. (1950), Discussions on Cloud Physics, Cent. Proc. Roy. Met. Soc. pp. 63-65.

Rau, W. (1944), Gefriervorgange des Wassers bei tiefen Temperaturen (Vorläufige Mitteilung). Schriften dtsch Akad. Luftfahrtforsch 8, (2) pp. 65-84.

Richards, W. T. (1932), The Persistence and Development of Crystal Nuclei Above the Melting Point, Journ. Am. Chem. Soc. Vol. 54, pp. 479-495.

Richards, W. T., Kirkpatrick and Hutz (1936), Further Observations Concerning the Crystallization of Undercooled Liquids, Journ. Am. Chem. Soc., Vol.58, pp. 2243-2248.

Schaefer, V. J. (1946), The Production of Ice Crystals in a Cloud of Supercooled Water Droplets, Science, Vol. 104 (N.S.) No. 2707, p. 457.

Schaefer, V. J.(1947),Properties of Particles of Snow and the Electrical Effects they Produce in Storms, Trans. A.G.U., Vol. 28, No. 4, pp. 587-614.

Schaefer, V. J. (1948), The Production of Clouds Containing Supercooled Water Droplets or Ice Crystals under Lab. Cond., Bull. Am. Met. Soc. Vol. 29, pp. 175-182.

Schaefer, V. J. (1949a) The Detection of Ice Nuclei in the Free Atmosphere, Journ. Met. Vol. 6, No. 4, pp. 283-285.

Schaefer, V. J. (1949b), The Formation of Ice Crystals in the Laboratory and in the Atmosphere, Chem. Rev. Vol. 44, No. 2, pp. 291-320.

Schaefer, V. J. (1950), The Formation of Frazil and Anchor Ice in Cold Water, Trans. A.G.U. Vol. 31, No. 6, pp. 885-893.

Smith-Johannsen, Robert (1948), Some Experiments in the Freezing of Water, Science, Vol. 108, pp. 652-654.

Stickley, A. R. (1938), Some Remarks on the Physical Aspects of the Aircraft Icing Problem, Journ. Am. Aeronautical Sciences, Vol. 5, pp. 442-446.

Sutherland, W. (1900), The Molecular Constitution of Water, Phil. Mag. Vol. 50, pp. 460-489.

Swinbank, W. C., (1947), Collisions of Cloud Droplets, Nature Vol. 159, pp. 849-850.

Tammann, G. (1925), States of Aggregation, New York, Van Nostrand Company.

Timonoff, V. E. (1936), On the Establishment of a Working Hypothesis of Ice Phenomena in Lakes and Rivers, Assoc. Int. Hydrol.Scientifique Bull. Vol. 23, pp. 351.

Vonnegut, B. (1947), The Nucleation of Ice Formation by Silver Iodide, Journ. Appl. Phys., Vol. 18, No. 7, pp. 593-595.

Vonnegut, B. (1948), I Production of Ice Crystals by Adiabatic Expansion of Gas. II Nucleation of Supercooled H_2O Droplets by AgI Smokes. III Infl. of Butyl Atc. on Shape of Snow Crystals formed in Lab. G. E. Res. Lab., Schenectady, Occasional Report No. 5,Project Cirrus.

Vonnegut, B. (1949a) A Note on Nuclei for Ice Crystal Formation, Bull. Am. Met. Soc. Vol. 30, No. 5, p. 194.

Vonnegut, B. (1949b) Nucleation of Supercooled Water Clouds by Silver Iodide Smokes, Chem. Rev. Vol. 44, pp. 277-289.

Weickmann, H. (1942) Experimentelle Untersuchen zuv Bildung von Eis and Wasser an Keimen bei tiefen Temperaturen, Zeut. Wiss. Enr. Luftfahrtforsch Ber Nr. 1730, Berlin-Adlershof.

Weyl, W. A. (1951), Transitions in Glass, from Phase Transformations in Solids by Smoluchowski, Mayer & Weyl. Published by John Wiley & Sons, Inc. New York, N.Y., pp. 296-334.

Williams, G. P. (1959), Frazil Ice, A Review of its Properties with a Selected Bibliography, The Engineering Journal, Vol. 42, No. 11, pp. 55-60.

Workman, E. J. and S. E. Reynolds, (1949), Electrical Phenomena Resulting from the Freezing of Dilute Solutions, Phys. Rev.,Vol. 75, Ser. 2, pp. 347-348.

Workman, E. J., and S. E. Reynolds (1950), Electrical Phenomena Occurring during the Freezing of Dilute Aqueous Solutions and their Possible Relationship to Thunderstorm Electricity, Phys. Rev. Vol. 78, No. 3, p. 254-259.

Young, S. W. (1910), Mechanical Stimulus to Crystallization in Supercooled Liquids, Journ. Am. Chem. Soc. Vol. 33, pp. 148-162.

Young, S. W. and W. J. Van Sicklen (1913), The Mechanical Stimulus to Crystallization, Journ. Am. Chem. Soc. Vol. 35, pp. 1067-1078.